

UNCLASSIFIED

AD NUMBER
AD817747
NEW LIMITATION CHANGE
TO Approved for public release, distribution unlimited
FROM Distribution authorized to U.S. Gov't. agencies and their contractors; Critical Technology; JUN 1967. Other requests shall be referred to Air Force Aero Propulsion Laboratory, Attn: Aerospace Power Division, Wright-Patterson AFB, OH 45433.
AUTHORITY
afapl ltr, 12 apr 1972

THIS PAGE IS UNCLASSIFIED

817747

AN INVESTIGATION OF THE CAPABILITY OF A  
COMBUSTION DRIVEN SELF-EXCITED MHD GENERATOR  
TO PRODUCE HIGH ENERGY ELECTRICAL IMPULSES

AVCO EVERETT RESEARCH LABORATORY  
a division of  
AVCO CORPORATION  
Everett, Massachusetts

This document is subject to special export controls and each transmittal to foreign governments or foreign nationals may be made only with prior approval of the Aerospace Power Division, Air Force Aero Propulsion Laboratory, Wright-Patterson Air Force Base, Ohio.

## FOREWORD

This Final Technical Report, "An Investigation of the Capability of a Combustion Driven Self-Excited MHD Generator to Produce High Energy Electrical Impulses," (Project # 5350, Task # 535004) has been prepared by Avco Everett Research Laboratory, 2385 Revere Beach Parkway, Everett, Massachusetts, for the Air Force Aero Propulsion Laboratory, Research and Technology Division, Air Force Systems Command, United States Air Force, Wright-Patterson Air Force Base, Ohio, under Contract AF 33(615)-2846.

This research was performed under the technical monitorship of Air Force Project Engineer Lt. Robert R. Barthelemy, APIE-2, Plasma Dynamics Technical Area of the Aero-space Power Division. The principal investigators for Avco Corporation were Mr. Thomas R. Brogan and Mr. Arne C. J. Mattsson. The work was accomplished between May 1965 and December 1966, and the report was submitted in January 1967.

This work was partially funded with Laboratory Director's Funds of the Air Force Aero Propulsion Laboratory.

This Technical Report has been reviewed and is approved.

*Robert R. Barthelemy*  
ROBERT R. BARTHELEMY  
Captain                      USAF

## ABSTRACT

The program described in this report is directed to the design, construction and performance evaluation of a single circuit output, Faraday magnetohydrodynamic generator channel. The design corresponds to a conventional DC generator with the field coil and load in series. As a second objective, the feasibility of employing a combustion driven self-excited MHD generator for the production of repeated high energy (tens of megajoules) electrical impulses has been investigated. In this application the MHD generator combines the functions of electrical energy generation, storage, and delivery in a single unit basically identical with a conventional self-excited MHD generator configuration. Such a combination is effected by utilizing the generator field coil as an energy storage device and the generator channel as both energy source and circuit breaker. The report describes the channel design analysis, channel construction, modifications to an existing MHD generator (the Mark V) and the testing program. The net power capability of the channel design was strongly compromised in favor of other characteristics judged to be desirable for the pulse application, where high net output from the channel is not the prime requirement. Thus, the maximum net output from the single circuit channel has been approximately fourteen (14) megawatts. Difficulties encountered during the testing program include voltage mismatch between electrode and insulating wall segments in the transition section between burner and channel, arcing in this transition section, and two dimensional current flow effects due to the shorted Hall currents. Solutions to these problems are indicated. An analysis of channel configurations designed primarily for single circuit net output, rather than pulse operation, is also presented. The program was concluded before evaluation of the impulse mode of operation could be carried out.

## TABLE OF CONTENTS

	<u>Page</u>
I. INTRODUCTION	1
II. GENERATOR DESIGN	7
A. GENERAL DESIGN	7
1. Continuous Electrode Faraday Configuration	7
2. Repeated Impulse Operation	7
B. BURNER AND NOZZLE	23
1. Design Requirement and Operating Conditions	23
2. Burner	23
a. Injector Assembly	23
b. Main Burner Chamber Liner	26
3. Burner Nozzle	26
4. Heat Transfer	30
C. MAGNET	37
1. Magnet Design	37
2. Magnet Modifications	40
D. CHANNEL	46
1. Channel Design	46
a. Electrode Walls	49
b. Insulating Walls	51
c. Cooling Water Passage Design	51
d. General	53

TABLE OF CONTENTS  
(Continued)

	<u>Page</u>
2. Channel Assembly	55
3. Channel Extension Section	59
E. AUXILIARY SYSTEMS	62
1. General Arrangement	62
2. Burner Systems and Controls	62
a. Cooling Water System	62
b. Oxygen System	64
c. Nitrogen System	64
d. Fuel System	64
e. Seed Control	68
f. Pilot Burner	74
3. Electrical Control	74
a. Magnet Control	77
b. Generator Control	81
4. Load Resistors	82
F. INSTRUMENTATION	84
1. Burner Monitoring Instrumentation	84
2. Channel Monitoring Instrumentation	85
III. TESTING PROGRAM	87
A. INTRODUCTION	87
B. GENERATOR TESTING	93
IV. CHANNEL DESIGNS FOR HIGH NET POWER OUTPUT	109
V. CONCLUSION	115

## LIST OF ILLUSTRATIONS

<u>Figure</u>		<u>Page</u>
1	Basic Components for a Rocket Driven MHD Generator Installation	2
2	Photograph of the Mark V MHD Generator	3
3	General Arrangement of the Mark V Pulse Generator	4
4	Mark V Single Circuit and Impulse Generator Electrical Circuits	8
5	Relative Power/Length vs Static Pressure for Shorted Hall Currents, JP-4 + O <sub>2</sub> , P <sub>c</sub> = 8 atm	9
6	Generator Excitation Curve and Channel Exit Pressure Level	14
7	Generator V-I Curves for Reduced Conductivities	16
8	Voltage Across Electrodes for Reduced Conductivities	17
9	Channel Exit Pressure and Maximum Shape Factor for Reduced Conductivities	18
10	Static Pressure Profile During Charging	19
11	Mach Number Profile During Charging	20
12	Static Pressure Profile During Pulse	21
13	Schematic of Pulse Burner	24
14	Copper Backplate Assembly	25
15	Pulse Nozzle Assembly	28
16	Heat Flux Inputs for Injector Plate	31
17	Heat Flux Inputs for Chamber Liner	32
18	Heat Flux Inputs for Nozzle Section I	33
19	Heat Flux Inputs for Nozzle Section II	34
20	Heat Flux Inputs for Nozzle Section III	35
21	Heat Flux Inputs for Nozzle Section IV	36

LIST OF ILLUSTRATIONS  
(Continued)

<u>Figure</u>		<u>Page</u>
22	A Photograph Showing the Copper Portion of the Magnet	38
23	A Photograph Showing the Magnet Completely Assembled	39
24	Cross Section of Copper Magnet and Reinforcement Structure in the Mark V Generator	41
25	Longitudinal Centerline Field Strength, Mark V Generator Magnet, Showing Power Section Location	42
26	Modified Magnet Insulation	44
27	Channel Layout	47
28	Heat Flux vs Channel Length	48
29	Cross Sections of the Copper Extrusions	50
30	Water Seal Assembly, Square Bars	52
31	Water Seal Assembly, Rectangular Bars	54
32	Hot Gas Side of a Completely Assembled Channel Electrode Wall	56
33	Outside of a Completely Assembled Channel Electrode Wall	57
34	Photograph of a Completely Assembled Channel Insulating Wall	58
35	Photograph of the Completely Assembled Channel	60
36	Photograph of Channel Extension Section Mounted on the Exhaust System	61
37	General Arrangement of Equipment and Systems for the Mark V Pulse Generator	63
38	Cooling Water System Schematic	65
39	Oxygen System Schematic	66
40	Nitrogen System Schematic	67

LIST OF ILLUSTRATIONS  
(Continued)

<u>Figure</u>		<u>Page</u>
41	Burner Backplate and Fuel Manifold Assembly	69
42	Main Fuel System Schematic	70
43	Secondary Fuel System Schematic	71
44	Auxiliary Fuel Storages	72
45	Fast Acting Valve Schematic	73
46	Exploded View of Fast Acting Valve	75
47	Fuel System Schematic of Igniter and Pilot Burners	76
48	Schematic of Pulse Generator Circuitry	79
49	New Rectifier Bank Mounted in Discharge Circuit	80
50	Load Resistor Schematic	83
51	Channel Monitoring Instrumentation	86
52	Characteristics for Excitation Test #2	89
53	Axial Channel Pressure Distribution for Excitation Test #2	91
54	Excitation Characteristics for Single Circuit Net Power Test #1	94
55	Excitation Characteristics for Single Circuit Net Power Test #2	95
56	Excitation Characteristics for Single Circuit Net Power Test #3	97
57	Excitation Characteristics for Single Circuit Net Power Test #5	99
58	Excitation Characteristics for Single Circuit Net Power Test #7	101
59	Excitation Characteristics for Single Circuit Net Power Test #8	102

LIST OF ILLUSTRATIONS  
(Continued)

<u>Figure</u>		<u>Page</u>
60	Typical Pressure Distribution for Single Circuit Operation	104
61	Magnet Voltage During Pulse Test	106
62	V-I Characteristics for the 56 Kg/sec Generator	110
63	Channel Layout for the 56 Kg/sec Generator	111
64	V-I Characteristics for the 90 Kg/sec Generator	113
65	Channel Layout for the 90 Kg/sec Generator	114

## I. INTRODUCTION

This is the Final Report of Contract AF 33(615)-2846, "Production of High Energy Electrical Impulses with an MHD Generator," between the USAF Aero Propulsion Laboratory and the Avco Everett Research Laboratory, a division of Avco Corporation.

The design, construction and performance evaluation of a prototype rocket engine driven, self-excited MHD generator (the Mark V) has been described previously.<sup>1, 2, 3</sup> The Mark V was originally designed for a maximum net output of twenty (20) megawatts at a mass flow of 60 kilograms/second into fifty individual loads connected to segmented electrode pairs. The generator delivered a maximum net output of 23.6 megawatts at 87% of the design mass flow, providing a demonstration that essentially unlimited amounts of power can be produced for limited durations with simple and inexpensive equipment using a conventional rocket engine as the energy source. However, the multiplicity of outputs each floating at a different potential with the segmented electrode configuration is a practical inconvenience. Therefore, the program described in this report is directed to the design, construction and performance evaluation of a single circuit output Faraday channel in the Mark V generator. The design corresponds to a conventional DC generator with the field coil and load in series. As a second objective, feasibility of employing a combustion driven self-excited MHD generator for the production of repeated high energy (tens of megajoules) electrical impulses has been investigated. In this application the MHD generator combines the functions of electrical energy generation, storage, and delivery in a single unit basically identical with a conventional self-excited MHD generator configuration. Such a combination is effected by utilizing the generator field coil as an energy storage device and the generator channel as both energy source and circuit breaker.

In its simplest form, the rocket driven MHD generator consists of a combustion chamber, channel, magnet and suitable auxiliaries, as shown in Figure 1. Other equipment performing essentially the same functions but designed for light weight could be appropriate for mobile and air or space borne applications. Figure 2 is a photograph of the self-excited Mark V generator. The combustion chamber burning gaseous oxygen and seeded alcohol is on the left. The structural steel encloses the heat sink, room temperature copper magnet winding that is driven by a portion of the generator output. The channel is inside the magnet. Above the magnet are the power take-offs from the electrodes. The exhaust duct on the right conveys the spent gases to the atmosphere. Figure 3 shows the arrangement of the hot generator components (burner, channel and exhaust breech) about the self-excited magnet. The major equipment changes and modifications required in this program were modified field coil insulation, a new burner nozzle, a new MHD generator channel, modified fuel injection system, and modified electrical and burner control systems.

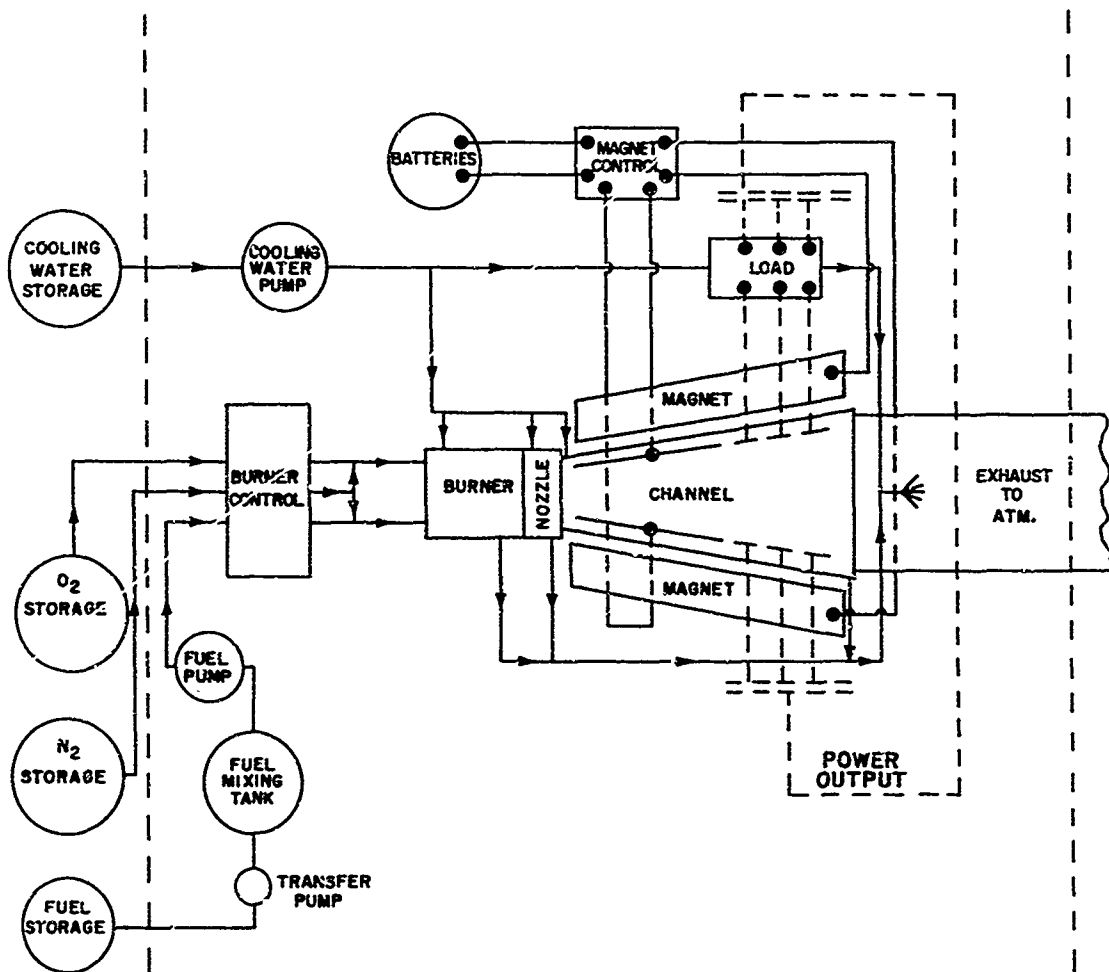


Fig. 1 Basic Components for a Rocket Driven MHD Generator Installation



Fig. 2 Photograph of the Mark V MHD Generator

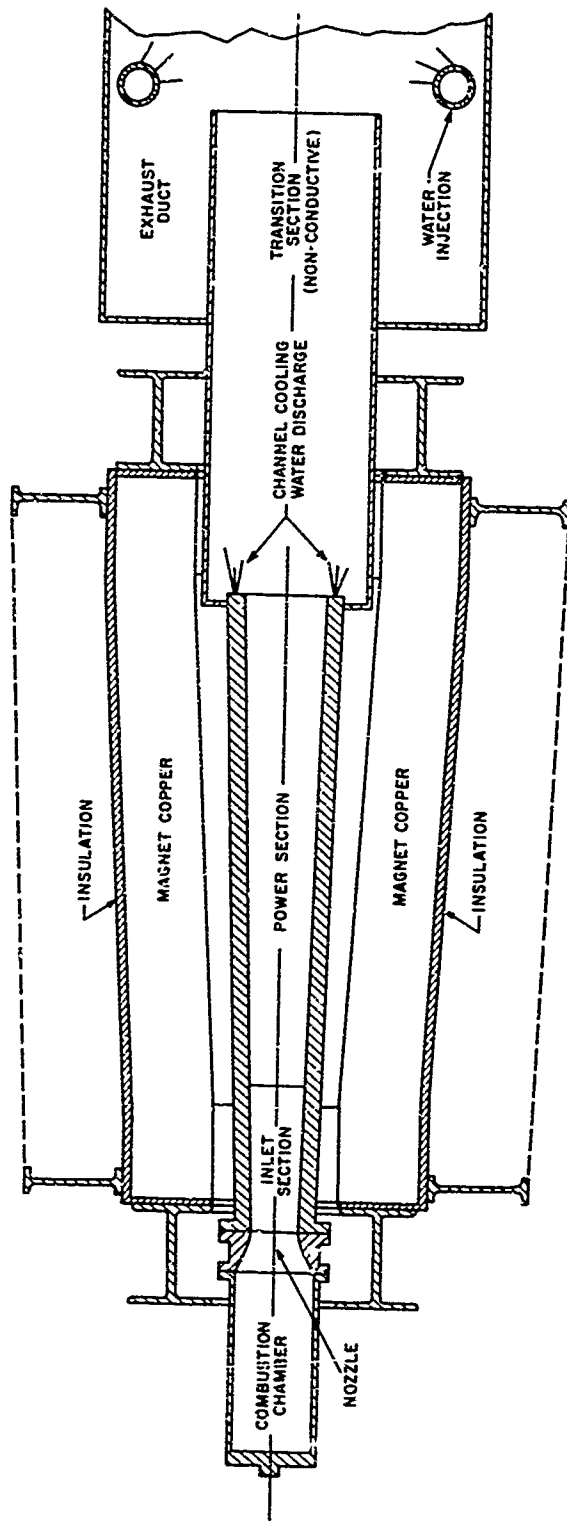


Fig. 3 General Arrangement of Mark V Generator

The fact that the Mark V MHD generator is self-excited means that the single circuit Faraday configuration with the Hall potentials shorted is the only single circuit configuration which could be considered. Thus, the generator configuration is equivalent to that of the conventional series connected DC machine with the field coil and load in series. The design problem consists in determining a suitable configuration which minimizes the effects of the shorted Hall potentials, and at the same time provides a good match between the channel and the field coil and load. The aerodynamic design of the channel, as well as considerations of the pulse mode of operation are discussed in Section II. This Section then goes on to discuss modifications to the magnet, combustion chamber, auxiliary equipment, and instrumentation to accommodate the new channel design, and describes in detail the design and construction of the new channel. Section III describes the performance evaluation of the single circuit generator and the new channel. The program was concluded before evaluation of the pulse configuration was carried out.

The net power output capability of the channel design in the single circuit mode was strongly compromised in favor of other characteristics judged to be desirable for the pulse application, where high net output from the channel is not the prime requirement. Thus, the maximum net output from the single circuit channel has been approximately fourteen (14) megawatts.

Difficulties encountered during the testing program include voltage mismatch between electrode and insulating wall segments, arcing in the transition section between burner and channel, and two dimensional current flow effects due to the shorted Hall currents. These problems are also discussed in Section III.

Section IV contains the results of a design study with high net power output being the prime requirement, and using the present magnet and flow facilities.

Section V contains the conclusion of the work performed under this contract.

#### REFERENCES

1. Final Report, Contract AF 33(657)-8380, "Design, Construction and Test of a Prototype Self-Excited MHD Generator," Avco Everett Research Laboratory, April 1964.
2. Final Report, Contract AF 33(615)-1862, "Detailed Performance Evaluation of a Self-Excited MHD Generator," Avco Everett Research Laboratory, May 1965.
3. Mattsson, A., Ducharme, E., Morrow, I., Govoni, E., and Brogan, T. R., "Performance of a Self-Excited MHD Generator," Avco Everett Research Laboratory RR 238, November 1965. See also Mechanical Engineering, November 1966, pp 34-36.

## II. GENERATOR DESIGN

### A. GENERAL DESIGN

As a part of this program effort was devoted to performance analysis of the single circuit output-impulse Mark V configuration. Basically, the steps in the performance analysis required detailed solutions of the gas-dynamic equations of momentum, energy and continuity, and of Ohm's law, including numerous real effects discussed in the text below. The results of the performance analysis are summarized in Figures 5 through 12 and Tables I and II.

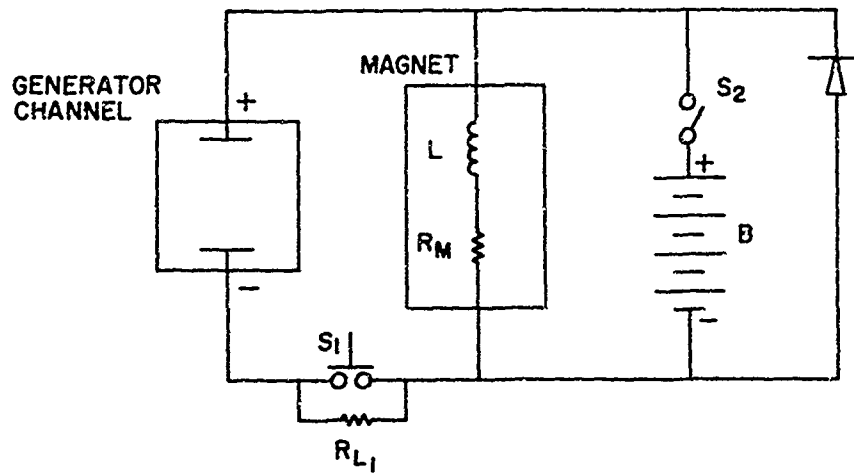
#### 1. Continuous Electrode Faraday Configuration

The single-circuit impulse configuration of the Mark V is shown schematically in Figure 4. On startup, which uses batteries for pre-excitation as before,  $S_1$  is closed so that the entire generator output is across the field coil. When the design current (20,000 amperes at 1610 volts) is reached,  $S_1$  is opened to put the load resistor in series with the magnet. The value of the load resistor,  $R_{L1}$ , is set to drop a voltage equal to the  $L di/dt$  across the magnet at design current; that is, about 1000 volts. Thus, the steady net output will be 20 Mw at 1000 volts of design.

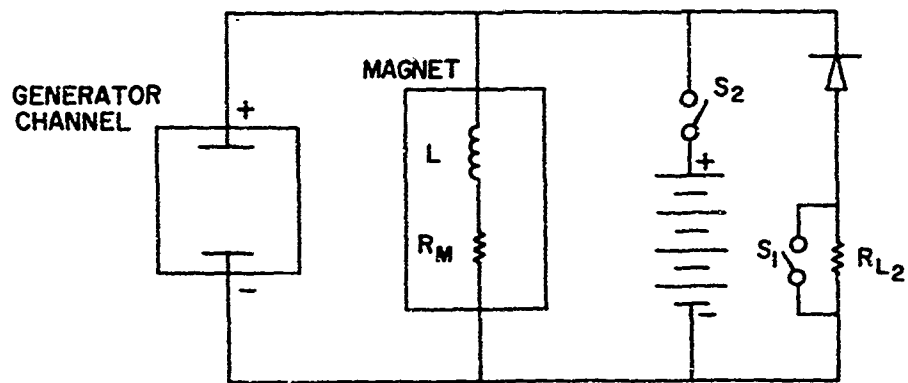
#### 2. Repeated Impulse Operation

For impulse operation the generator is started and excited as described above. When the design current is reached, the generator impedance is greatly increased when the seed is cut off and the magnet discharges through the silicon rectifier to the impulse load. The maximum voltage which can be developed is equal to the design current times the impulse load resistance. Switch  $S_1$  is used as protective circuitry to dissipate the energy stored in the magnetic field in an orderly fashion, by means of shorting out the impulse load, in case of an emergency shutdown. Switch  $S_1$  in both diagrams is the same circuit breaker.

The energy stored in the Mark V field coil at the design field strength is about 70 megajoules, while the design net power output of the generator is 20 megawatts. Since the field coil energy storage is much greater than the net energy/unit time delivered from the generator, repeated short duration pulses with an average power level approximating the net power output of the channel may be delivered if the pulse energy is less than 20 megajoules. This is because after each pulse is delivered at levels below 20 megajoules, the field coil remains in an essentially fully charged condition



SINGLE CIRCUIT OUTPUT OPERATION



PULSE OPERATION

Fig. 4 Mark V Single Circuit and Impulse Generator Electrical Circuits

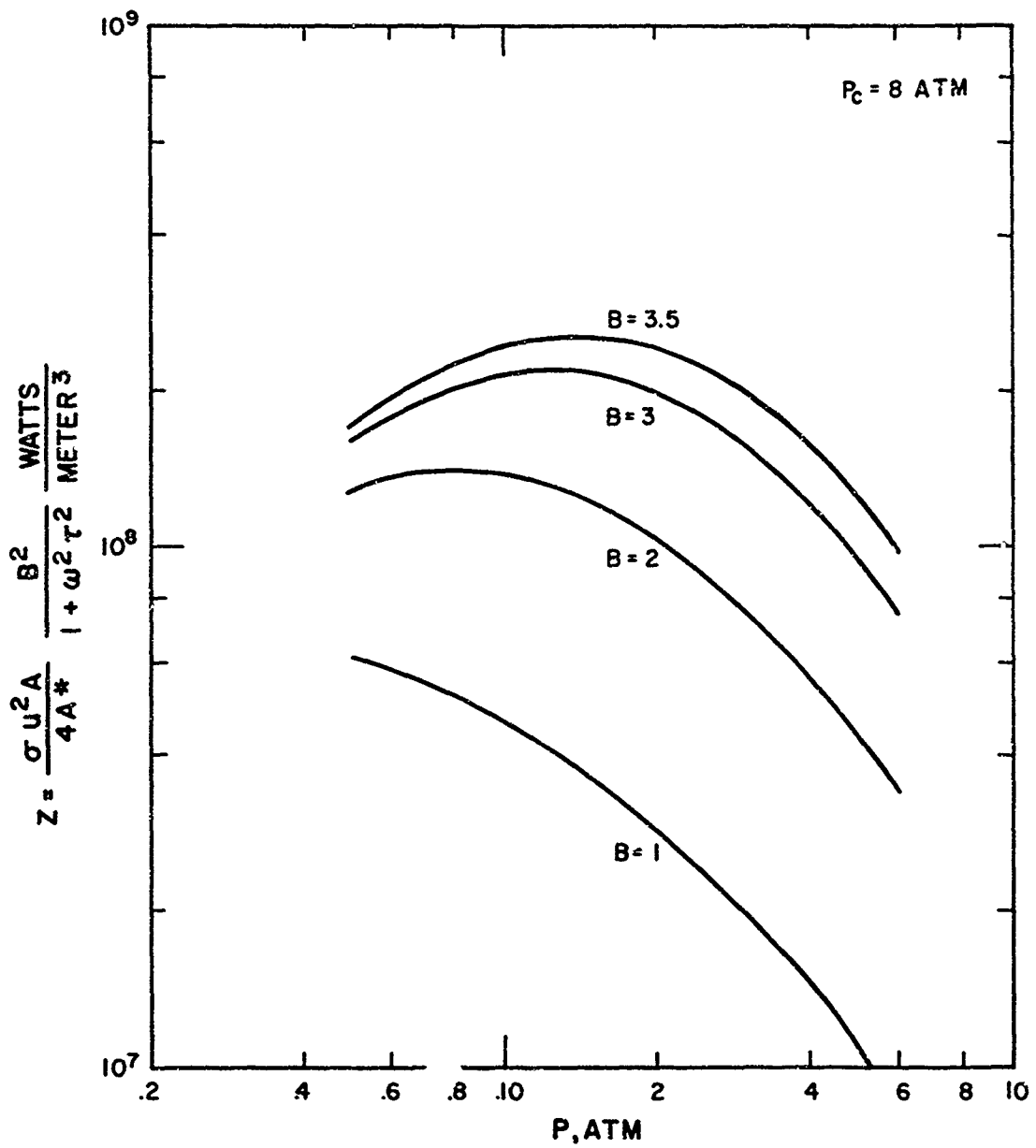


Fig. 5 Relative Power/Length vs Static Pressure for Shorted Hall Currents, JP-4 + O<sub>2</sub>, P<sub>c</sub> = 8 atm

The energy extracted in the pulse is replaced by re-introducing the seed into the combustion chamber, and the process can be repeated. However, only single pulses were studied in the present program.

There are two crucial questions regarding the repeated impulse operations: First, can the conductivity be "extinguished" with the burner operating; and second, can the channel withstand the high voltages developed during the impulse? With regard to the first question, the answer is probably a qualified yes if a metal wall burner and channel is employed so that seed absorption on the walls is minimized. The conductivity of unseeded combustion gases is commonly about 1% of the seeded case using, say, 1 mole % seed. Moreover, the calculations which follow indicate that the conductivity must be reduced to about 1% of its seeded value in order to deliver the minimum impulse voltage desired (5 KV). Thus, the seeding system must be capable of rapid and thorough seed cutoff to seed levels approximating  $10^{-4}\%$  from an initial value of 1%. High net output was not a prime requirement for the impulse program. The capability of the channel to withstand the high impulse voltage is unknown, since the program was concluded before impulse testing could be carried out. In fact, certain phenomena encountered during the single circuit testing would indicate that difficulties would have been encountered at the channel inlet. What is certain, however, is that the impulse mode of operation dominated the channel design phase of the program, leading to compromises with the channel net output capability in favor of pulse performance, while the single circuit net output testing dominated the test program. Thus, neither the single circuit nor impulse objectives was fully achieved.

Compromises to the channel in favor of the impulse mode made at the expense of the channel net power output include:

1. Omission of exit diffuser of complicated construction in order to eliminate voltage insulation problems downstream of the power generating section.
2. This leads to inefficient use of the available pressure ratio of eight, since the channel must discharge at a sufficiently high static pressure to avoid separation. Thus, the effective pressure ratio of the generator is little more than 2.
3. Reaction mode design operation at a Mach number of 1.6 is less efficient when compared with much more optimum partial impulse operation with an inlet Mach number near 2. The lower inlet Mach number was used in order to eliminate any possibility of boundary layer separation on impulse.

As a result of these compromises, there was absolutely no margin in the net power output capability of the channel design. Thus, in operation, eddy currents, current concentrations due to Hall effects, and electrode drop limited the maximum net output to approximately 14 mega-

watts. Lest this be construed as a demonstration that a 20-megawatt, single circuit, continuous electrode Faraday channel could not be built, the design of such a channel optimized for net power output using the same flow results in approximately a net power output of 35 megawatts. The design of such a channel is described in Section IV.

The performance analysis has considered the excitation and impulse discharge phase of the operation. Fuel and oxidizer mass flow and combustion pressure were selected on the basis of previous experience with the Mark V combustion chamber in such a way that the burner would operate reliably. A mass flow of 50 kilograms/sec at a combustion pressure of 8 atm allowed reliable operation of the burner. Gaseous oxygen and JP-4 were selected as the main combustibles, and the seed is dissolved in ethyl alcohol and added separately. One percent seed concentration by volume at 3000°K is employed. The combustion chamber efficiency used is 95%.

Single-circuit output implies shorted Hall potential. Therefore, with the mass flow and combustion pressure chosen, the performance analysis consists of finding a suitable efficient Hall field shorted configuration which provides a good impedance match with the magnet and rapid excitation. Rapid excitation implies output voltage much greater than the magnet IR drop at the design current in the magnet, which was set at 20,000 amperes. This limit was placed as a maximum magnet operating point so as not to overload the magnet reinforcement structure.

With short circuited Hall currents, the power, W, per unit length, l, is:

$$\frac{W}{l} = \frac{\sigma}{1 + (\omega\tau)^2} u^2 B^2 A \alpha (1 - \alpha)$$

where  $\sigma$  is the gas conductivity,  $\omega\tau$  the Hall coefficient,  $u$  the gas velocity,  $B$  the magnetic field strength,  $A$  the channel area, and  $\alpha$  the local loading coefficient. Since, for a given magnetic field coil, the magnet dissipation/unit length is proportional to  $B^2$ ,  $W/l$  should be maximized for rapid excitation and to permit voltage reversal to occur when the channel is nearly purged to conducting gas when the impulse is delivered. Figure 5 shows the value of the local  $W/l$  as a function of the static pressure for different magnetic fields. The channel area is taken as the ratio of the local area to that at the throat. The combustion pressure is 8 atm and the gas is the combustion products of JP-4 and  $O_2$  with 1% K seed. Note how the position of the maximum shifts to higher pressure as the field increases. This indicates the effect of the shorted Hall potential which increases with increasing field. At design field, the maximum is quite broad and occurs at between 1.0 and 2.5 atm corresponding to inlet Mach numbers between 1.5 and 1.8. The high inlet Mach numbers also lead to higher voltage output which is desirable for rapid magnet charging.

A second important consideration is the channel discharge static pressure and its relationship to the design, particularly for the impulse mode. The full impulse voltage appears across the generator exit which, in addition, contains the gas of highest conductivity in the MHD channel. Therefore, to inhibit breakdown, it is desirable to avoid extending the channel beyond the last electrode; that is to say, to eliminate the diffuser. This means that the exit static pressure should be above one atmosphere when running near the design conditions. Static pressure below one atmosphere can be allowed at lower currents as long as boundary layer separation, due to lack of a diffuser, did not prevent excitation.

We adopted a quasi-steady-state analyses for the flow in the channel during delivery of the impulse. Assume that the seed concentration is reduced at a rate such that the flow in the MHD generator at any time can be characterized as a steady flow at reduced seed concentration. Assume that the reduction is carried out fast enough so that the generator current remains constant until voltage polarity reverses, at which time the magnet current is shared between the generator channel and the load, according to the instantaneous conductivity value in the channel. As we will see, the conductivity must be reduced to about 20% of the full load value to achieve polarity reversal. This corresponds to a seed concentration of 5% of the full load value. Thus, the actual impulse rise time is the time the last 5% of the seed is cut off. It would seem reasonable to assume that this will take a relatively long time compared to the time to establish steady flow in the channel which is of the order of two milliseconds due to the fact that the same small amount of seed will persist for several milliseconds after cutoff is initiated. Thus, while the situation going from full load to zero voltage in the short time the seed is reduced to 5% of its full load value may be an unsteady aerodynamic solution, the quasi-steady-state assumption seems reasonable during rise and delivery of the impulse.

Since the inlet Mach number is within the range of relatively high power density, the design of the channel is directed toward reaction mode of operation. At high current levels, especially during the period of high Joule dissipation due to reduced electrical conductivity, some degree of impulse mode will appear when the flow is decelerated. When the flow is decelerated, as in the impulse mode, the stability of the boundary layer on the electrode walls, where the  $j \times B$  force as well as friction retard the boundary layer, is a very important consideration in the design. The stability of a turbulent boundary may be measured by the "shape factor,"  $H$ , where  $H = \delta^*/\theta$  and  $\delta^*$  is the boundary layer displacement thickness and  $\theta$  the momentum thickness. The "shape factor" for a turbulent flow may be estimated using the momentum integral plus semi-empirical correlations of flow with adverse pressure gradients. An adverse gradient; i. e., the  $j \times B$  force in a generator tends to increase  $H$ , a pressure drop tends to reduce  $H$ . It is generally accepted that value of  $H > 1.6$  for a turbulent flow indicates incipient separation.

With these considerations in mind five configurations were examined in some detail, and pertinent data are contained in Table I for

condition of flow, seed and combustion pressure, and 20,000 amperes load current.

TABLE I

Case	Inlet M	Discharge Pressure		Voltage	Remarks
		No Load	Full Load		
1	1.6	1.0	1.6	1400	Low output
2	1.6	0.72	1.15	1610	Good, $H < 1.5$
3	1.7	0.75	1.25	1580	Boundary layer separation on impulse
4	1.7	0.55	1.0	1710	Low exit pressure
5	1.8	0.55	1.0	1740	Low exit pressure, separation on impulse

As can be seen from the table, the best performance is achieved by high inlet Mach number and low discharge pressure. However, Case 2 was selected as the configuration which most closely fulfills the design objectives. Discussion of this design follows.

A channel configuration consisting of a square cross section with straight diverging walls was selected based on practical design considerations. Boundary layer corrections were made in the fluid dynamical calculation for both electrode and insulating walls, taking into consideration the momentum-thickness, shape factor, compressibility, and cooling effects. The stability of the boundary is indicated by the value of maximum shape factor ( $H_{max}$ ), which occurs at the channel exit.

In Figure 6 the V-I curves of the channel with different magnetic field strength are shown as solid lines identified with maximum local field strength ( $B_{max}$ ). The straight line through the origin is the D. C. characteristic of the magnet and is labeled  $IR_C$ . The other curve intercepting the origin represents the excitation characteristic of the generator, giving the generator voltage output at various magnetic fields or magnet currents. Each point on the dynamic characteristic represents an operating point while the field coil is being excited. The difference between these two curves is the available voltage in overcoming the momentary inductive load ( $L di/dt$ ). As can be seen in the curve, this is 1000 volts at a magnet current of 20,000 amperes. The static pressure at the generator channel exit is also shown as a function of magnet current. As can be seen in the figure, at zero current; i.e., startup, the discharge pressure is 0.72 atm. Due to

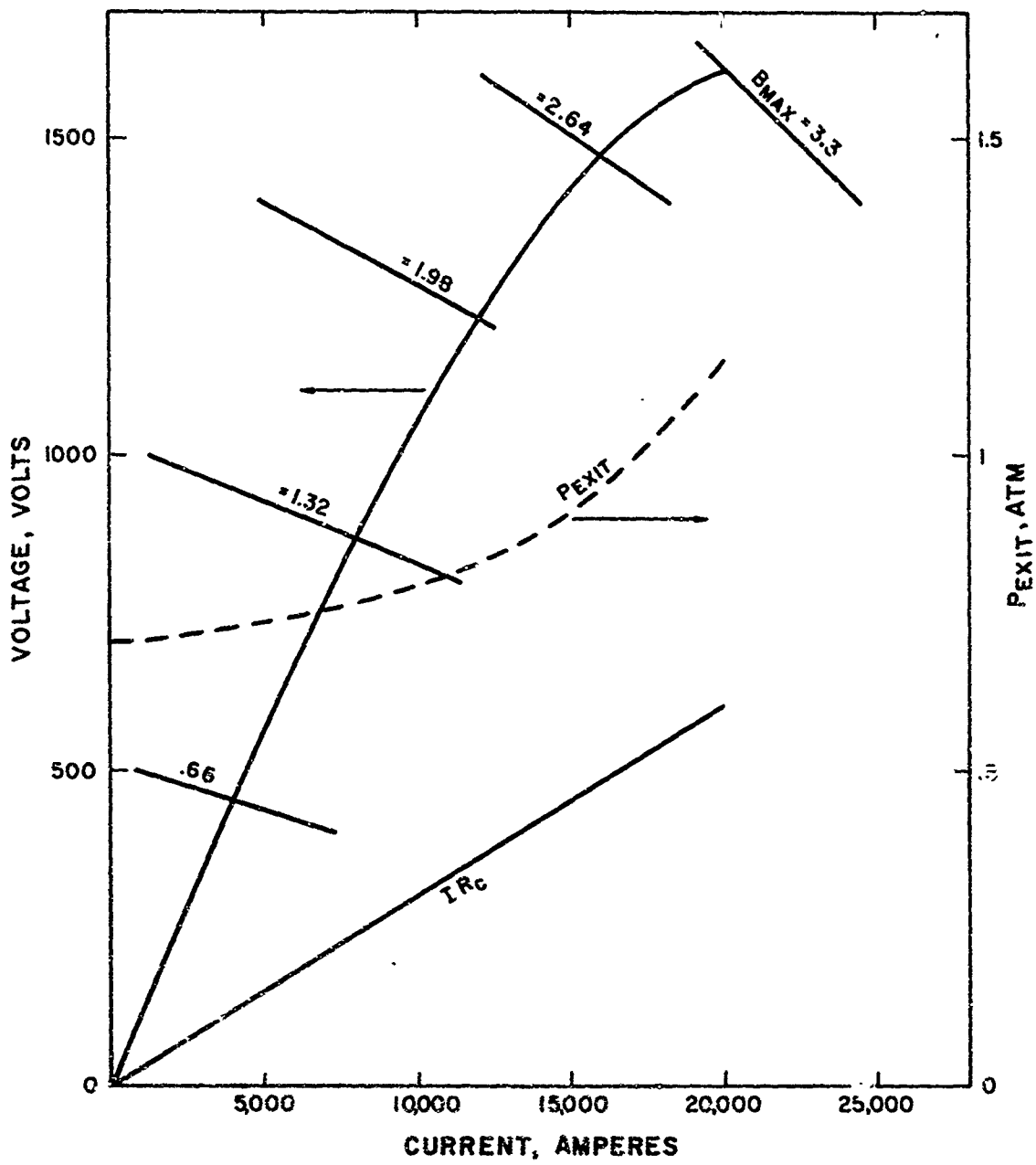


Fig. 6 Generator Excitation Curve and Channel Exit Pressure Level

drag in the gas, the pressure rises to 1.0 atm at 15,000 amperes and to 1.15 atm at the design current of 20,000 amperes.

Figure 7 shows the generator channel V-I curves as the electric conductivity of the working gas is reduced to a fraction  $\sigma/\sigma_0$  of the original value, due to a reduction of seed concentration. The current passing through the generator channel can be taken as a constant as long as the terminal voltage is positive (generating mode) since the rectifier prevents current from transferring to the load with this polarity. As the conductivity drops further, the polarity reverses and the load resistor starts to take a part of the total current. The current in the generator channel then decreases as the terminal voltage becomes more negative. The dotted lines represent operating lines for different load resistors (0.25 $\Omega$ , 0.5 $\Omega$ , 1.0 $\Omega$ ) corresponding to delivery at  $10^{-7}$  joule pulses in 100, 50, and 25 milliseconds.

Figure 8 shows the generator terminal voltage and Figure 9 shows the generator channel exit pressure, and the maximum shape factor (H) encountered as the conductivity decreases ( $\sigma/\sigma_0$  varies from 1.0 to .01). It is interesting to note as the  $\sigma/\sigma_0$  decrease, the joule dissipation increases, and as the generator polarity is reversed and the load resistor starts to take a part of the total current, the total Lorentz force in the generator channel diminishes. The interplay of these two effects determines the allowable size of the load resistor for a specific channel if stable boundary layers are to be maintained. As the conductivity becomes very small, the magnetohydrodynamic effect vanishes, and the curves for different load resistors again tend to converge.

Figure 10 and Figure 11 show the theoretical static pressure and the Mach number profiles along the generator axis during the charging period. Quasi-steady flow is assumed at each magnetic field strength level. Figure 12 shows the static pressure profile along the generator axis during the pulse period with the electric conductivity level used as parameter. A relatively high load resistance of one ohm is used. Lower load resistance would lessen the friction of the current flowing through the general channel, thus giving a more favorable pressure profile. It should be noted that even under the unfavorable conditions considered, in no case is any adverse pressure gradient allowed to exist. This is very important as the stable boundary layer is essential in purging the residue seed in the generator channel. The control of the seed concentration is of critical importance in insuring the effectiveness of the generator channel as a circuit breaker.

The final design parameters for the single-circuit-pulse generator are summarized in Table II:

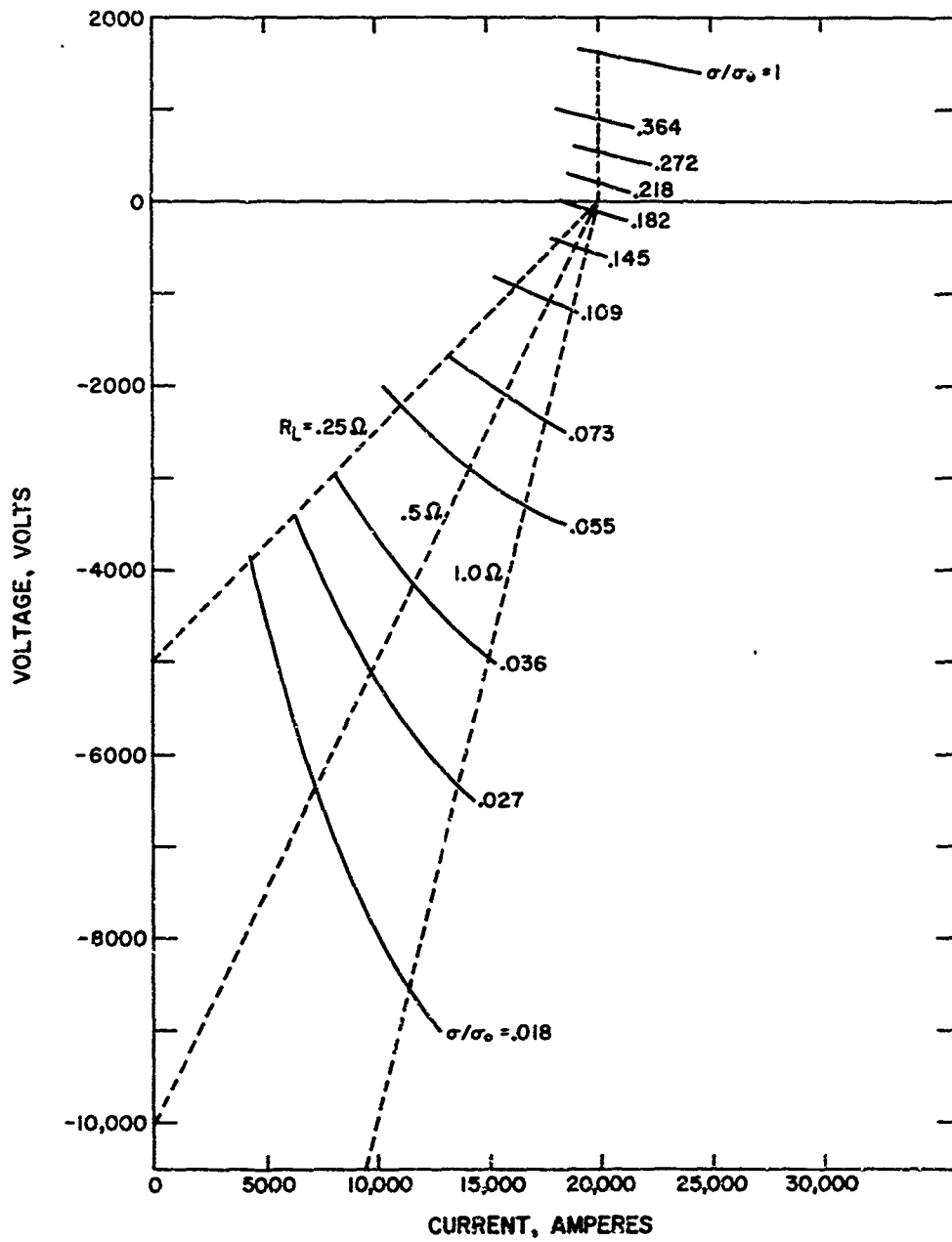


Fig. 7 Generator V-I Curves for Reduced Conductivities

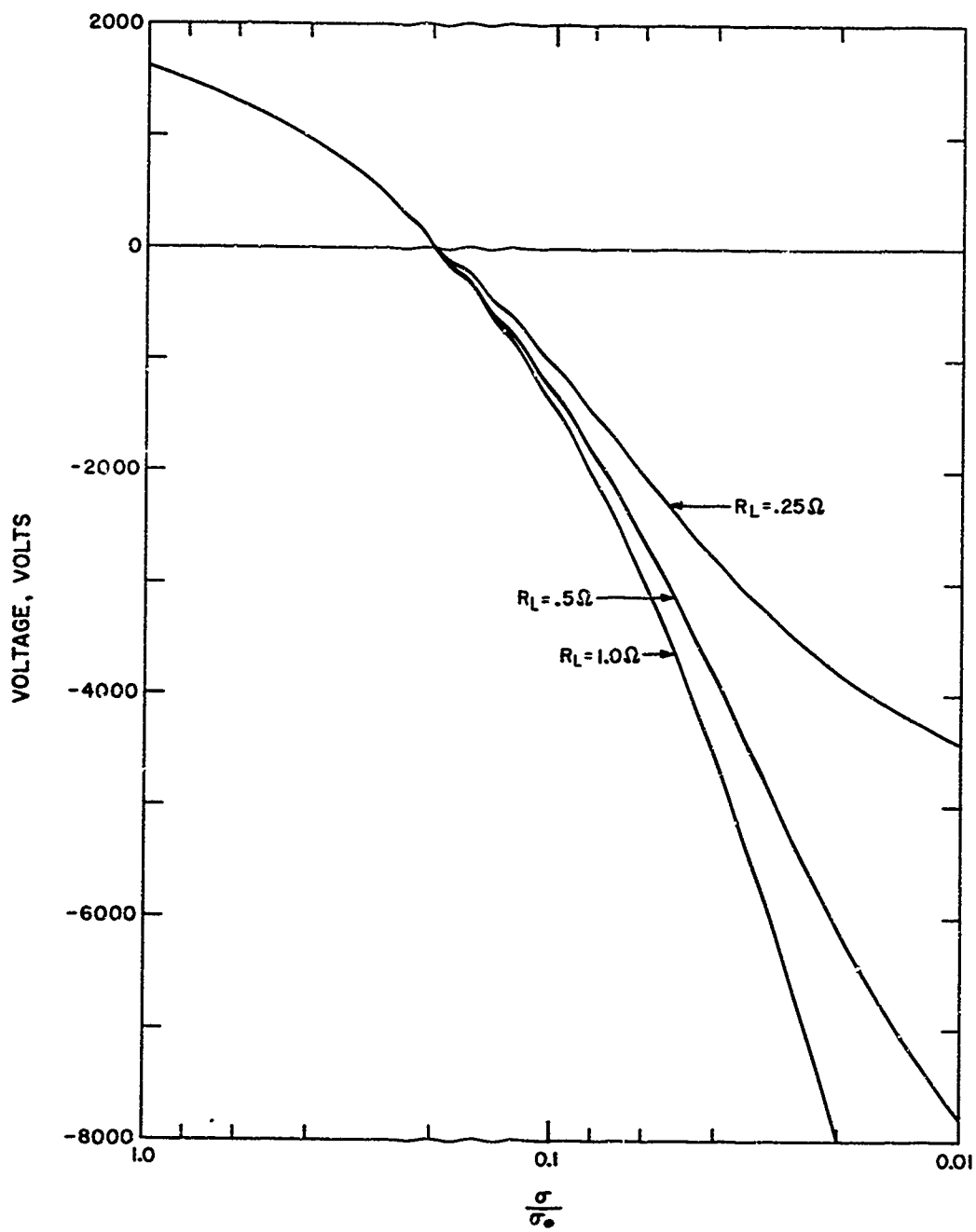


Fig. 8 Voltage Across Electrodes for Reduced Conductivities

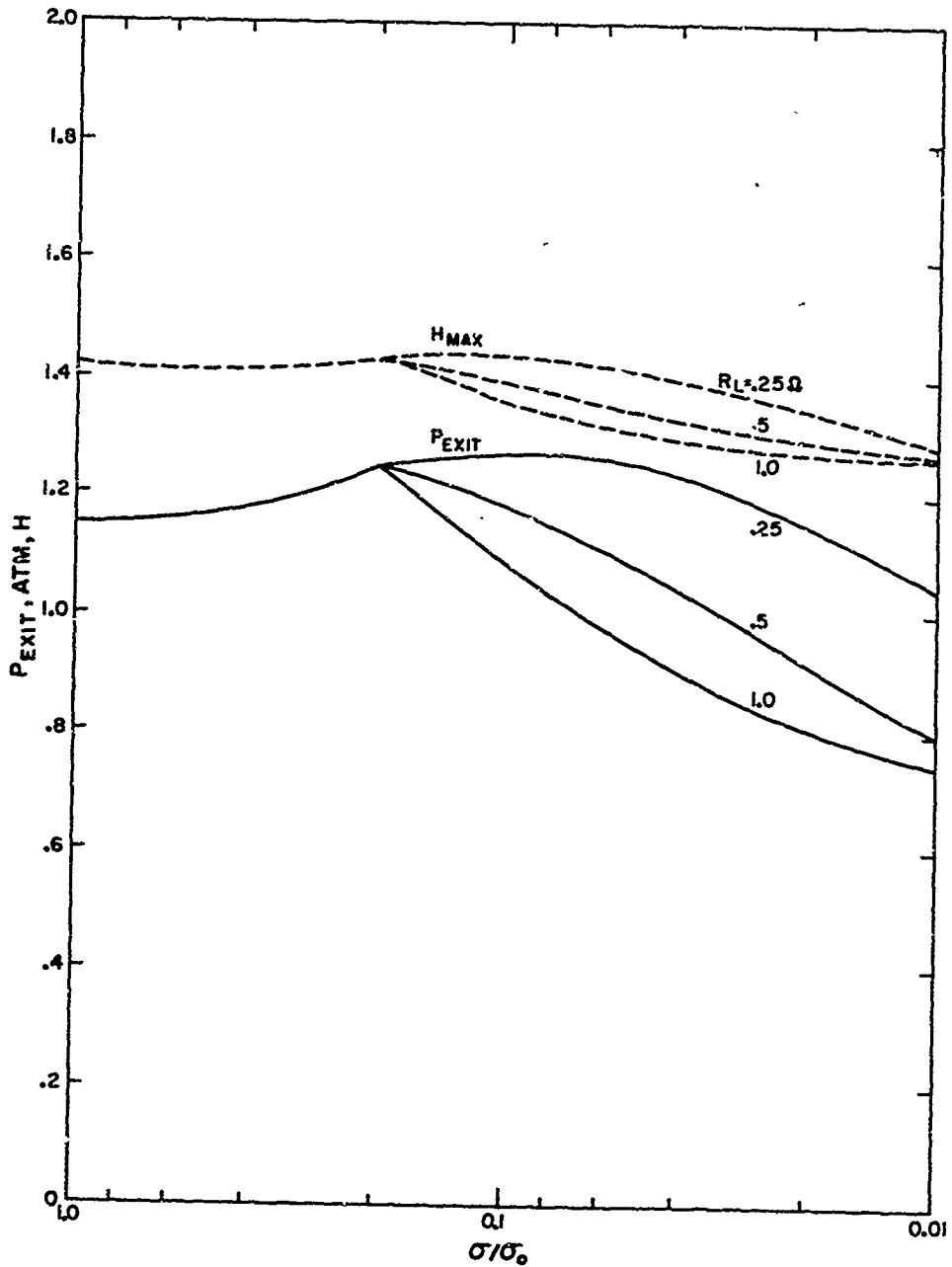


Fig. 9 Channel Exit Pressure and Maximum Shape Factor for Reduced Conductivities

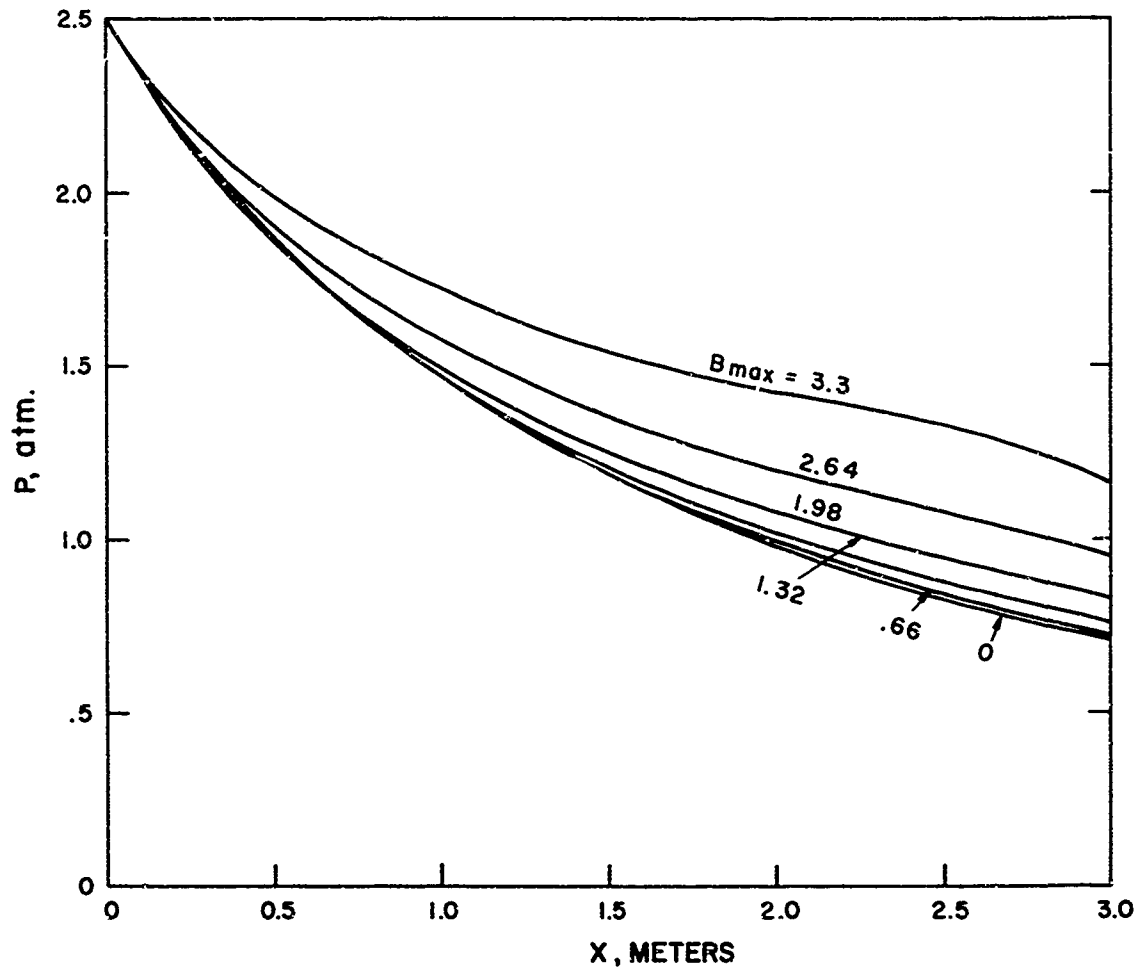


Fig. 10 Static Pressure Profile During Charging

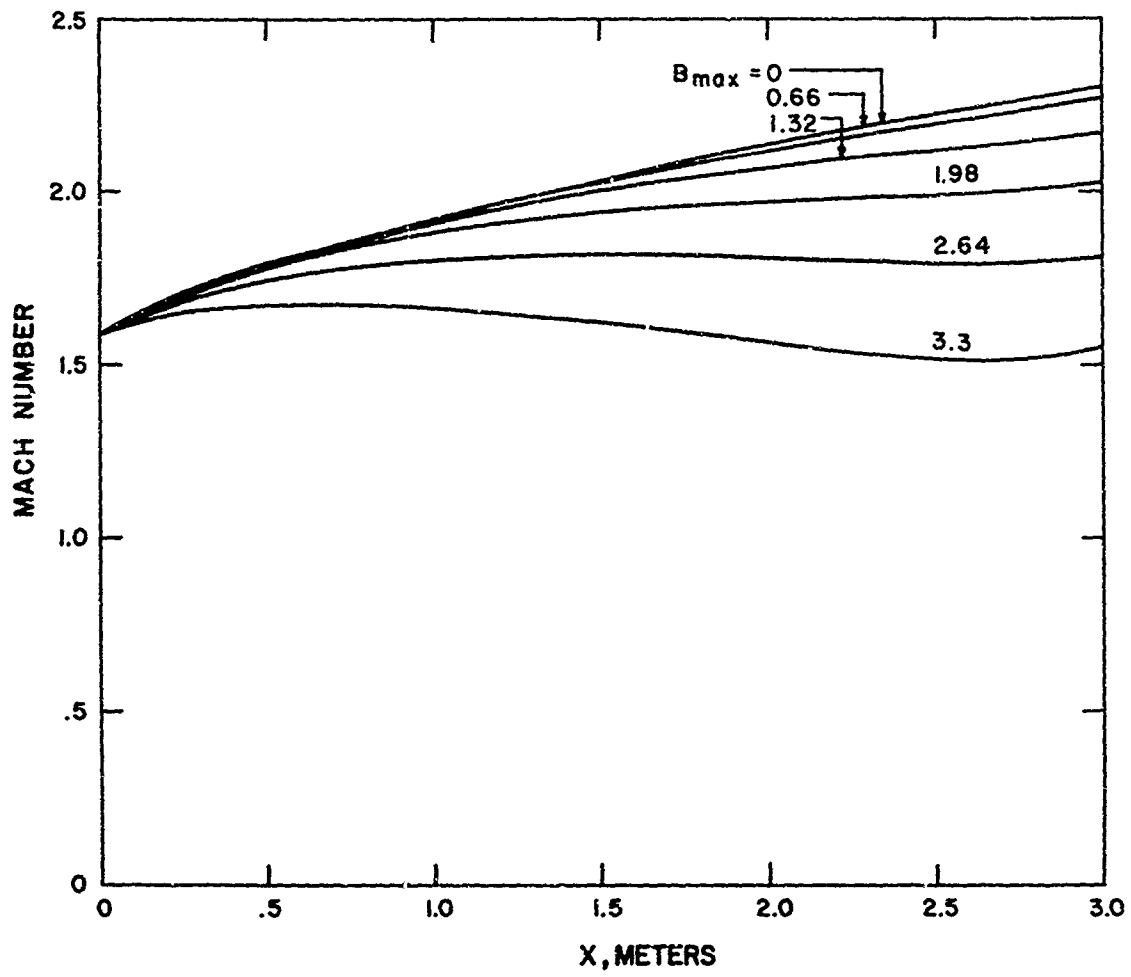


Fig. 11 Mach Number Profile During Charging

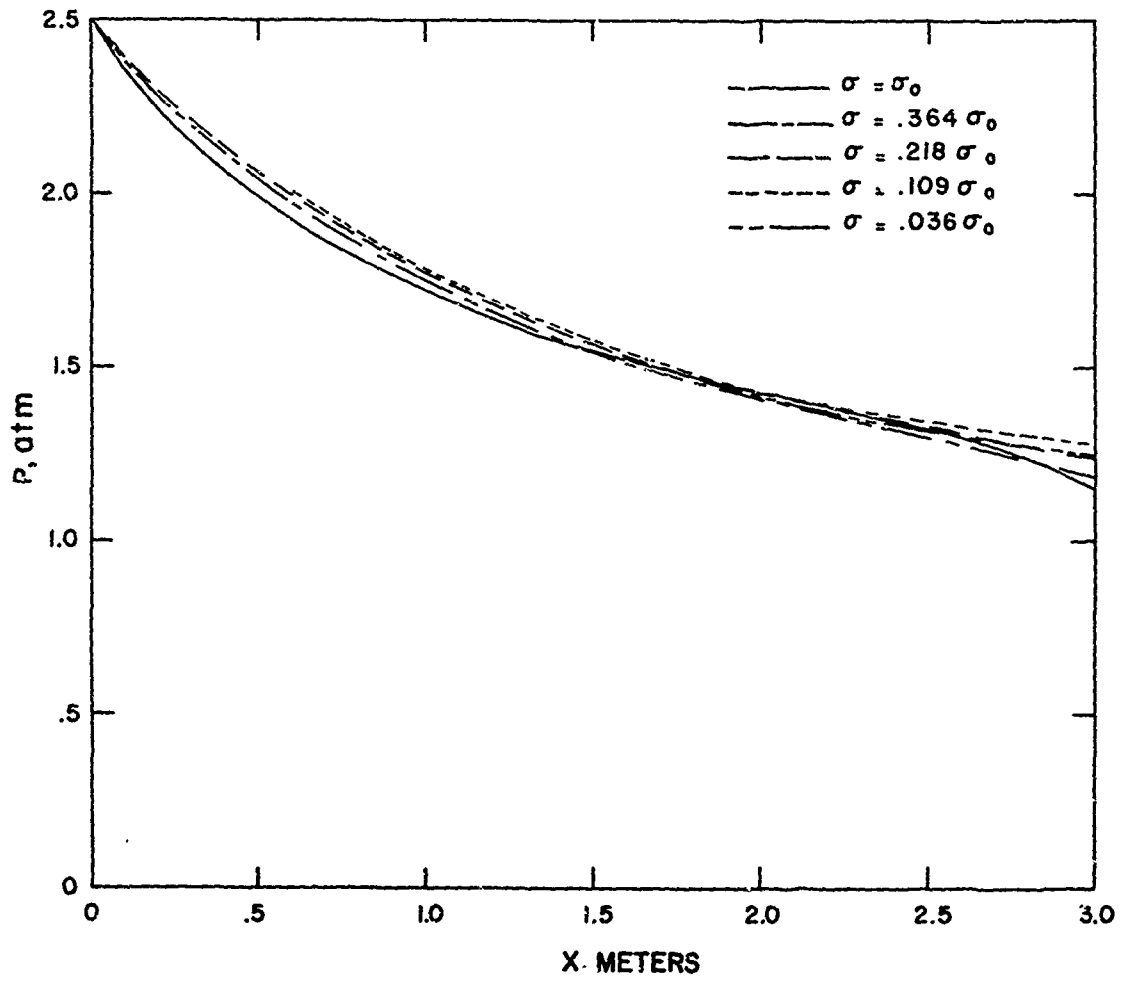


Fig. 12 Static Pressure Profile During Pulse

TABLE II

Combustibles	JP-4 + O <sub>2</sub> + Separate KOH in Alcohol Seed (1%) (Seed may be increased)
Mass Flow	50 Kg (110 lb.) per second
Combustion Pressure	8 atm
Design Output Current	20,000 amperes
Design Output Voltage	1610 volts
Design Gross Output	32.2 megawatts
Design Net Output	20.0 megawatts (20,000 amperes at 1000 volts)
Channel Inlet Mach Number	1.6
Channel Discharge Pressure - No Load	0.72 atm abs
Channel Discharge Pressure - Full Load	1.15 atm abs
10 <sup>7</sup> Joule Impulse Voltage	
100 msec	5,000 volts
50 msec	10,000 volts
25 msec	20,000 volts

These were the parameters utilized to perform the detailed design of the new burner nozzle and channel, as well as the modifications to the magnet and auxiliary systems to the existing Mark V generator. These designs and modifications are discussed in detail on the next page.

## B. BURNER AND NOZZLE

### 1. Design Requirement and Operating Conditions

The burner used in this program is the same as that used in the Mark V program with the exception of the nozzle and backplate assembly. The original burner was designed for a mass flow of 60 Kg/sec, composed of 40 Kg/sec gaseous oxygen, 19.0 Kg/sec ethyl alcohol, and 1.0 Kg/sec potassium hydroxide, with a combustion pressure of 8 atmospheres. In the pulse program the burner was designed to be operated at a mass flow of 50 Kg/sec, with 38 Kg/sec of gaseous oxygen, 10.0 Kg/sec of JP-4, and various amounts of ethyl alcohol and potassium hydroxide at a combustion pressure of 8 atmospheres. Although total mass flow was lower than in the Mark V program, the higher energy release of the new fuel approximated the design operating conditions of the original program.

The only new components in the MHD pulse burner designed under the subject contract were the nozzle and backplate assembly; however, the design of all burner components is discussed for general information. Figure 13 is a schematic of the pulse burner showing its components; the backplate, liner and nozzle assemblies. In the center of the injector assembly is the pilot burner. The pilot burner is intended to run continuously so as to provide a constant source of ignition in the main burner. The pilot is started by a small igniter burner. Both the pilot and igniter burners operate on gaseous methane and gaseous oxygen. The all-gas system provides simple and reliable operation. The pilot burner operates at a chamber pressure of 13.5 atmospheres and a mass flow of 0.1 Kg/sec.

### 2. Burner

#### a. Injector Assembly

Due to the multiple plenums used in the Mark V fuel system, the time required to purge these manifolds was excessive for the pulse program, and therefore the burner backplate was modified so that each of the 60 fuel nozzles had its own individual feed. The main fuel for pulse operation was JP-4 and the secondary fuel was ethyl or methyl alcohol and potassium hydroxide.

The copper backplate assembly is shown on Figure 14. The injector assembly is divided by a series of plates or diaphragms to provide passages for cooling water and oxygen. Starting from the left side of the figure, first is a plate which forms the back wall of the combustion chamber and contains the oxygen nozzles, which have a rounded entrance

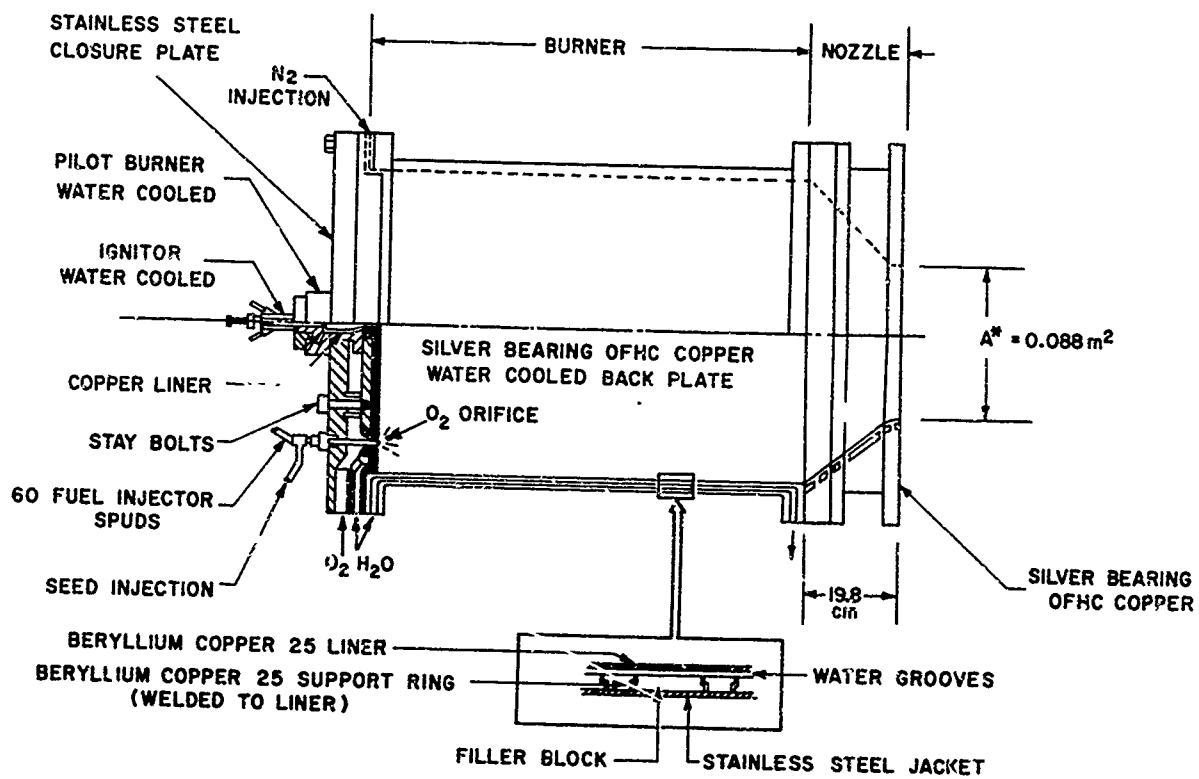


Fig. 13 Schematic of Pulse Burner

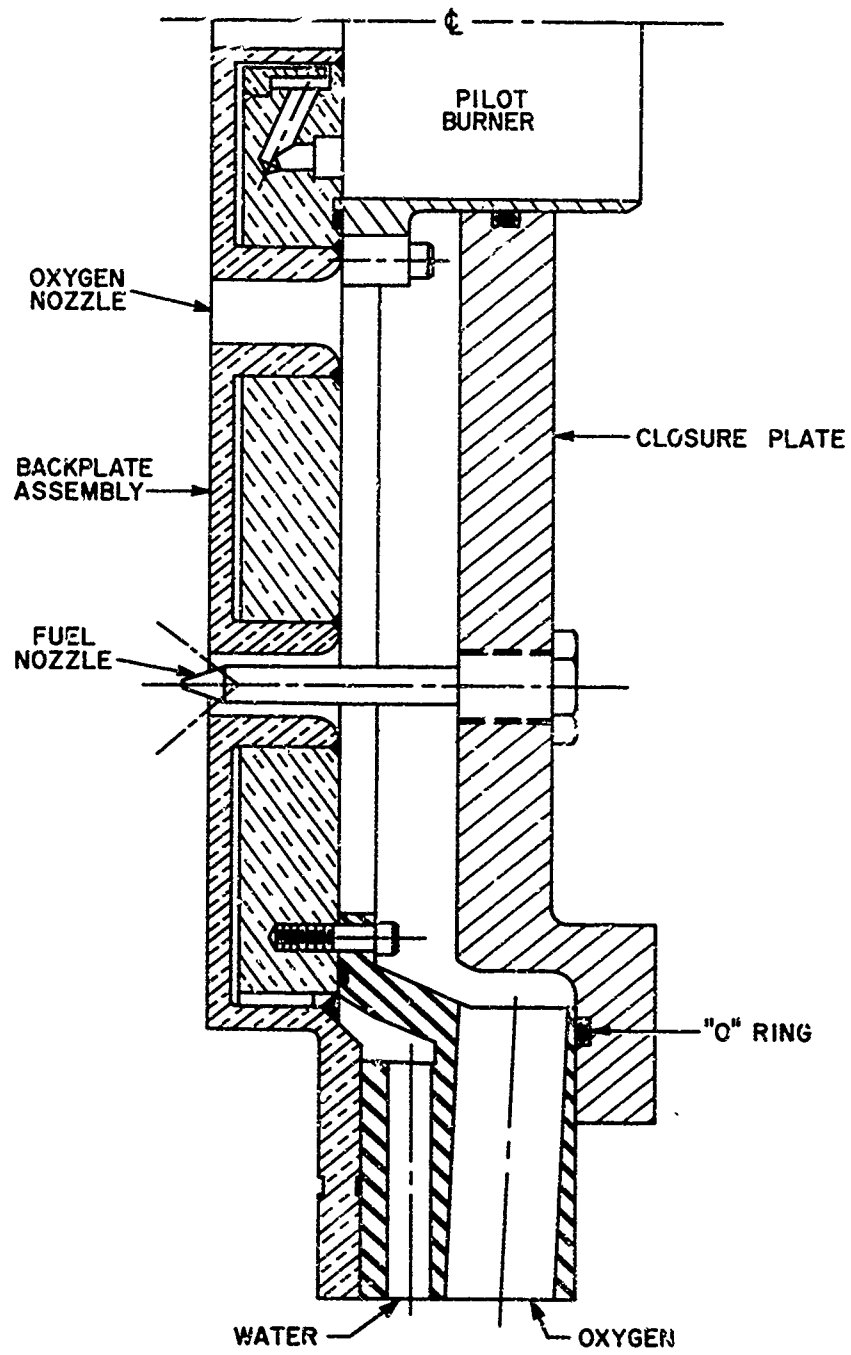


Fig. 14 Copper Backplate Assembly

for a smooth flow and are sized to produce sonic velocity at the throat. Behind this plate is the cooling water passage which is formed by the addition of a support plate. The third plate closes the oxygen passage and contains the fuel injectors. The center of the injector assembly is designed to accept the pilot burner and igniter assembly. The cooling water flow passage in the backplate was designed to cool the pilot burner throat.

#### b. Main Burner Chamber Liner

The burner chamber shown on Figure 13 consists of an inner liner and an outer jacket with a cooling water passage in between. The inner liner is subject to external water pressure, and to prevent failure by buckling is reinforced with several rings. To provide a reasonably high and uniform cooling water velocity, the spaces between reinforcing rings are taken up by filler rings. The inner liner is fixed at the nozzle end and is free to expand axially at the backplate end, an "O" ring seal being provided at this point. It operates at a heat flux of 600 watts/cm with a cooling water flow of 3400 liters/minute. Because the burner is operated inside a building, elementary safety considerations dictated that the outer shell of all portions of the burner should be amply strong. The outer jacket of the chamber section, for instance, has a theoretical bursting pressure of 185 atm which gives a safety factor over normal chamber pressure of 22.

#### 3. Burner Nozzle

Due to the new channel geometry a new burner nozzle was required. Based on previous experience with water cooled rocket nozzles, several guide lines were used for the design. These were:

1. The nozzle must be radially restrained because of the large dimensions and the transition from a round to rectangular cross section.
2. A fully developed turbulent boundary layer along with an axial velocity change was assumed to calculate heating loads.
3. A high strength, high thermal conductivity material was desired.

The nozzle inlet brings about several unique problems in estimating the heat flux as the boundary layer thickness is changing while the velocity is increasing. The heat transfer rates used in the design were a combination rocket engine practice and data obtained from the Mark V, and gave values from 735 watts/cm<sup>2</sup> at the nozzle inlet to 1255 watts/cm<sup>2</sup> at the nozzle throat.

The selection of a nozzle material was of prime importance in designing a suitable nozzle configuration with the proper cooling throughout. Since the combustion gas temperature is in excess of the melting point of most materials, a highly conductive material suitable for water cooling was desirable. The wall was required to withstand high water side and high gas side pressures in addition to the large stresses caused by the thermal loads. From the design point of view the highest stresses were found at the instant of burner shutdown when high mechanical and thermal stresses exist together without the presence of chamber pressure.

Alloys considered for the nozzle were beryllium copper 10 and 25, OFHC (oxygen-free, high conductivity) copper, OFHC silver bearing copper, zirconium copper (with .13% Zr) and chromium copper. In making a material choice such factors as yield strength, ductility, and corrosion resistance at operating temperatures were the prime considerations. A low expansion coefficient is desirable from the thermal stress point of view; however, low expansion coefficients usually mean low conductivities for the same material, with the disadvantage of low conductivity outweighing the low expansion coefficient. As expansion coefficients vary little for the copper-base alloys, it could not be used as a prime factor in material selection.

The beryllium copper alloys hold their strength at temperatures in excess of 320°C; however, they become more brittle with increasing temperature and are quite notch sensitive. The thermal conductivity of BeCu (alloy 25 and alloy 10) is approximately 30% and 50% of the conductivity of copper, respectively. Because of the brittleness and lower thermal conductivity of BeCu alloys, its use was not recommended for the application. Zirconium copper has 90% of the conductivity of copper and has yield strength over 2700 Kg/cm<sup>2</sup> at temperatures of 320°C, remains ductile, but depends upon cold working for its strength. Chromium copper also has good high temperature properties, but must be heat treated to attain its strength; since some degree of distortion accompanies all heat treatment, the use of chromium copper was ruled out. The transition from a round to a square cross section required a welded assembly from the strength and manufacturing point of view, and thus ZrCu was eliminated, since the strength gained by cold working was reduced to the level of pure copper by welding. After a thorough evaluation of the above materials, silver bearing "oxygen-free, high conductivity" copper was selected as the best material for the nozzle, since the silver improves the alloy's ductility at elevated temperatures and does not influence other properties to a great degree.

Figure 15 shows the nozzle assembly, except for the throat section, with their respective cooling water connections. The nozzle is made in four sections; the first two reduce the 0.508-meter liner diameter to approximately a 0.43-meter diameter. The third section forms the round to square transition, with the fourth section forming the nozzle throat and burner flange. The first two sections and the last section are cooled by

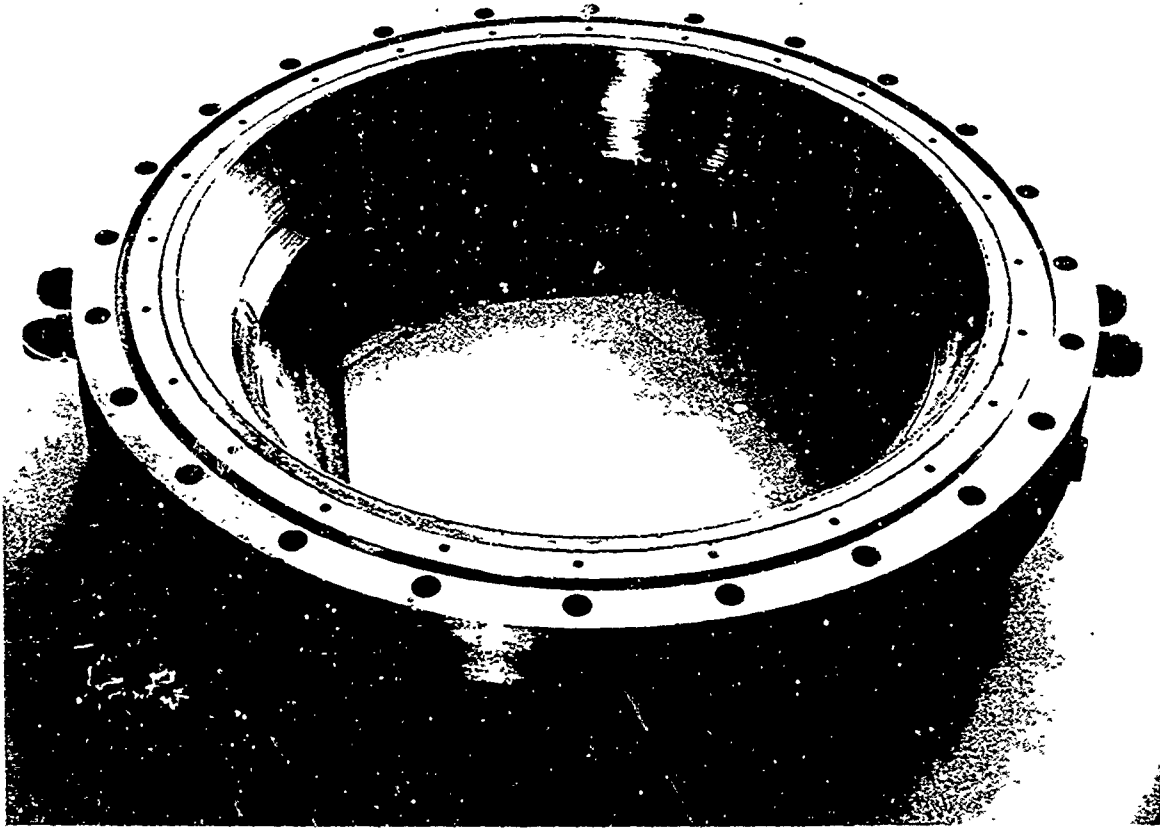


Fig. 15    Pulse Nozzle Assembly

water circulating circumferentially, while the third or transition section is cooled axially. The total water flow for the nozzle is 3200 liters/minute. The entire assembly is bolted together and attaches to the existing liner and liner shell. Advantages of this design are that there is no separate outer jacket, no water seals, is half the length of the Mark V nozzle and simpler to manufacture and maintain.

Because of the high level of thermal and mechanical stresses present in a nozzle of this type, a joint of the maximum strength possible for the given material was desired. This was copper-to-copper weld; however, the heat necessary to insure proper weld penetration would have caused overpenetration in certain locations, ruining the water cooling passages. Therefore, alternative methods of closing the cooling water grooves were investigated and the results indicated that Everdur 1010, an alloy of 95% copper, was the most feasible welding rod to use, as its melting point is considerably lower than pure copper; consequently, less heat is required for welding.

Of the four sections which comprise the nozzle, only the welds on the transition section withstood the water pressure test when received. The thinner nozzle ring had several areas of porous welds which resulted in water leaks; however, these were of a very minor nature and quickly repaired with a simple low temperature soldering cycle. The larger reducing ring had many water leaks due to poor weld penetration and porosity, which required replacement of the cooling water groove cover rings.

Since the inside contour of the nozzle was finish machined, a great probability existed that welding would damage the thin nozzle wall; therefore, it was decided to furnace braze this insert ring, using Sil-Flos, a copper based brazing alloy, which melts at 735°C. The insert ring was machined to close tolerances so as to leave a braze groove width of approximately 0.05 mm. Such clearances were necessary to achieve a high strength joint since Sil-Flos in such a joint will have a strength greater than that of the base material. This repair cycle was successful, and so the cover ring on the other cooling water groove was machined out and replaced. This ring was furnace brazed, using a lower temperature brazing alloy (Easy flow 45, melting at about 570°C.) This braze was unsuccessful, due to improper control of the vendor's furnace temperature during the heating cycle, which caused some of the volatiles (zinc, cadmium) in the braze material to boil off leaving a porous braze.

A repeat cycle was completed successfully, using the same brazing alloy (Sil-Flos) as used on the first side. It was possible to do this and not melt the braze on the first side since there exists sufficient copper alloying in the brazed joint to raise the melting point of the original brazed material.

The nozzle throat section also had to undergo a repair cycle due to a vendor error in machining. The repair consisted of welding in a

section on the hot gas surface of the throat section and remachining to the original dimensions. Inspection and pressure checking revealed the repair work was unacceptable.

After a second repair cycle, a thorough inspection was performed, including X-rays of the cooling water passages to check for flow obstructions and weld integrity. This inspection revealed that the second repair cycle was satisfactory; however, the integrity of the everdur welds used to seal the cooling water grooves appeared doubtful, so a test section was removed from water groove covers which revealed a weld depth of only 0.005 to 0.030 inches, rather than the 0.090 inches required. In view of this the entire cover plate was removed, a new plate machined, and was furnace brazed in place.

#### 4. Heat Transfer

Figures 16 through 21 show the measured values of heat flux for the various burner components. The injector plate operated at a heat flux of 262 watts/cm<sup>2</sup>, with a cooling water flow of 530 liters/minute; the liner, 600 watts/cm<sup>2</sup> and 3400 liters/minute; nozzle Section II, 740 watts/cm<sup>2</sup> and 185 liters/minute; nozzle section III, 850 watts/cm<sup>2</sup> and 1140 liters/minute, and nozzle section IV or the nozzle throat, 1160 watts/cm<sup>2</sup> and 320 liters/minute. The measured and predicted heat flux values were in close agreement as measured values are approximately 95% of the predicted values.

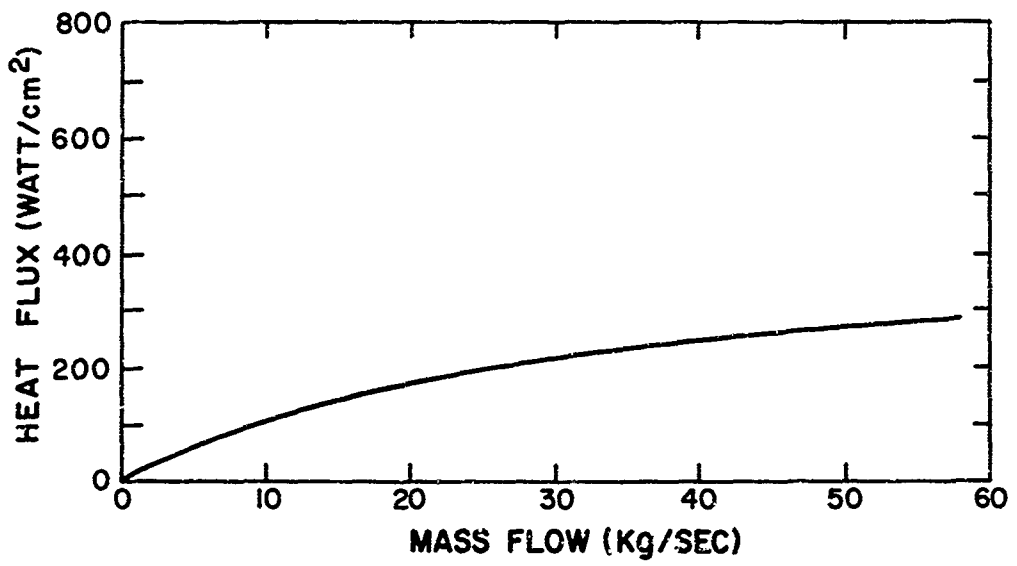


Fig. 16 Heat Flux Inputs for Injector Plate

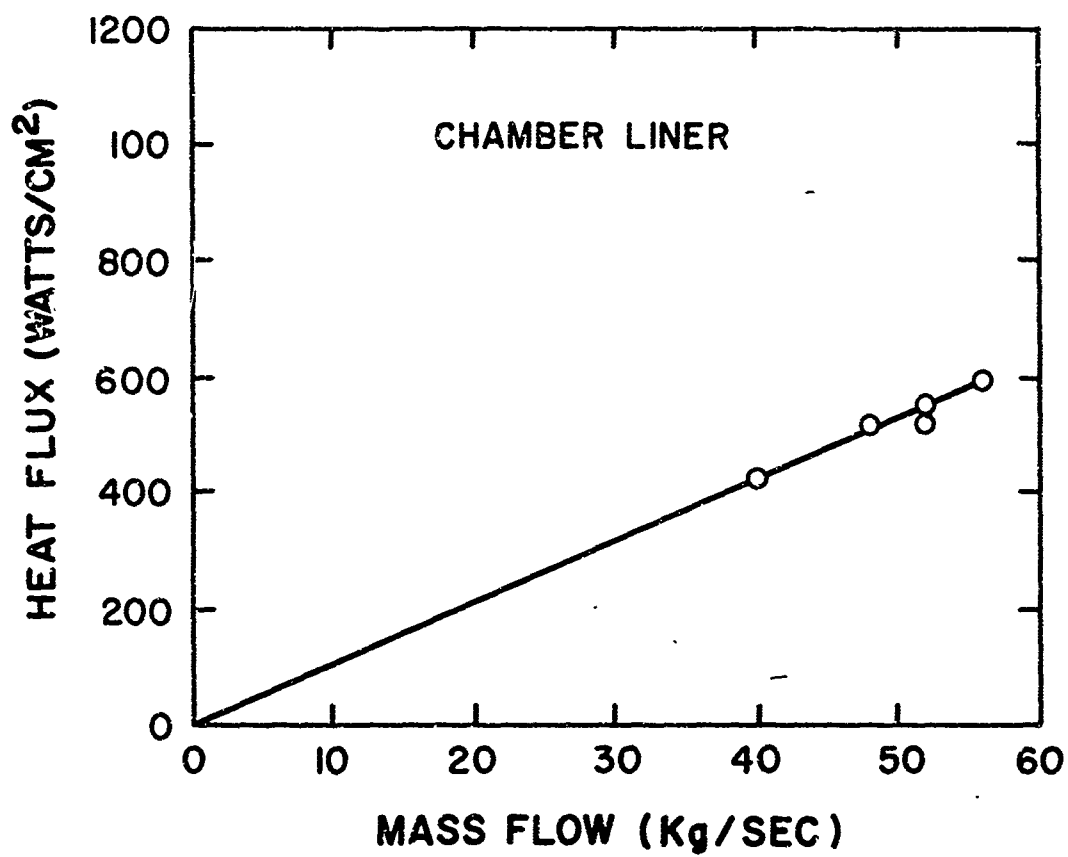


Fig. 17 Heat Flux Inputs for Chamber Liner

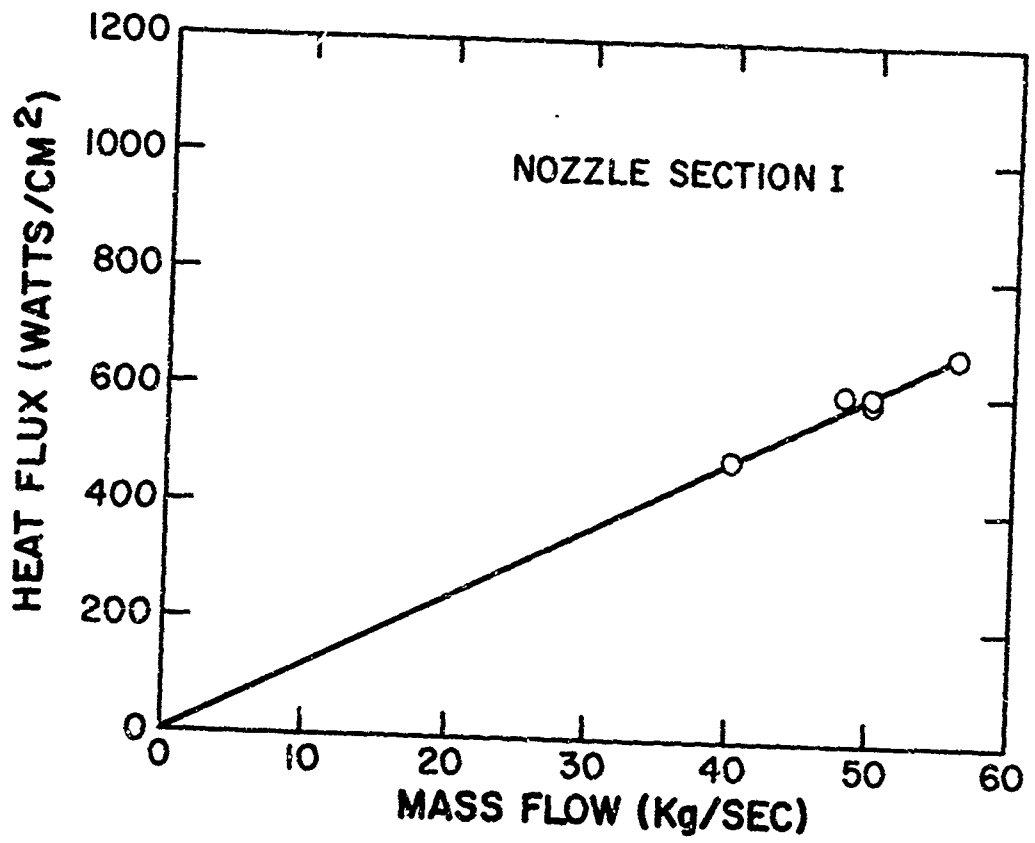


Fig. 18 Heat Flux Inputs for Nozzle Section I

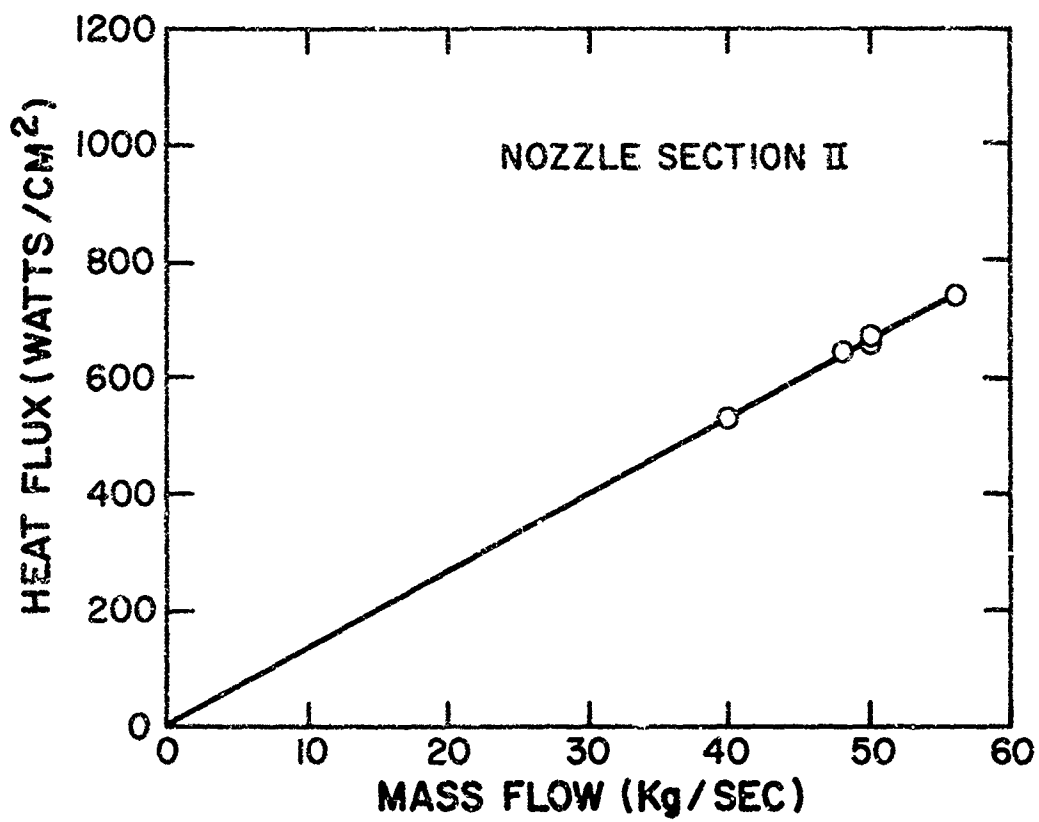


Fig. 19 Heat Flux Inputs for Nozzle Section II

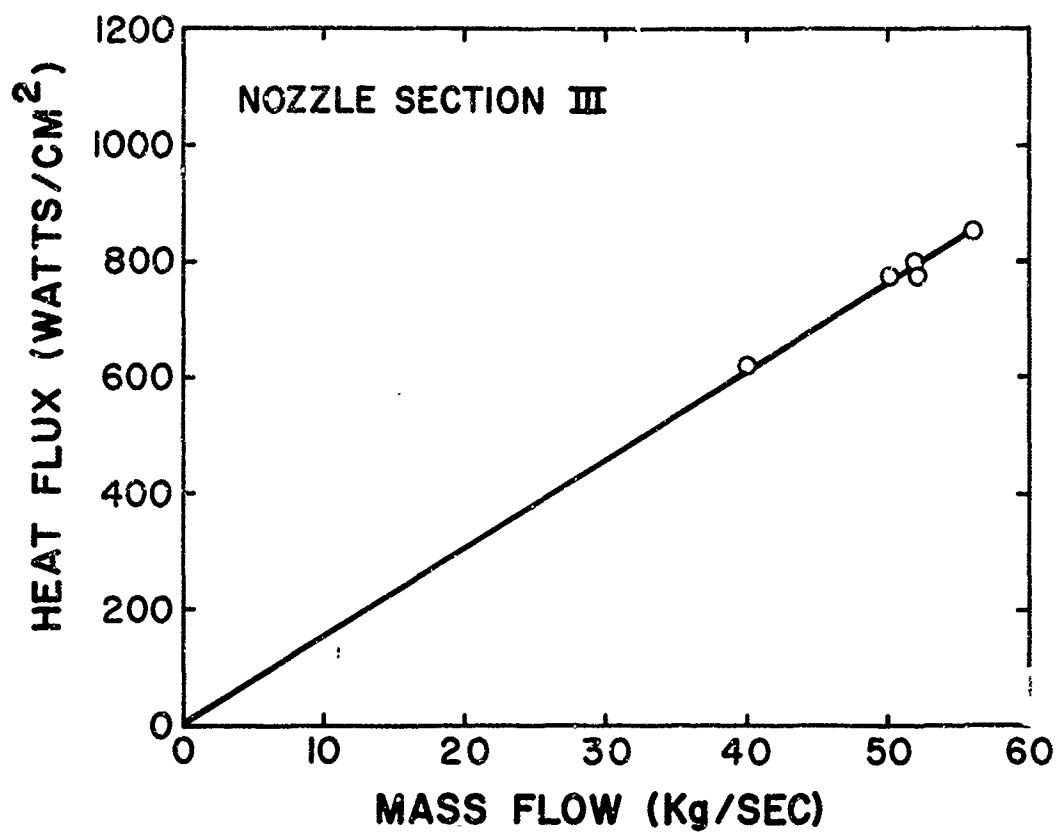


Fig. 20 Heat Flux Inputs for Nozzle Section III

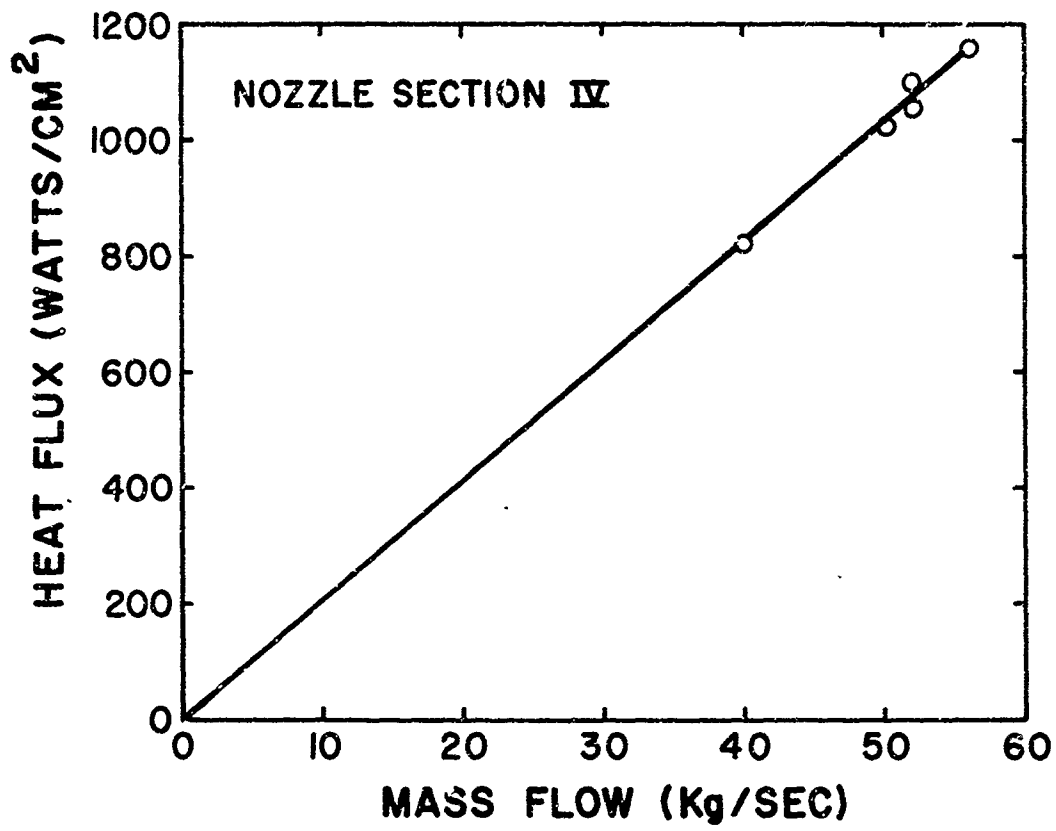


Fig. 21 Heat Flux Inputs for Nozzle Section IV

## C. MAGNET

### 1. Magnet Design

The magnet used in the subject contract is the same as that used throughout the Mark V generator program, designed under Contract No. AF 33(657)-8380.

The specifications of the magnet are as follows:

Field strength	35,000 gauss inlet; 30,000 gauss outlet
Width of openings	0.81 meter inlet; 1.16 meter outlet
Active length	3.18 meter
Overall length	4.52 meter
Power requirement	16-20 Mw
Current	22,000 amps
Resistance	0.0318 ohms
Inductance	0.27 henries
Weight of copper	61,000 Kg
Number of turns	316
Conductor material	ETP copper
Conductor dimensions	0.00368 x 0.496 meter
Insulation	Mylar
Type of cooling	Heat sink

Figure 22 is a photograph of the copper portion of the magnet, while Figure 23 shows the completely assembled magnet once the reinforcing structure had been added.

The high values of field strength and current in the generator magnet produce large forces on the conductors. The magnitude of these forces at any point is equal to the factor product  $j \times B$ . These forces are far too large to be contained by the mechanical strength of the conductors, and therefore the reinforcement system is necessary. The magnet may be

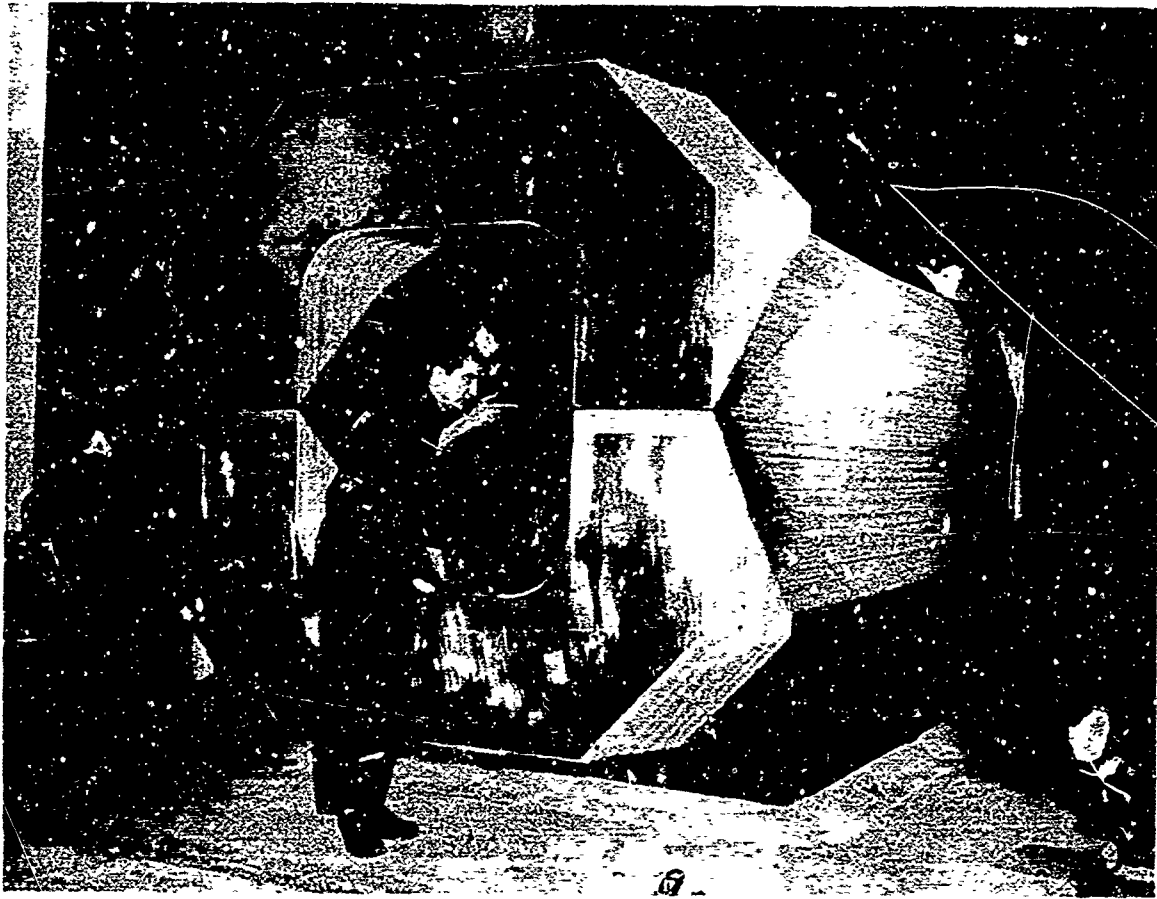


Fig. 22 A Photograph Showing the Copper Portion of the Magnet



Fig. 23 A Photograph Showing the Magnet Completely Assembled

envisioned as a pressure vessel with an internal pressure of 61 atm. The total of all forces absorbed by the reinforcing system is of the order of  $4.5 \times 10^6 K_p$ .

The reinforcement system was designed to be built quickly and cheaply with little regard for space or weight. Accordingly, standard structural shapes were used as much as possible. The primary reinforcement consists of 0.6-meter I-beams arranged in pairs along the sides of the magnet and connected by tie rods. Support for the ends is provided by rectangular I-beam structures joined by longitudinal tie rods. To prevent buckling of the plates under compressive loading, a top structure is provided which clamps the stack of conductors to the magnet base. A cross section of the magnet including a cross section of the new channel at the exit is shown in Figure 24.

The copper conductors must, of course, be insulated from the reinforcing structure and on flat surfaces this was done with sheets of polyester-fiberglass material. Along the sides of the magnet the surfaces were too irregular to permit the use of sheet insulation. On the sides a small space was left between the conductors and the steel beams. This space was filled with an epoxy potting mixture. The inside of the magnet was coated with a similar epoxy mixture but thickened with a flow control agent to a putty-like consistency. The inside coating is intended to prevent accidental short circuiting of the power connections to the channel and to provide some short-term protection for the magnet in the event of a bad hot gas leak in the channel wall.

## 2. Magnet Modifications

As can be seen from the above specifications, this magnet was designed to operate at a maximum voltage of 820 (V) and a current of 22,000 amperes; giving a maximum field strength of 3.55 Webers/square meter. In this program the maximum steady state magnet operating voltage was to be 1610 (V) and a current of 20,000 amperes, giving a maximum field strength of 3.3 Webers/square meter. Figure 25 shows the center-line field strength and location of the channel power section within the field. During impulse operation the voltage across the magnet will vary depending on the time required to discharge an energy of  $10^7$  joules. For example, for a  $10^7$  joule discharge in 50 milliseconds, a maximum voltage of 10,000 (V) will be obtained. This large increase in magnet operating voltage, which would be experienced during pulse operation led to a study into the quality of the existing magnet insulation.

The insulating value of the 0.010-inch thick Mylar used between copper plates is 5000 (V) per mill at  $150^\circ\text{C}$ , which is more than sufficient to withstand the expected voltage. The remainder of the magnet insulation; that is, between the support structure and the magnet, as well as between the supporting members themselves and ground, was insufficient

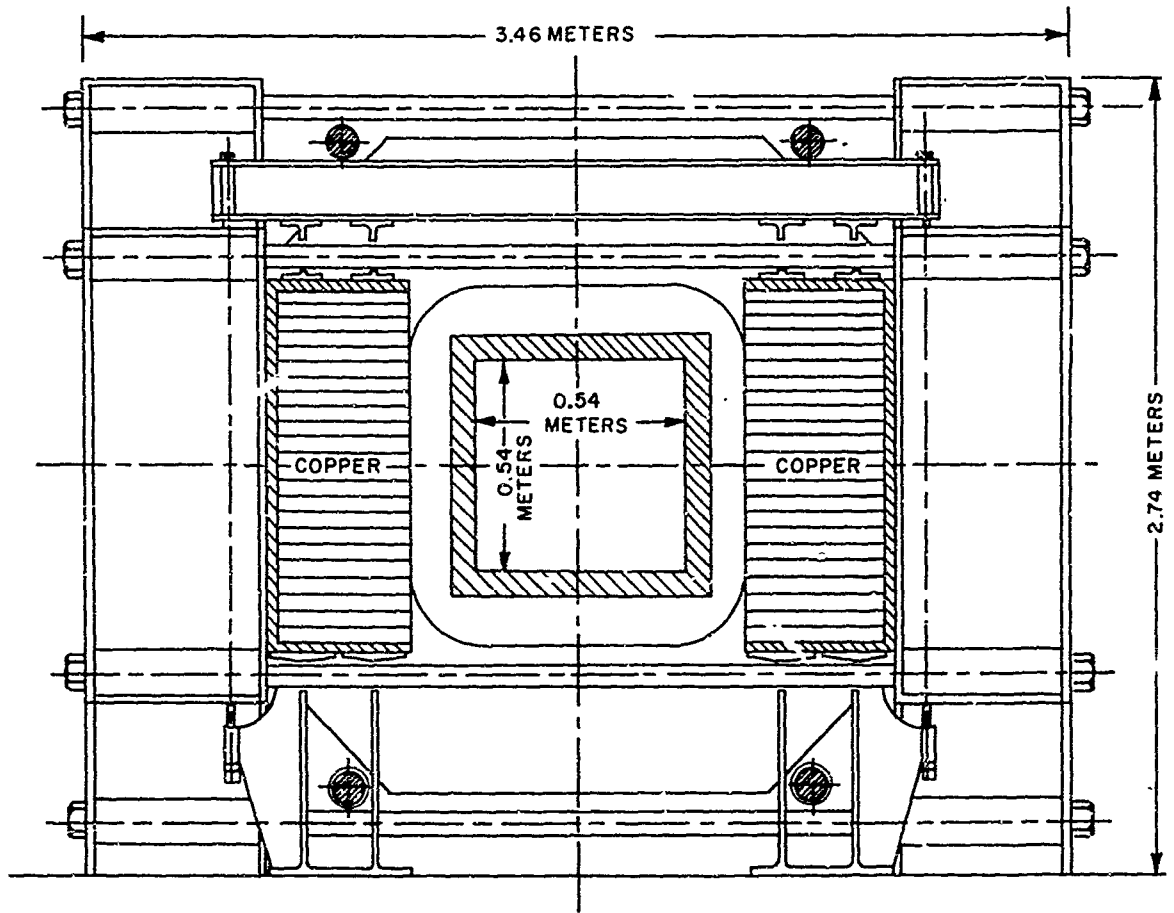


Fig. 24 Cross Section of Copper Magnet and Reinforcement Structure in the Mark V Generator

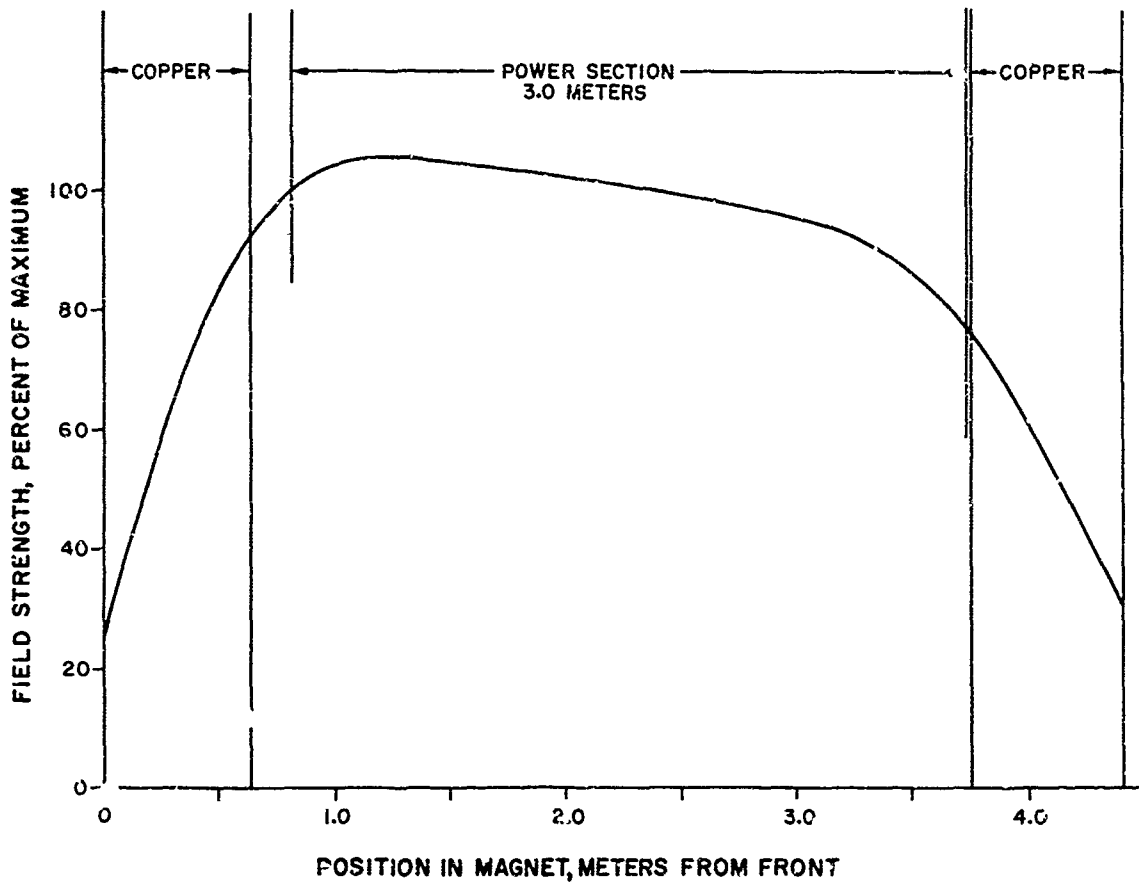


Fig. 25 Longitudinal Centerline Field Strength, Mark V Generator Magnet, Showing Power Section Location

for impulse operation. The experience of the previous Mark V generator program, when arcs occurred throughout the structural system to ground, indicated that the existing insulation would not be sufficient to meet the conditions described above.

The steps taken to locate the areas where additional insulation was required were the following: The magnet assembly drawing was studied to determine components requiring insulation that are not visible by a physical examination of the magnet itself. The magnet was inspected visually. The integrity of the copper insulation was tested using a D. C. power supply and measuring the voltage drop between loops.

The visual inspection of the magnet showed that the epoxy which separates the copper from the structural beams contained fissures in the region between beams. These fissures existed under some of the support steel, leaving only a short air gap between copper and steel. Although the voltage between turns was relatively low (32 volts for a pulse delivered at a maximum voltage of 10,000 V), the presence of these fissures introduced the possibility of shorting out a significant number of turns using the reinforcement steel as a short circuit member. For this reason, it was decided to remove the structural side supports, open the fissures to allow repairing of epoxy, and to place a solid sheet of phenolic insulation, 1.27 centimeters thick, between the steel beam and the epoxy. The sheet of insulation thus serves as a backup against short circuits from the copper to steel in the event fissures should appear in the epoxy during the pulse program. Figure 26 shows a schematic which is typical for the new insulation of the magnet.

The loops formed by tie rods and beams should be broken and insulated for two reasons. First of all, any portion of the structure which forms an electrical loop and which intercepts an appreciable amount of flux could be subjected to additional forces during magnet buildup or shutdown. To prevent such forces from developing, the structure was provided with insulation to break the loop. Secondly, by providing the insulation for each component of the support structure, the possibility of any short circuits occurring was greatly reduced. Maximum insulation was, therefore, provided to the structural members by completely insulating all tie rods, thus breaking the loops.

The center portion of the tie rods was wrapped with fiberglass and coated with epoxy to effect this insulation, while the region which passes through the tubes in the support beams was sleeved with solid insulating tubes. Beneath the nut and washer on the tie rod an insulating washer was placed and permanently bonded to the insulating tube. The gap between the solid tube and fibreglassed section of the tie rod was closed on assembly by adding fibreglassed epoxy. Since the tie rods pass through holes in the magnet base and top support structure, their movement is restricted and the alignment of the tie rods with the fixed tubing on the support beams was critical, especially with the addition of the insulating sleeve. To insure

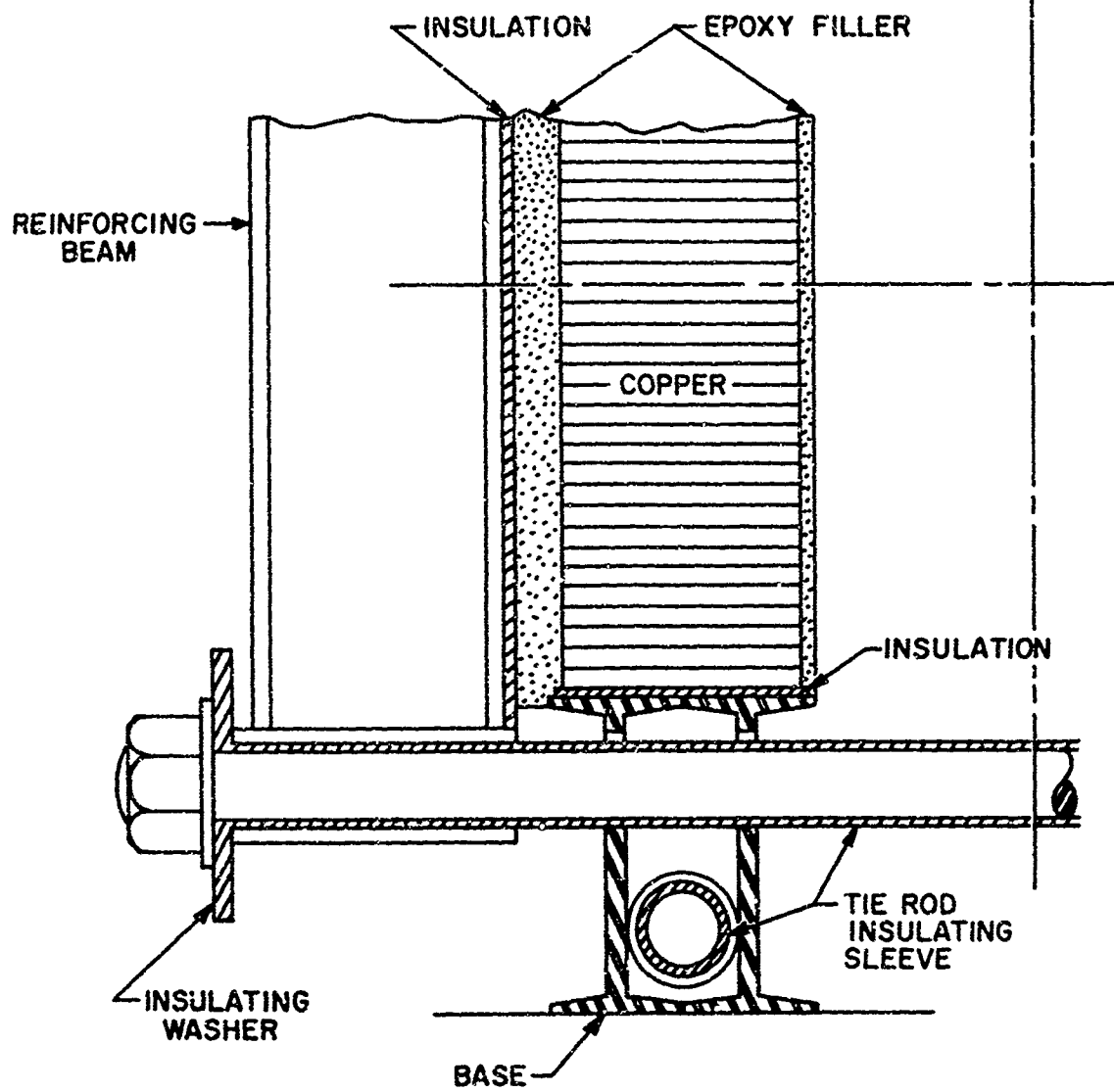


Fig. 26 Modified Magnet Insulation

proper alignment of the tie rods and beams, it was necessary to have the holes in the beams opened to a larger diameter.

During pulse operation, the maximum voltage developed is between the top and bottom copper plates of the magnet. The  $j \times B$  forces in the vertical direction are taken up by a top support structure which clamps the copper stack to the base through vertical tie rods. Any connection between the copper and the top support structure would therefore short circuit the magnet to ground through the base. To prevent this, the vertical tie rods were insulated in the manner previously described.

To provide adequate insulation between the magnet end supports and the copper, solid sheets of insulation were added. These sheets were extended to cover the entire copper surface which was not covered by the end support. The tie rods connecting the inlet and exit end supports were also fibreglassed and sleeved as previously described.

As a further protection between side supports, a sheet of mylar was added such that it is positioned under the beam and wrapped around it to the outside, so each beam is completely insulated from the other.

## D. CHANNEL

### 1. Channel Design

As a result of the design analysis and configuration study, the internal dimensions of the channel were determined, as well as the heat transfer rates, pressure distribution, and power output values necessary to design the channel.

The final channel length and cross section is as shown in Figure 27. The internal channel geometry is square from the nozzle to the exit with a nozzle throat area of 0.088 square meters. The length of the inlet section was selected so as to extend the channel to a location at which a physical connection between burner and channel could be accomplished. The power section starts at a point where the area is 0.117 square meters, with a field strength of 3.01 Webers/meter<sup>2</sup>, at a magnet current of 20,000 amperes. The length of the power section is 3.0 meters with the exit area being 0.292 square meters. The magnetic field strength at the exit is 2.47 Webers/meter<sup>2</sup>.

Figure 28 shows the predicted heat flux vs channel length for both the insulating and electrode walls. The total cooling water requirement was approximately 9090 liters/minute. The limiting design factor was not heat flux but electrical insulation which required fine segmentation in order to stand off the high voltages to which the channel would be subjected.

The first step taken in the design was to determine the general arrangement of the various channel components. In this step it was sought to apply the experience gained during the previous Mark V program. The previous Mark V channel was a segmented design which required several thousand cooling water connectors between individual pegs and electrodes. These cooling water connectors were located close to the gas surface, and a loss of refractory would expose the seal to the working fluid, resulting in damage to the water seals. Another problem was that of thermal stresses in copper bars located in the inlet and exit sections. The channel was not easily maintainable in that it was difficult to remove electrodes and repair damaged cooling water seals. It was also necessary to effect all repairs from the inside since the channel walls were not removable.

The new channel design did not require axial segmentation in the power section insulating walls, since the generator is single circuit, but it did require transverse segmentation. The power section electrode wall acts as a single electrode, and therefore no axial segmentation is required here. The inlet section electrode and insulating walls must, however, provide axial segmentation in order that the burner may be insulated from the power section.



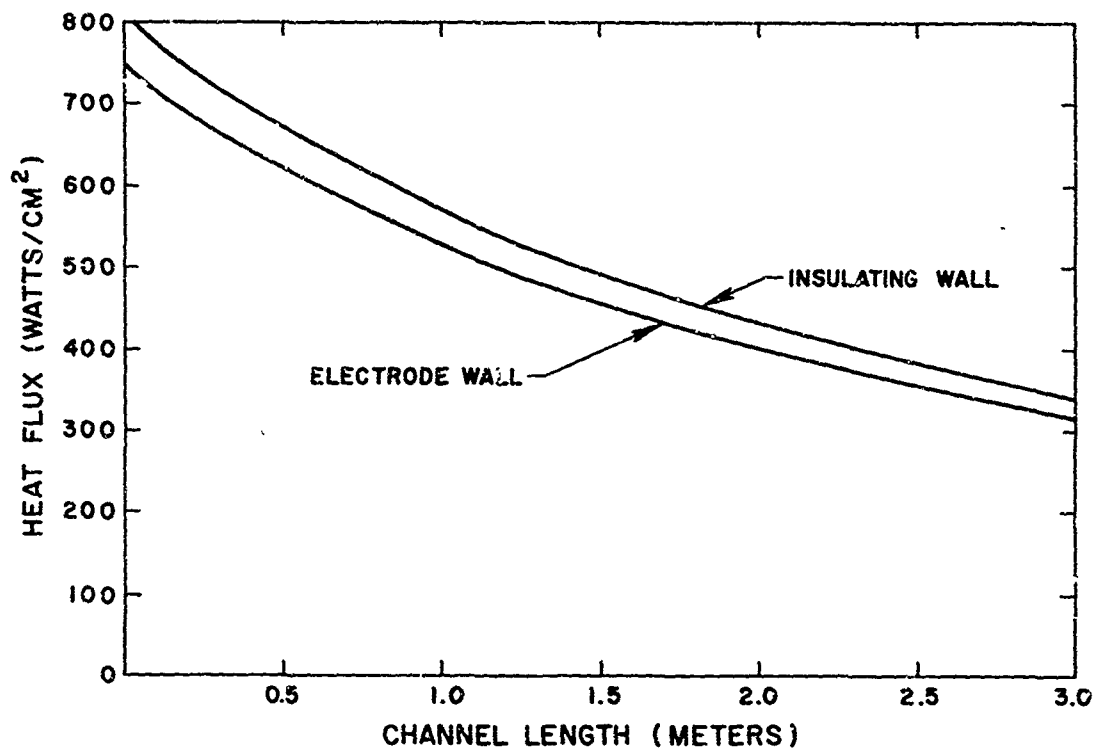


Fig. 28 Heat Flux vs Channel Length

The design conditions for this channel were, therefore, improved over the previous Mark V channel, since little axial segmentation was required. The overall design goal for this channel was to be simplicity; that is, the number of cooling water connectors was to be held to a minimum, the connectors were to be located as far away from the working fluid as possible, the size of components and temperature distribution was to be carefully controlled, no unnecessary joints or bends were to be allowed, all components designed with ease of maintenance considered, and finally, the size was such that at least one wall could be removed to allow access.

A description of the final design is presented below with emphasis on the most significant components. In the overall mechanical design, a considerable effort was placed on the arrangement of the cooling water passages required for the non-axially segmented electrode and insulating walls of the power section, and the segmentation required in the inlet and power section insulating walls. In the final design the entire inside surface of the channel in contact with the working fluid is fabricated from two basic copper extrusions, the cross sections of which are shown in Figure 29. The extrusion which is square in cross section is used to form the electrode walls in the working section of the channel. The sizing of these extrusions was based on the heat transfer requirements and allowable stresses, as well as on a cross section which could be physically extruded by the copper mill, still maintaining sufficient area for cooling water flow, and providing electrical insulating capability for the insulating walls.

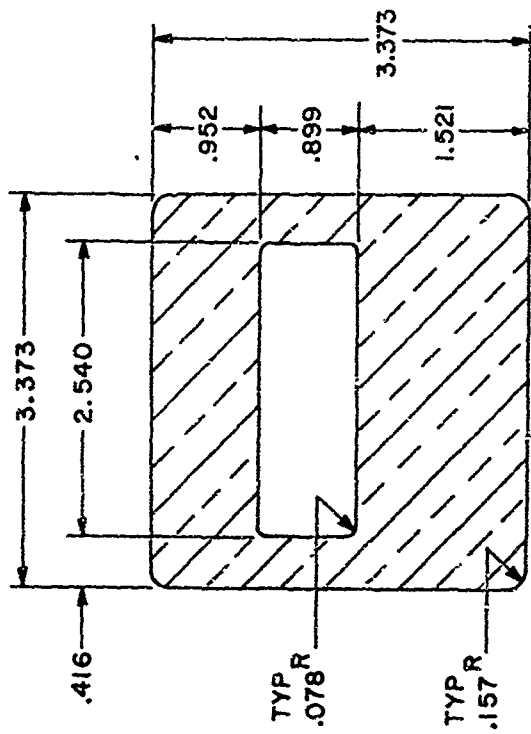
#### a. Electrode Walls

The side walls of the channel are the electrode walls. A sketch of the electrode configuration may be seen in Figure 27. As can be seen in the figure, the inlet section consists of 16 square extrusions and 38 narrow extrusions arranged normal to the flow direction, with an insulating gap of 0.159 centimeters between each bar. The bars are mounted onto an insulating plate made of glass-epoxy laminate which forms the outside wall.

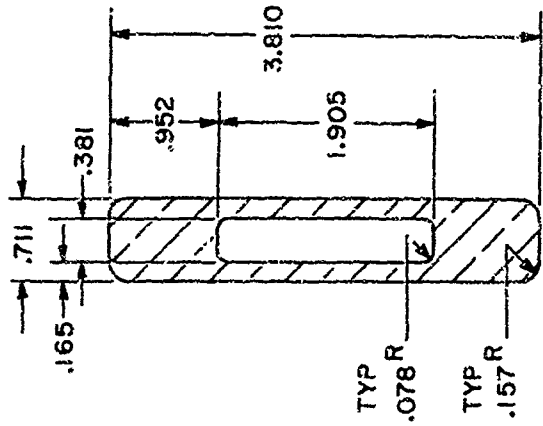
The electrodes in the power section consist of square extruded bars, arranged axial to the flow direction, for the remaining length of the channel. These extrusions are mounted onto a solid slab of stainless steel which connects all the bars electrically, thus forming a single electrode slab.

In order to keep the bars straight and of constant cross section while still maintaining the divergence of the channel, two bars are added to each side of the main group as indicated in Figure 27.

The electrode design consists of the water cooled copper bar with grooves to contain the electrode material which was stabilized zirconia. The grooves are perpendicular to the gas flow and their dimensions are



SQUARE EXTRUSION



RECTANGULAR EXTRUSION

NOTE  
(1) ALL DIM. IN CENTIMETERS

Fig. 29 Cross Sections of the Copper Extrusions

varied to maintain a more nearly constant electrode surface temperature throughout the channel.

The cooling water requirement for each electrode wall is 2085 liters/minute with a pressure drop of approximately 6.8 atmospheres.

#### b. Insulating Walls

The top and bottom walls of the channel are the insulating walls. The design of the insulating walls is similar in principle to that of the electrode walls. As indicated in Figure 27 the inlet section consists of the square extruded bars arranged exactly as in the electrode walls. The rectangular bars in the insulating section are normal to the gas flow and continuously decreasing in length to match up with a similar rectangular bar which has an axial orientation and is continuous from the point of intersection to the channel exit. To provide the necessary insulation, there is a 0.159 centimeter gap filled with aluminum oxide refractory material between each of these bars.

The axial bars in the power section are straight and of constant cross section which requires eleven additional bars on each side of the main group of 38 bars to accommodate the divergence of the channel. The copper bars are mounted on a plate made of glass-epoxy laminate, which forms the outside wall. The cooling water requirement for each insulating wall is 2155 liters/minute, with a pressure drop of approximately 12.25 atmospheres.

#### c. Cooling Water Passage Design

To provide cooling water to each of the extruded copper bars within the channel, a system of common manifolds was designed. These manifolds are an integral portion of the inlet walls on which the copper bars are mounted.

To conduct the cooling water from the manifold to the copper bars, a sealing arrangement was designed for each of the two basic extrusions.

Figure 30 shows a typical sealing arrangement used for the square extrusion. As can be seen in the figure, the copper bar is independently fastened to the channel wall and has a water passage located on the back surface of the bar. This arrangement makes it possible to insert the water seals from the outside without disturbing the bar on the inside of the channel. The "O" ring seal is inserted from the outside together with a retaining ring. The retaining ring thus controls the "O" ring squeeze and

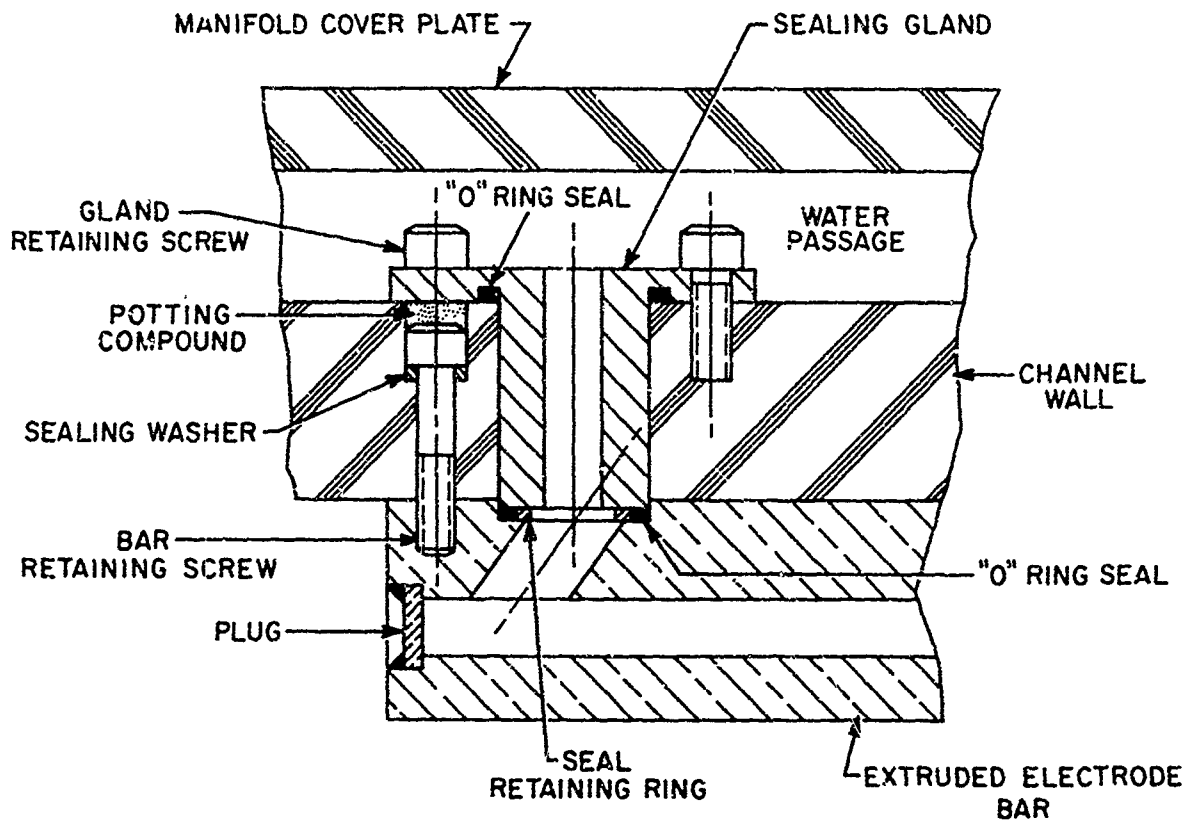


Fig. 30 Water Seal Assembly, Square Bars

prevents movement of the "O" ring. The gland is then installed and is sealed by another "O" ring when it seats in the cooling water manifold. The gland is held in place as indicated by retaining screws.

Figure 31 shows a typical sealing arrangement used for the rectangular extrusion. As can be seen in the figure, the copper bar is independently fastened to the channel wall and has a water passage located on the back surface of the bar. For these narrow bars, however, it was necessary to silver solder a tube into the water inlet of each bar. The solder joint thus provides the water seal at that point. When mounted in position, the water tube projects to the channel wall which is machined so that a tapered seal and seal retaining screw may be inserted from the outside.

The seals described are typical of those used for both inlet and outlet of all bars. For each wall a common inlet manifold located in the channel inlet wall feeds the inlet bars. After leaving these bars, the water flows through a manifold to feed the bars for the power section, from where it is discharged into the exhaust system of the generator.

To provide cooling water to the bars which are added in the power section, an external manifold system is used with each tube connected to the manifold by a non-conductive hose.

The use of the cooling water seal designs presents no problems in the short bars of the inlet section where there is little movement due to thermal expansion. The long bars in the power section, however, required special attention in order to control the thermal expansion, and the effect of this expansion on the cooling water seals. For this reason, the end of these bars in which the water seal is located has been locked in position by the insertion of a dowel pin in the proximity of the water seal. The remainder of the bar is then allowed to expand towards the exit end of the channel.

The screws required to keep the bars straight and flat against the wall have been designed so as to move with the bars.

Another important consideration was the design of the cooling water entrance into the bars. It is imperative that the cooling water reach the very beginning of the bar. This became a problem in the entrance to some of the narrower bars where it was impossible to physically place the inlet tube at the very beginning of the bar. To insure proper cooling in these bars a special insert was designed and brazed into the bar to divert the cooling water to the desired location.

#### d. General

The channel is mounted on an integral chassis assembly. This chassis assembly is designed to match up with rails that are located

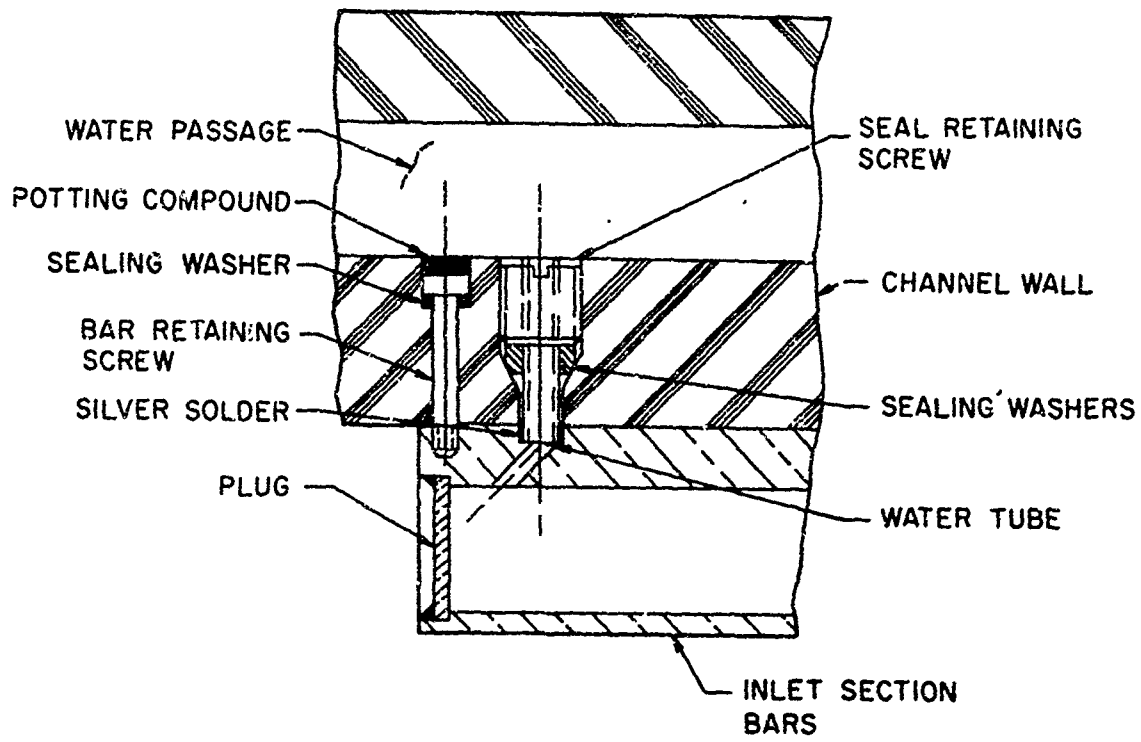


Fig. 31 Water Seal Assembly, Rectangular Bars

within the generator field coil. Thus, the channel may be easily removed for maintenance purposes.

The electrical connection from the channel to the magnet is achieved through a series of copper bus bars mounted to the channel electrodes by aluminum power tap lugs. The bus bars are then shorted together to a single bar. The final connection between magnet and channel was tailored to fit when the fully assembled channel was inserted into the magnet, and lined up with the burner nozzle flange and exhaust system.

## 2. Channel Assembly

The design of the channel is such that each of the four walls must be assembled as a single unit. For this reason, it was unimportant which wall was assembled first. In the final assembly, to join the four walls and form the channel, it is first necessary to mount the bottom insulating wall to the integral chassis, and place this unit on the channel rollout stand. The channel inlet flange was mounted onto the burner flange with the burner located in the operating position, the bottom wall assembly was then rolled into the magnet, and the rails were adjusted to insure proper alignment of the completed channel with the burner nozzle.

After installing the other three walls, the prefabricated channel bus bars and cooling water piping were mounted, and the channel was reinserted into the magnet to tailor the connection of the electrical bus bars to the magnet and cooling water inlet manifolds to the water system piping.

Figures 32 and 33 are photographs showing both surfaces of a completely assembled electrode wall. Figure 34 shows a completely assembled insulating wall.

Figure 32 shows the copper bars assembled onto the wall plates. The inlet of the channel is to the left of the photograph, and is comprised of 16 square bars and 38 narrow bars arranged normal to the flow direction, with an insulating gap of 0.159 centimeters between each bar. These insulating gaps were filled with aluminum oxide refractory material before final assembly. The remainder of the wall is the power section electrodes arranged axial to the flow direction and mounted onto the stainless steel slab. The grooves, which can be seen in the electrodes, are to retain the electrode material.

Figure 33 shows the exterior of the electrode wall, and the integral cooling water manifolds and seals previously described. The cooling water enters the groove on the top of the inlet wall and water passes through the glands and tubes into the copper bars. The water passes downward to the exit of the bars, out the lower glands and tubes into the common lower manifold. The water then flows horizontally to the left and into the entrance glands of the electrodes. The water cools the electrodes from which it is

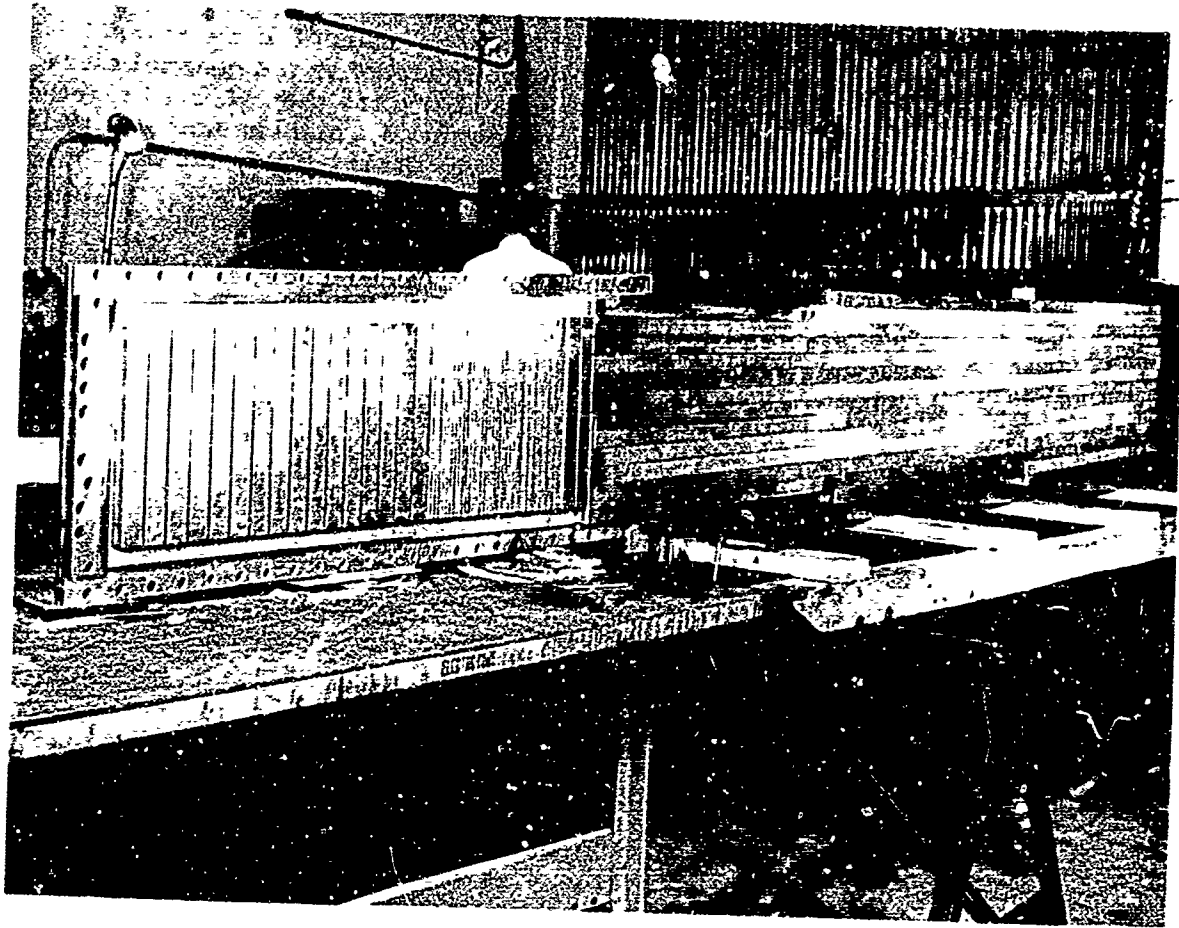


Fig. 32 Hot Gas Side of a Completely Assembled Channel Electrode Wall

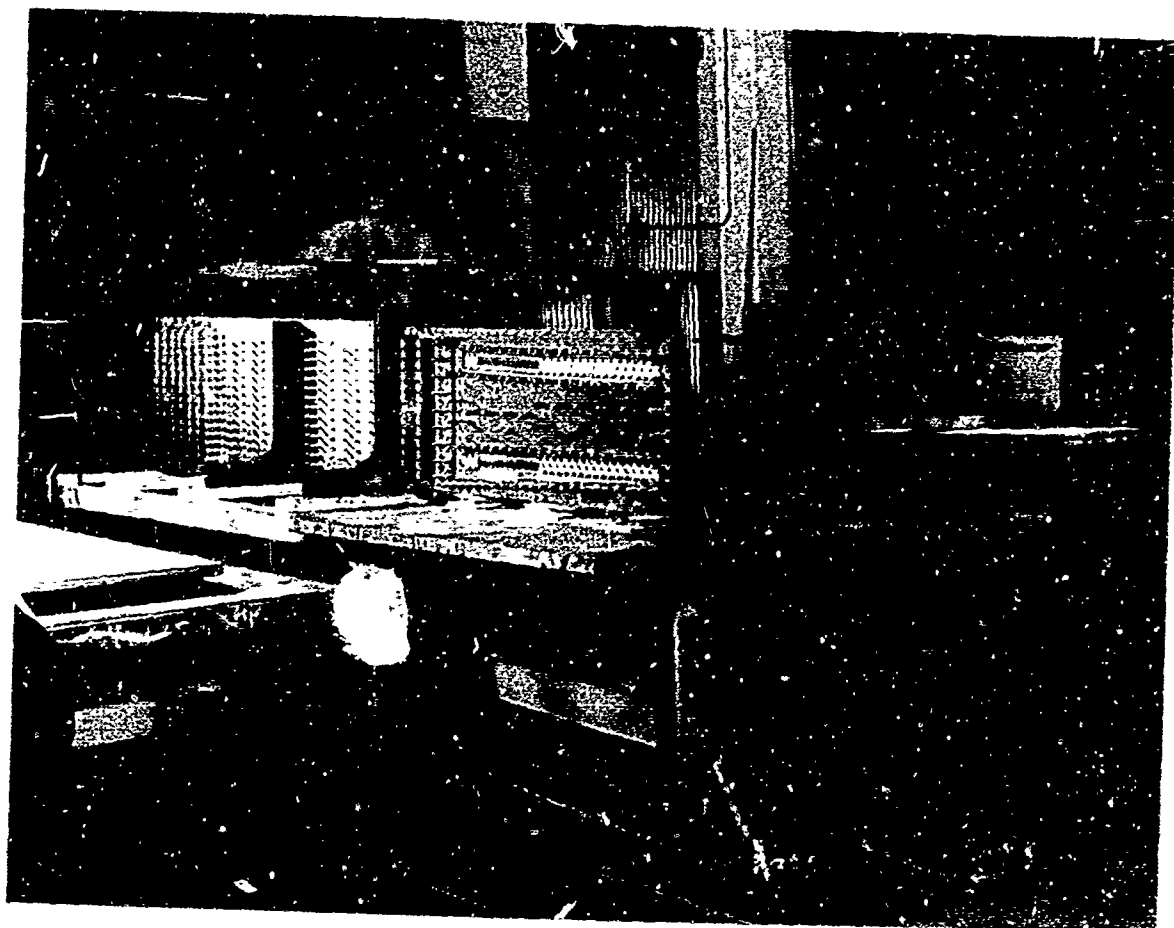


Fig. 33 Outside of a Completely Assembled Channel Electrode Wall

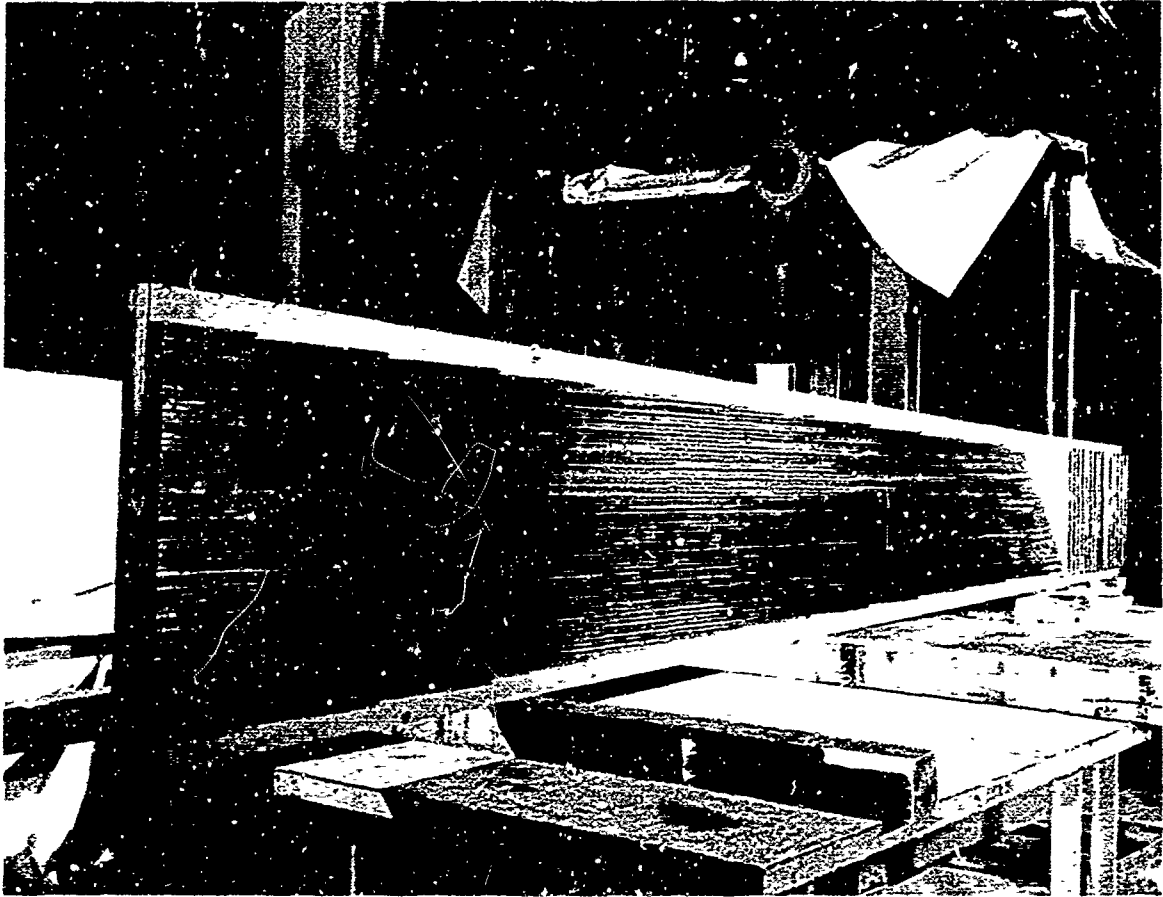


Fig. 34 Photograph of a Completely Assembled Chan. l Insulating Wall

discharged directly into the working fluid at the channel exit. The studs protruding from the inlet section are used to retain the water manifold closure plate, while the studs in the power section are to mount the electrical bus bars. The channel rollout stand can be seen directly behind this wall assembly, and in the background is a partially assembled insulating wall.

Figure 35 is a photograph of the completely assembled channel mounted on the rollout stand. When this photograph was taken the channel was undergoing a static gas pressure check; hence, the plates mounted to each end.

### 3. Channel Extension Section

To duct the working fluid from the channel exit through the end of the magnet and into the generator exhaust system required the fabrication of a channel extension.

The section is fabricated of an electrically non-conductive material (transite), and is film cooled by the water discharged from the exit of the channel. A gas seal is affixed at the channel end by sealing bars which overlap the joint between channel and extension, and on the diffuser end by a gasketed flange which mates up to the diffuser.

Figure 36 is a photograph of the extension section mounted onto the generator exhaust system.

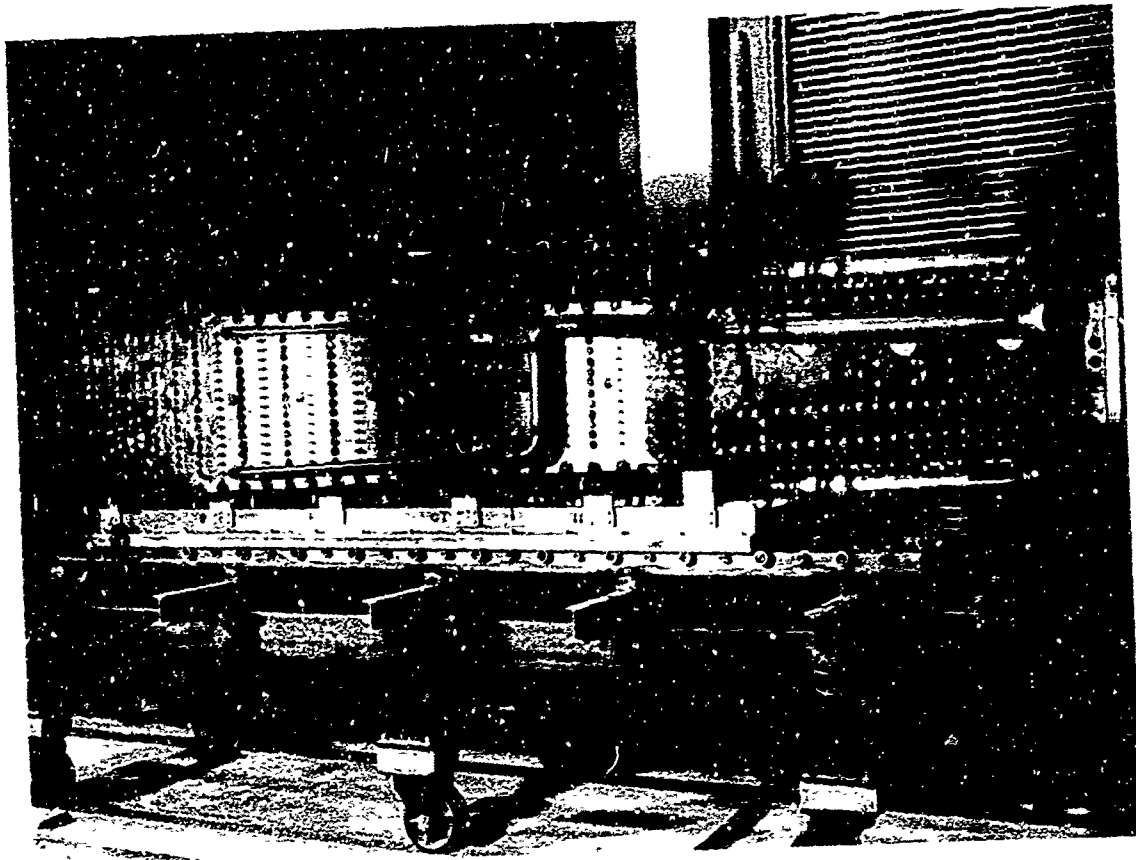


Fig. 35 Photograph of the Completely Assembled Channel

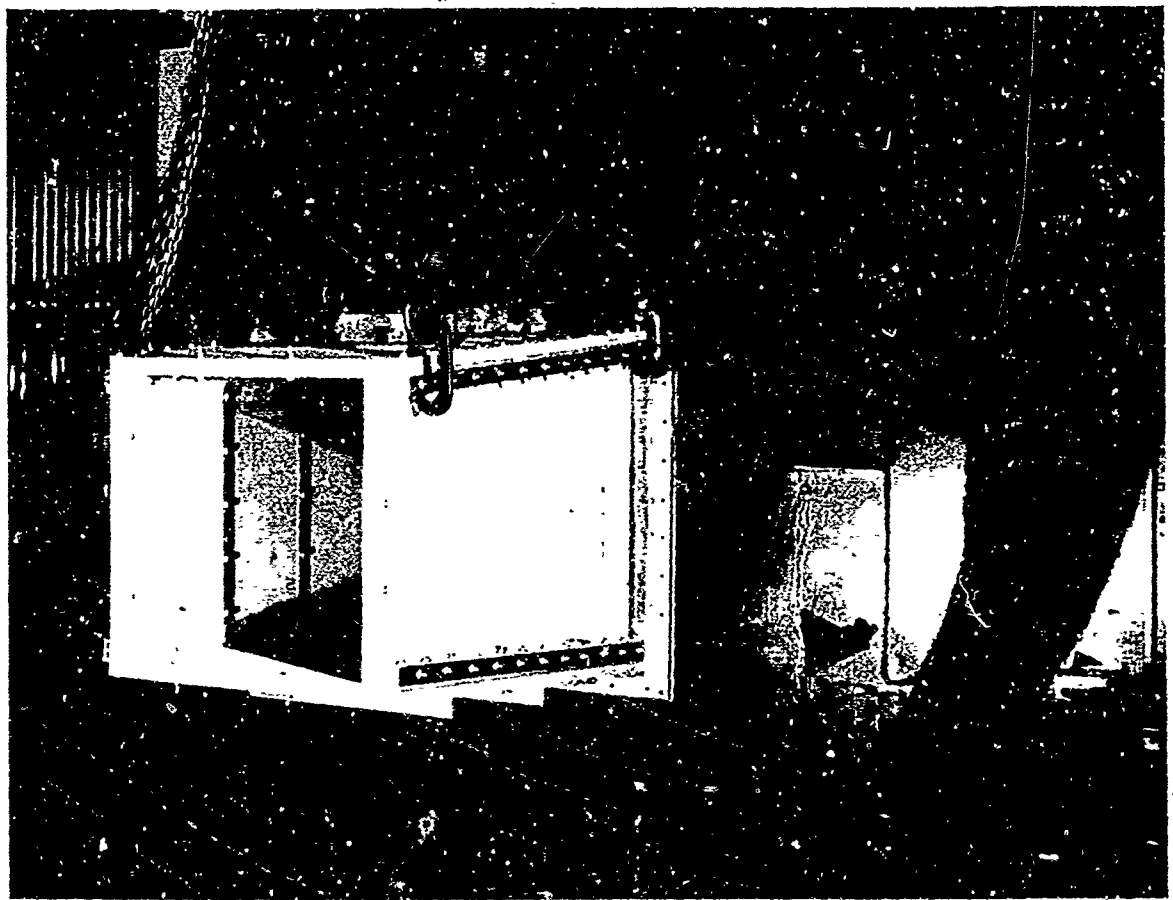


Fig. 36 Photograph of Channel Extension Section Mounted on the Exhaust System

## E. AUXILIARY SYSTEMS

### 1. General Arrangement

The generator itself consists of three essential items: burner, magnet and channel. These require the use of auxiliary systems to provide the necessary cooling water, fuels, and generator controls. The general arrangement of the equipment and systems may be seen in Figure 37.

The final design of these components is based on the parameters resulting from the design analysis and an intimate knowledge of the generator component requirements. These systems are designed to be as simple as possible and are fabricated from off-the-shelf items whenever practical.

### 2. Burner Systems and Controls

Each auxiliary system basically consists of a storage and a control system. Bulk storage facilities for oxygen, fuel and water are located outside of and away from the test cell.

A suitable control system, consisting of regulating and shut-off valves, is employed to control the flow of each system and to permit orderly starting and stopping of combustion. A nitrogen system is utilized for the purpose of purging the burner and channel of combustibles, immediately before and after operation of the burner.

The design of the control system has been performed with certain basic principles in mind: the fuel and oxygen flow to the main burner must be accurately measured, since any variation in the total mass flow or fuel oxidizer ratio has an important effect on generator performance. The shut-off valves which control the flows to the burner must be located as close to the burner as possible, so as to minimize the volumes to be purged. These valves are operated from the control room.

The starting and stopping sequence used in all burners is based on AERL's experience with similar burners. The general description of the design and arrangement of each individual system and its control is as follows:

#### a. Cooling Water System

The water to be used for cooling purposes is stored in a 150,000-gallon concrete tank, and is pumped into the test cell at a maximum

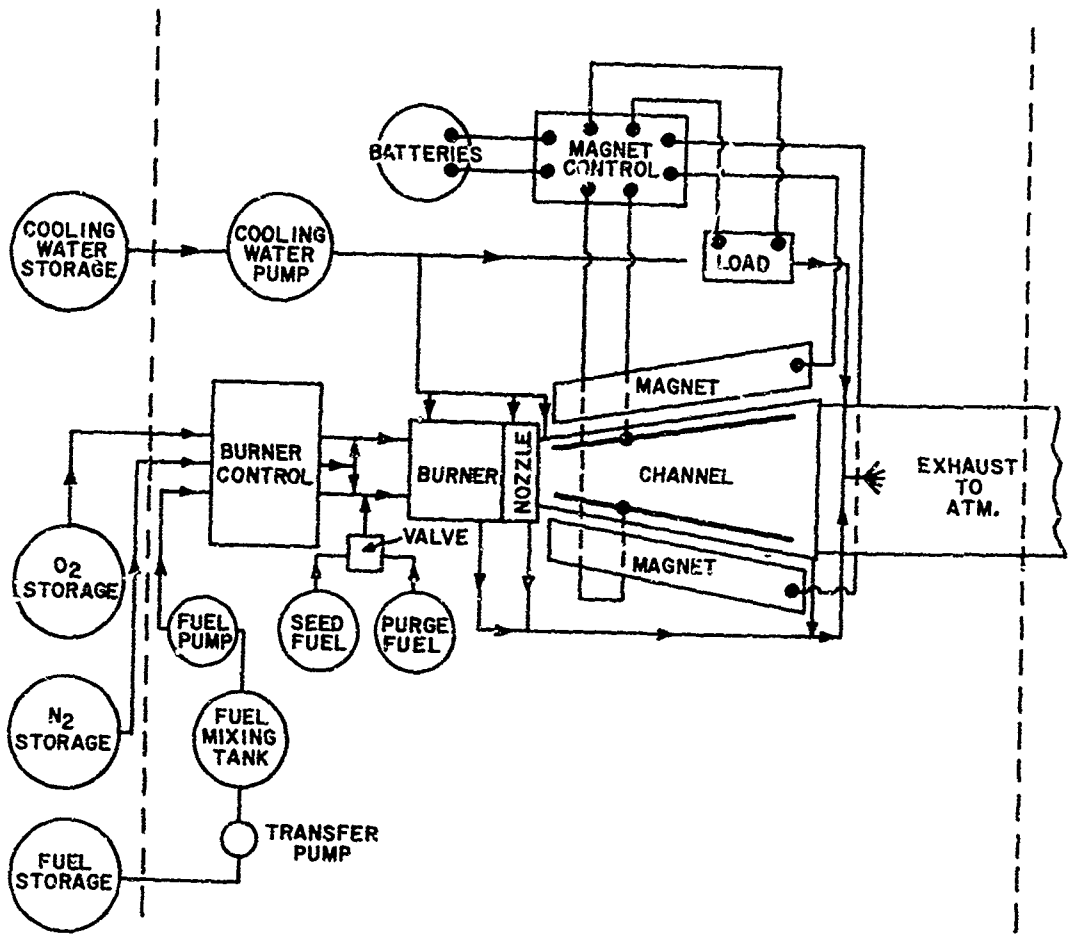


Fig. 37 General Arrangement of Equipment and Systems for the Mark V Pulse Generator

rate of 10,000 gpm with a pump discharge pressure of 250 psig. A schematic of the cooling water system may be seen in Figure 38. The flow is divided; 5000 gpm for the stainless steel tubes used as load resistors, 1500 gpm for the burner and nozzle, and 2500 gpm for the channel. All cooling water is discharged into the exhaust duct where some is converted to steam and goes off into the atmosphere and the rest drains out of the duct to a drain basin outside the building.

#### b. Oxygen System

During burner operation, oxygen from the outdoor storage enters the building as indicated in the Oxygen System Schematic shown in Figure 39. Oxygen for the main burner is throttled by valve 1 to about 100 to 400 psi, depending on required mass flow. The flow rate is measured by the venturi, 4, and the valve, 1, is regulated from the control room to maintain the desired flow. A nitrogen purge connection, valve 3, permits purging the oxygen line, burner, and generator channel. Oxygen for the pilot and igniter flows through a branch line and manual shut-off valves 2 and 5 to a regulator, 6, which reduces the pressure to 500 psi. From the regulator, oxygen flows through the manual back-up valves, 7 and 9, through the solenoid valves, 8 and 10, to the igniter and pilot burners.

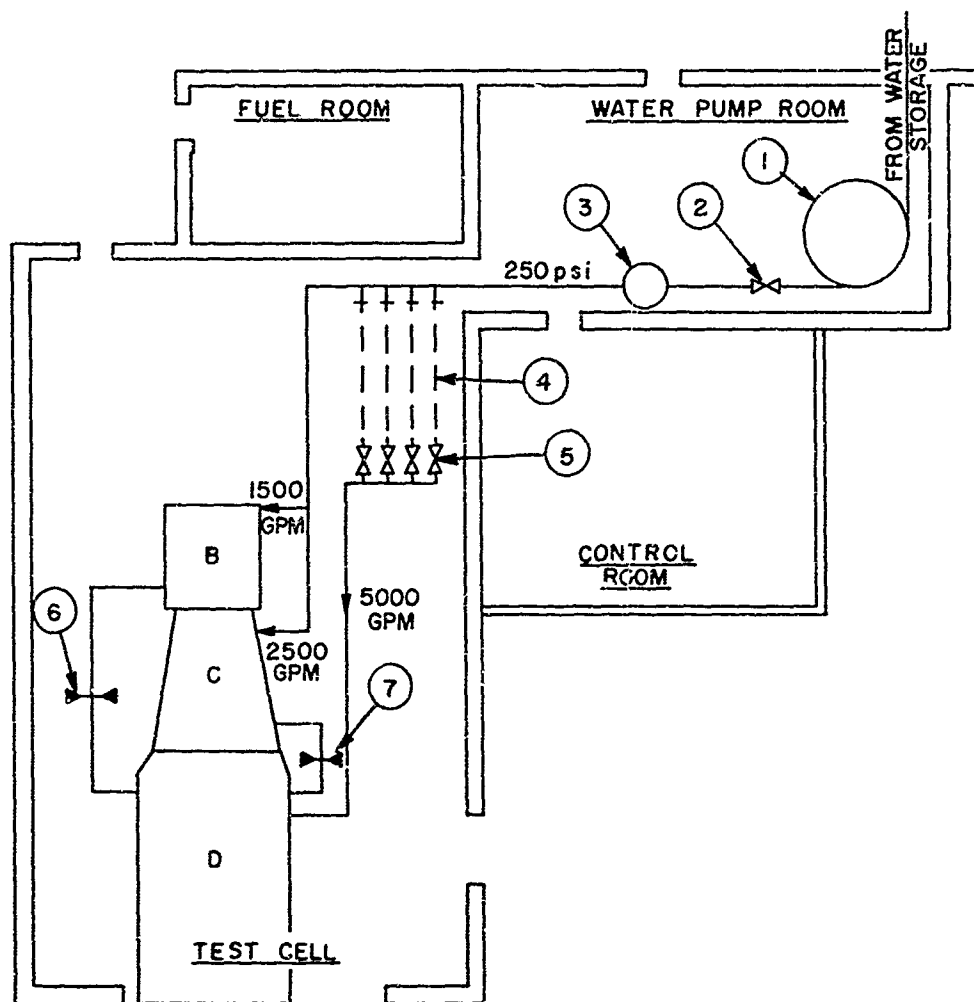
#### c. Nitrogen System

Nitrogen from the outdoor storage enters the building as shown in Figure 40 (a schematic of the nitrogen system), and flows through a main shut-off valve, 11, then to the main burner, through valves 12 and 13. Valve 12 is a throttle for regulating nitrogen flow. Valve 13 is a fast acting remote control valve which works simultaneously with a similar valve in the fuel line to switch from "purge" to "fuel" or vice versa. Nitrogen for purging fuel injectors of the igniter and pilot burners flows through valve 14 and regulator 15 to solenoid valves 17 and 19 at the burners. Valves 16 and 18 are manual back-up valves to be used in the event that a solenoid valve fails to operate. Valve 3 connects to the main oxygen line for purging of the main burner oxygen injectors.

#### d. Fuel System

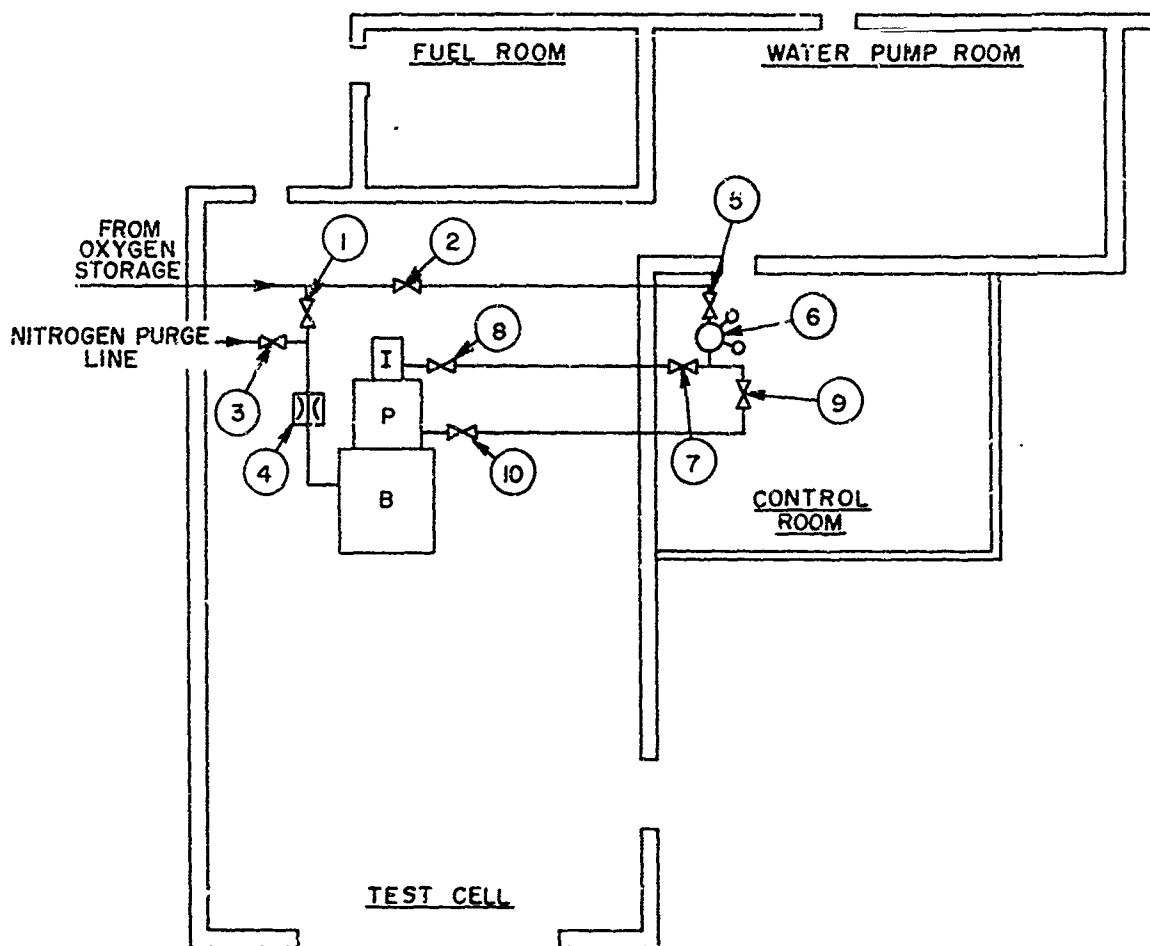
The original fuel system piping was altered due to the relocation of the main burner, and a new fuel system was added to permit a rapid and sharp cutoff of the seed flow which is required for pulse operation.

The seed material (KOH) is dissolved in methyl alcohol and injected to the main combustion chamber with a separate feed for each of



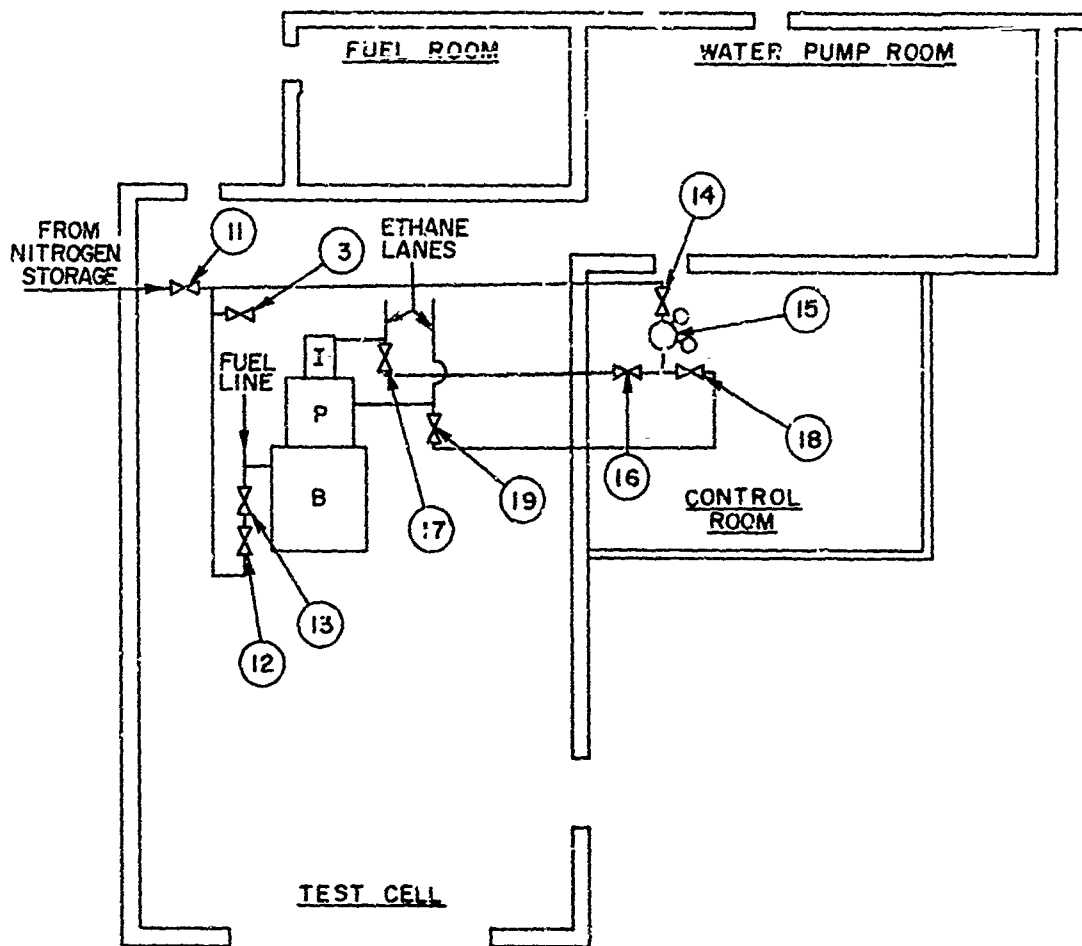
- B = Burner
- C = Channel
- D = Exhaust Duct
- 1 Cooling water pump
- 2 Main cooling water shut-off valve
- 3 Strainer
- 4 Load resistors
- 5 Control valves for load resistor cooling water
- 6 Burner cooling water restriction orifices
- 7 Channel cooling water restriction orifices

Fig. 38 Cooling Water System Schematic



- I = Igniter Burner  
P = Pilot Burner  
B = Main Burner
- 1 Main oxygen control valve and shut-off (remote controlled)
  - 2 Auxiliary oxygen shut-off valve
  - 3 Nitrogen purge valve for oxygen line, burner, channel, and exhaust stack (manual control)
  - 4 Oxygen venturi
  - 5 Main oxygen shut-off for igniter and pilot burners (manual control)
  - 6 Oxygen regulator for pilot and igniter burners
  - 7 Oxygen shut-off valve for igniter burner (manual control)
  - 8 Oxygen valve for igniter burner (remote controlled)
  - 9 Oxygen shut-off valve for pilot burner (manual control)
  - 10 Oxygen valve for pilot burner (remote controlled)

Fig. 39 Oxygen System Schematic



- I = Igniter Burner
- P = Pilot Burner
- B = Main Burner
- 3 Nitrogen purge valve for oxygen line, burner, channel, and exhaust stack (manual control)
- 11 Main nitrogen shut-off valve (manual control)
- 12 Nitrogen throttle valve for main fuel system purge (manual control)
- 13 Nitrogen purge valve for main fuel system (remote controlled)
- 14 Nitrogen purge shut-off valve for igniter and pilot burners (manual control)
- 15 Nitrogen regulator for igniter and pilot burners
- 16 Nitrogen shut-off valve for igniter burner (manual control)
- 17 Nitrogen purge valve for igniter burner (remote controlled)
- 18 Nitrogen shut-off valve for pilot burner (manual control)
- 19 Nitrogen purge valve for pilot burner (remote controlled)

Fig. 40 Nitrogen System Schematic

the 60 fuel injectors placed in the burner backplate. This injection system is shown in Figure 41. The flow of methyl alcohol (depending on the seed amount required) represented approximately 30% of the total fuel flow to the burner, and the remaining 70% of the main fuel flow was JP-4 or equivalent and is injected to the combustion chamber using the old fuel system as shown in Figure 42.

A three-way remote control valve, 7, is used to direct fuel flow either to the calibrating loop or the burner. The calibrating loop contains an orifice, 8, with hydraulic impedance equivalent to the burner fuel injectors. The sequence for starting the burner is to start the main fuel pump, 5, with the valve open to the calibrating loop, then adjust the bypass valve, 9, to produce the desired flow as indicated by the venturi, 6, and then divert the fuel flow by means of the three-way valve, 7, from the calibrating loop to the burner.

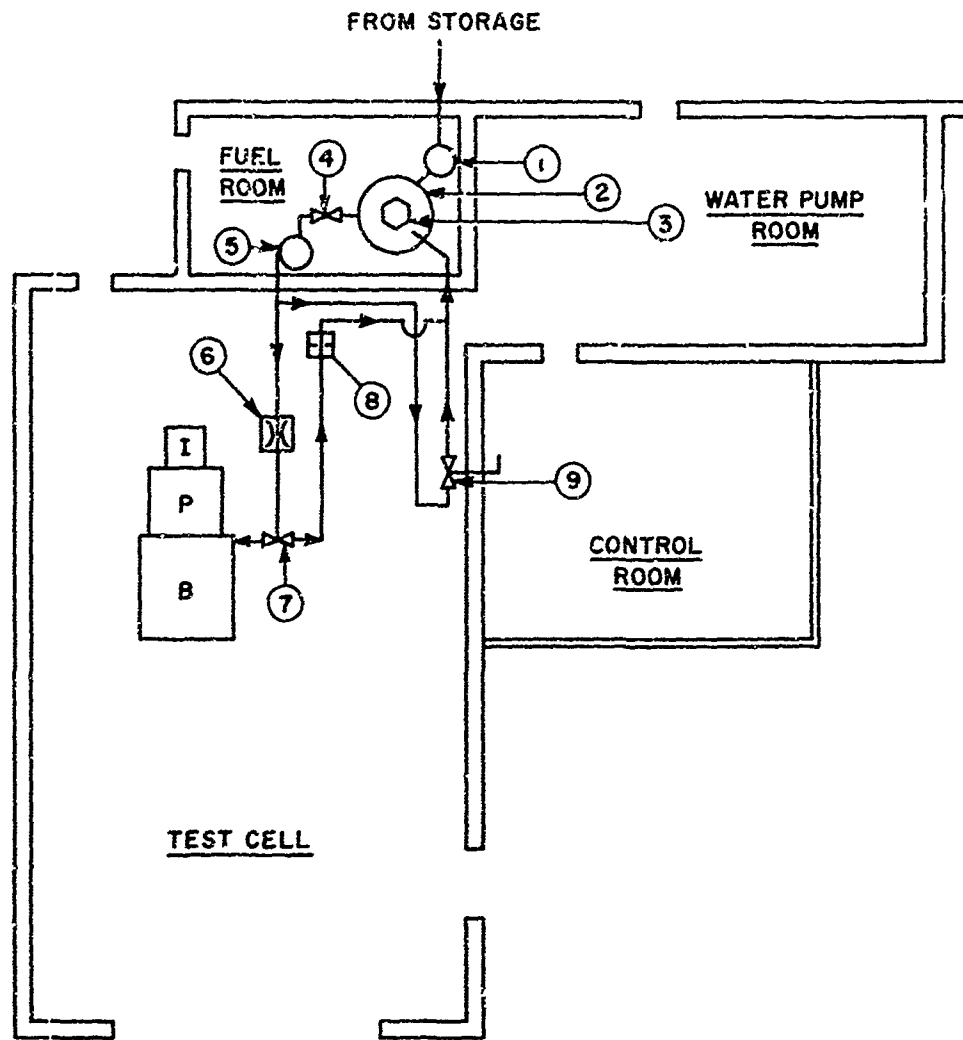
A schematic of the secondary main burner fuel system is shown in Figure 43. Due to the limited operating time required, pressurized fuel systems were incorporated rather than pumps. The fuels were stored in mixing tanks, then transferred to pressure tanks prior to testing. A photograph of the completed storage and pressure system for pulse operation is shown in Figure 44. These tanks are pressurized by individual nitrogen regulators connected to the main nitrogen storage supply. The larger tank in the photograph is the mixing and storage tank while the thin cylindrical tank is the pressure vessel. Initially, fuel is stored in the larger tank, and a measured amount of seed added to one of the tanks to give the desired gas conductivity. The seeded fuel is then pumped into the pressure vessel tank by means of the small transfer pump shown under the storage tank and pressurized. The other fuel system is identical to the first with the exception of no seed being in the fuel. The flow rate of the regulators is set equal to the fuel flow rate, thereby eliminating the possibility of pressure surges. Control of the various fuel flows is ascertained by monitoring a venturi regulated with a throttling valve.

The need for two separate auxiliary fuel networks was brought about by the generator pulse mode of operation which necessitated reducing the gas conductivity to approximately zero in the interval of several milliseconds. However, since the seeded fuel is approximately 30% of the total fuel flow, combustion cannot be maintained without having a replacement or a purge fuel, so a secondary system is required.

#### e. Seed Control

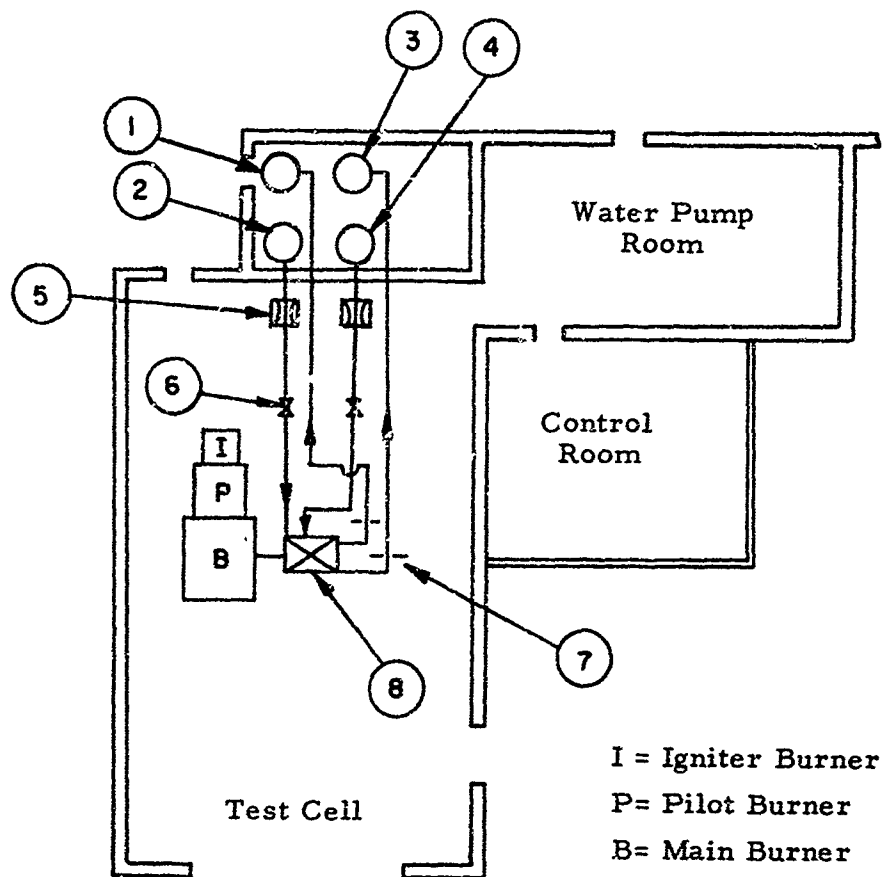
A specially designed, quick acting three-way fuel valve was used to change the flow from seeded fuel to purge fuel flow. Figure 45 shows the operating principle for the fast acting valve. Initially, seeded fuel is flowing from the right to the 60 circumferentially placed feeds. When the





- 1 Transfer Pump
- 2 Fuel Tank
- 3 Mixer
- 4 Main Fuel Shut-off Valve (manual control)
- 5 Fuel Pump
- 6 Fuel Venturi
- 7 Three-Way Fuel Valve (remote control)
- 8 Restriction Orifice
- 9 Fuel By-Pass Valve (manual control)

Fig. 42 Main Fuel System Schematic



1. Seeded fuel storage and return tank
2. Seeded fuel pressure tank
3. Purge fuel storage and return tank
4. Purge fuel pressure tank
5. Venturi (seeded and purge system)
6. Throttling valve (seeded and purge system)
7. Orifice
8. Flow control valve

Fig. 43 Secondary Fuel System Schematic

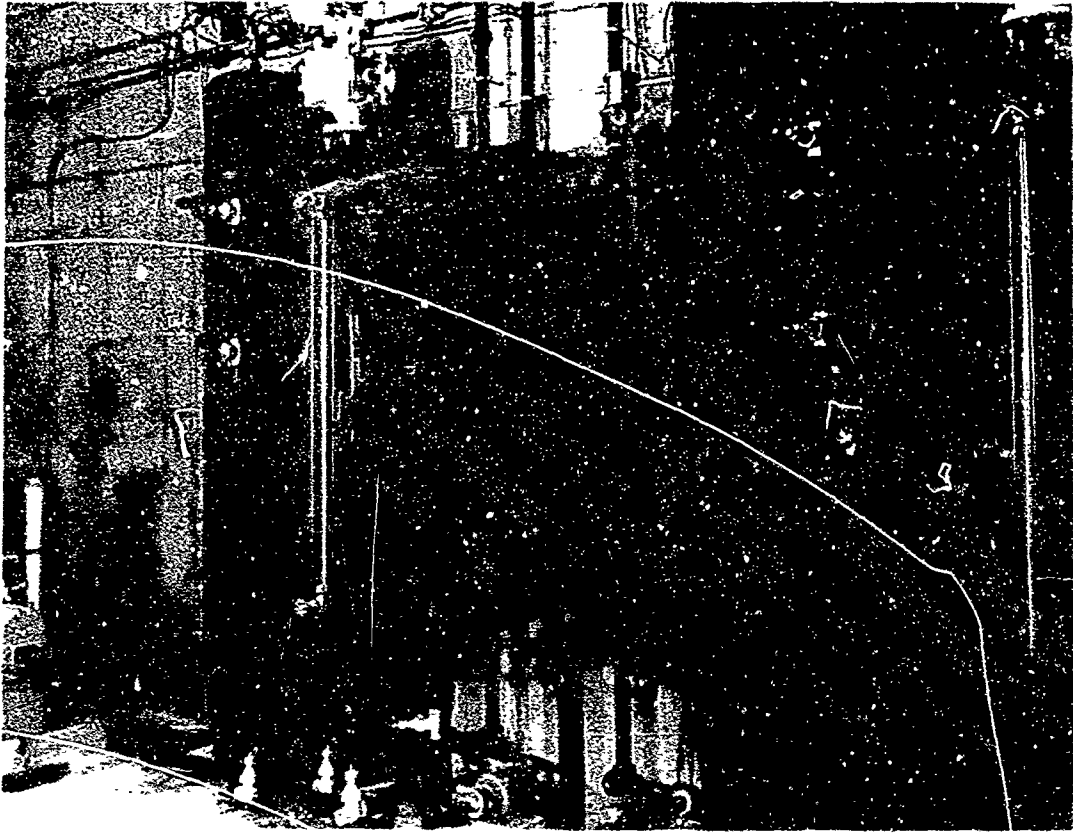
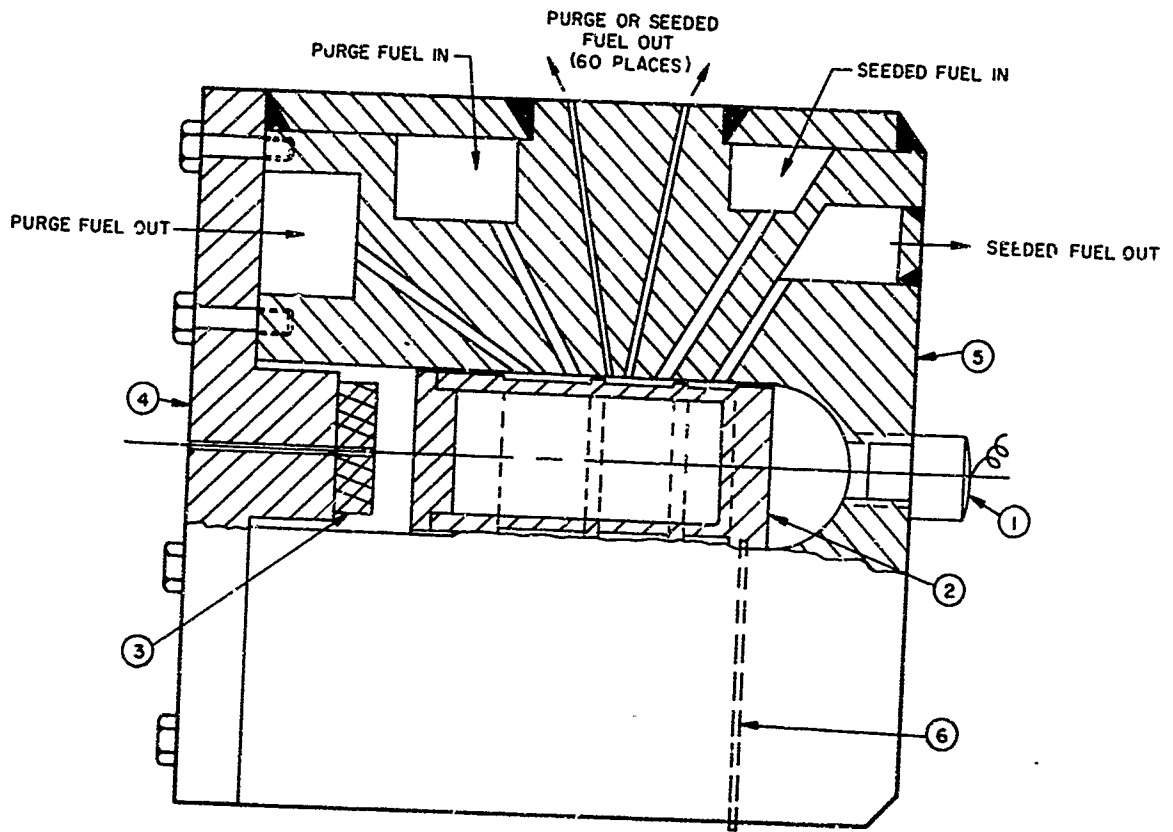


Fig. 44 Auxiliary Fuel Storages



- 1. Electrically operated explosive charge
- 2. Valve piston
- 3. Lead insert
- 4. Cover plate
- 5. Valve body
- 6. Shear pin

Fig. 45 Fast Acting Valve Schematic

pulse mode of operation is desired, an explosive charge is fired, giving a pressure of approximately 2200 psi in the chamber. This pressure causes failure of the shear pin positioning the valve piston, and the resultant piston movement substitutes purge fuel for seeded fuel. The operating time of this valve is of the order of 2 milliseconds, depending upon the size of the explosive charge. The energy of the piston is absorbed by the deformation of a lead plug at the end of the cylinder.

An exploded view of the fast acting, three-way valve used for pulse operation is shown in Figure 46. From left to right are the plate with a lead insert to absorb the energy of the piston, valve sleeve, valve body with the 60 individual fuel feeds, valve piston, valve sleeve and shear pin assembly, cover plate with explosive charge.

#### f. Pilot Burner

The fuel selected for use in the igniter and pilot burners is gaseous methane which is stored in bottles. A schematic of the fuel system to the igniter and pilot burners is shown in Figure 47. Methane flows from the pressure regulator to solenoid valves 29 and 31 which operate in conjunction with nitrogen purge valves 17 and 19 to permit switching from "purge" to "fuel" or vice versa. Valves 28 and 30 are manual back-up valves in the control room to be used in the event of solenoid valve failure.

The igniter and pilot burner control systems are of an automatic design in respect to sequencing and safety interlocks. The electrical circuit is designed to shut off the igniter combustion in six seconds and to shut off the pilot burner fuel and oxygen valves if the pilot burner does not ignite within this time period. However, if the pilot burner is properly ignited, it will keep operating, and, due to its interlock with the main burner control, permit starting the main burner. Safety interlocks are provided as follows: the main burner shuts off if the pilot burner goes out or if the magnet current becomes excessive. Both pilot and main burners are shut down if the discharge pressure of the cooling water pump drops to a minimum allowable value.

In addition, pressure switches in the various burner cooling circuits cause the burner to shut off if the pressure in any individual circuit becomes too low. An interconnection to the magnet battery circuit turns off the batteries in the event they are still connected when the burner is shut off.

### 3. Electrical Controls

The general electrical circuitry is similar to that described in the Final Technical Report for Contract Number AF 33(657)-8380, April

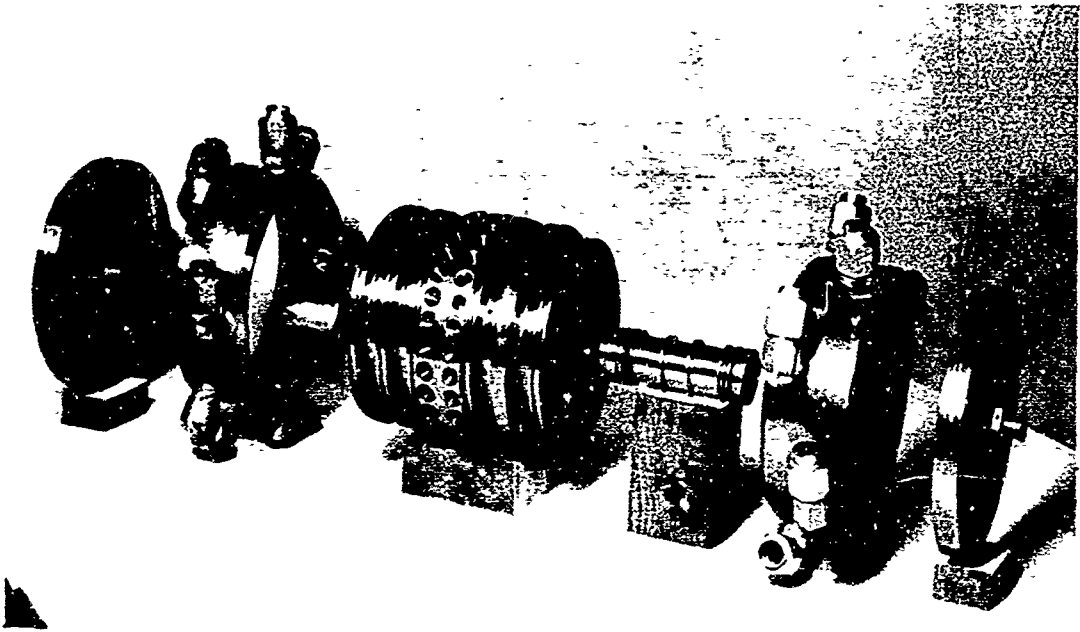
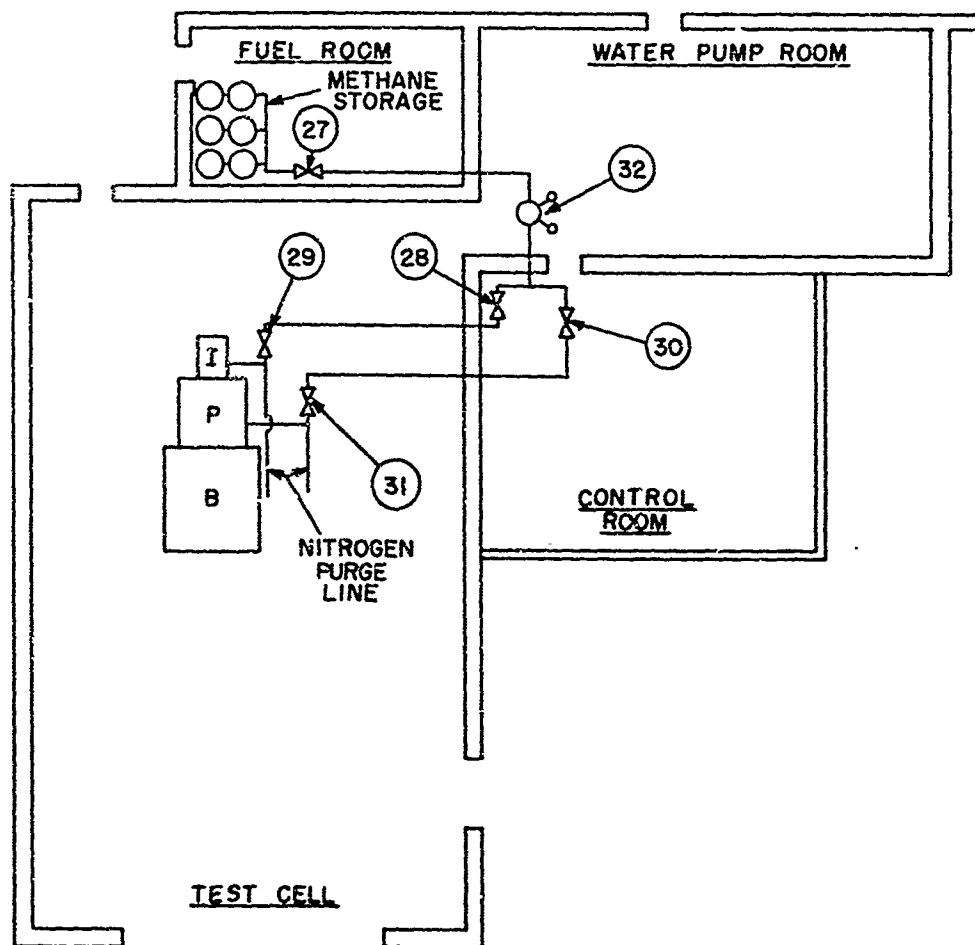


Fig. 46 Exploded View of Fast Acting Valve



- I = Igniter Burner
- P = Pilot Burner
- B = Main Burner
- 27 Main methane shut-off valve (manual control)
- 28 Methane shut-off valve for igniter burner (manual control)
- 29 Methane valve for igniter burner (remote controlled)
- 30 Methane shut-off valve for pilot burner (manual control)
- 31 Methane valve for pilot burner (remote controlled)
- 32 Methane regulator

Fig. 47 Fuel System Schematic of Igniter and Pilot Burners

1964, with the following exceptions: an additional sensing unit to detect reverse current to the battery bank; addition of two amplifiers to operate a fast acting valve and serve as an overexcitation device; a double pole switch capable of making and breaking at high currents and voltages; a modified rectifier bank to handle the higher anticipated voltages; and an adjustable electronic timer to delay the closing of the fuel servo valves and pulse load switch until the pulse is completed. Figure 48 shows a schematic of the pulse generator circuitry.

#### a. Magnet Control

The magnet control used in this program is basically that used in the previous Mark V program. Initial excitation of the magnet is provided by a battery bank which consists of 180 storage batteries. The battery bank, when fully connected, is capable of producing 1.1 Mw for a period of 45 seconds. The batteries are arranged in six parallel strings of 30 batteries in series. This array has an open circuit voltage of 360 volts and a current flow of 6000 amps at matched impedance. In addition, 10 or 20 batteries from each string may be disconnected, reducing the open circuit voltage to 240 or 120 volts, respectively. Power from the batteries to the magnet is controlled by a circuit breaker which is normally actuated from the generator control room. During normal startups, the breaker is opened by a signal from a low current detector when the generator output voltage exceeds the battery open circuit voltage. The magnet shorting loop, which protects the magnet from excessive voltage during shutdown, originally contained 88 silicon rectifiers, arranged such that there were 44 parallel circuits of two rectifiers in series, to provide a peak inverse voltage rating of 1200 volts. Parallel bleed resistors and series resistors provide for proper distribution of voltage and current, respectively, between the 88 rectifiers.

Since the pulse generator design has a higher output voltage than the original Mark V generator, expansion of the rectifier system to the peak reverse voltage rating of 2400 volts was required. The rectifier system was thus doubled in size. A photograph of the new rectifier bank is shown in Figure 49.

As an added safety to the magnet control circuitry, due to the higher generator voltage, a reverse current sensor was added to prevent damage to the battery bank as well as switches in each leg on the main feeds between the main battery breaker and the magnet. The operation of these switches is such that they close when the main battery breaker closes, completing the battery magnet circuit and open after the battery breaker opens.

One of the major modifications to the electrical system was the addition of new bus bar circuitry to allow the changeover between single circuit and pulse operation. This bus bar system allows the use of existing

## EQUIPMENT NOMENCLATURE

Device (1) is an amplifier device that takes a 50 to 250 mV signal and fires a SCR. This is adj. from 5,000 A to 25,000 A. It has a temp. drift of 1/2% of set point. It is the trigger device for purging burner for pulse. It applies to D-C to explosive charge for changing position of (Hi speed valve) in (P.C.) operation. In (S.C.) operation it opens circuit breaker.

Device (2) is the same as (1). It shuts burner down if activated. It is backup for (1). It is set slightly higher than (1) when in pulse or single circuit operation, or can be set at max. Current cut-off point in single circuit operation. It closes valves, (VMF), (VSF) and (VPF) in single circuit operation. In pulse operation it operates (5) and then closes valves (VMF) (VSF) and (VPF) after it is closed in (P.C.) circuit only.

Device (3) is the panic stop push button. When pushed closes main fuel, seed fuel and purge fuel valves in (S.C.) operation. In (P.C.) operation it closes circuit breaker first (5) then closes (VMF) (VSF) and (VPF).

Device (4) is the burner spring loaded main burner fuel valve dead man switch. It operates main fuel, seed fuel and purge fuel valves. When released it closes all three (3) valves in (S.C.) operation. In (P.C.) operation it closes circuit breaker first (5) then closes (VMF) (VSF) and (VPF).

Device (5) is a switch located on circuit breaker and mechanically moves with closing of circuit breaker. It breaks circuit to all three valves after it is closed in (P.C.) only.

Device (6) is an adjustable electronic timer-range 25 to 5,000 milliseconds. It is activated by device (1) in (P.C.) operation only. Preset time after device (1) has operated the high speed valve, which in turn (5) closes valves (VMF) (VSF) and (VPF).

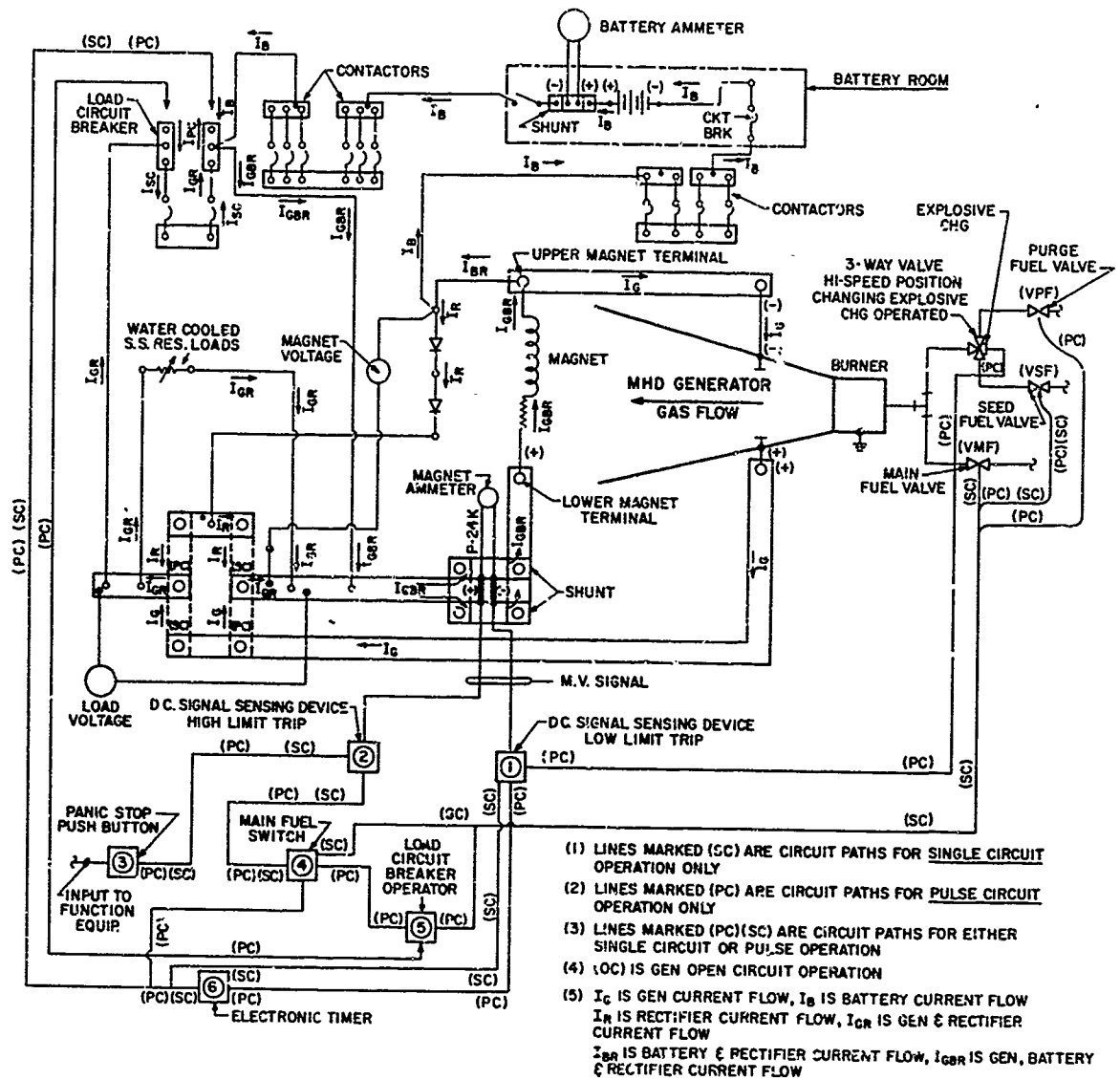


Fig. 48 Schematic of Pulse Generator Circuitry

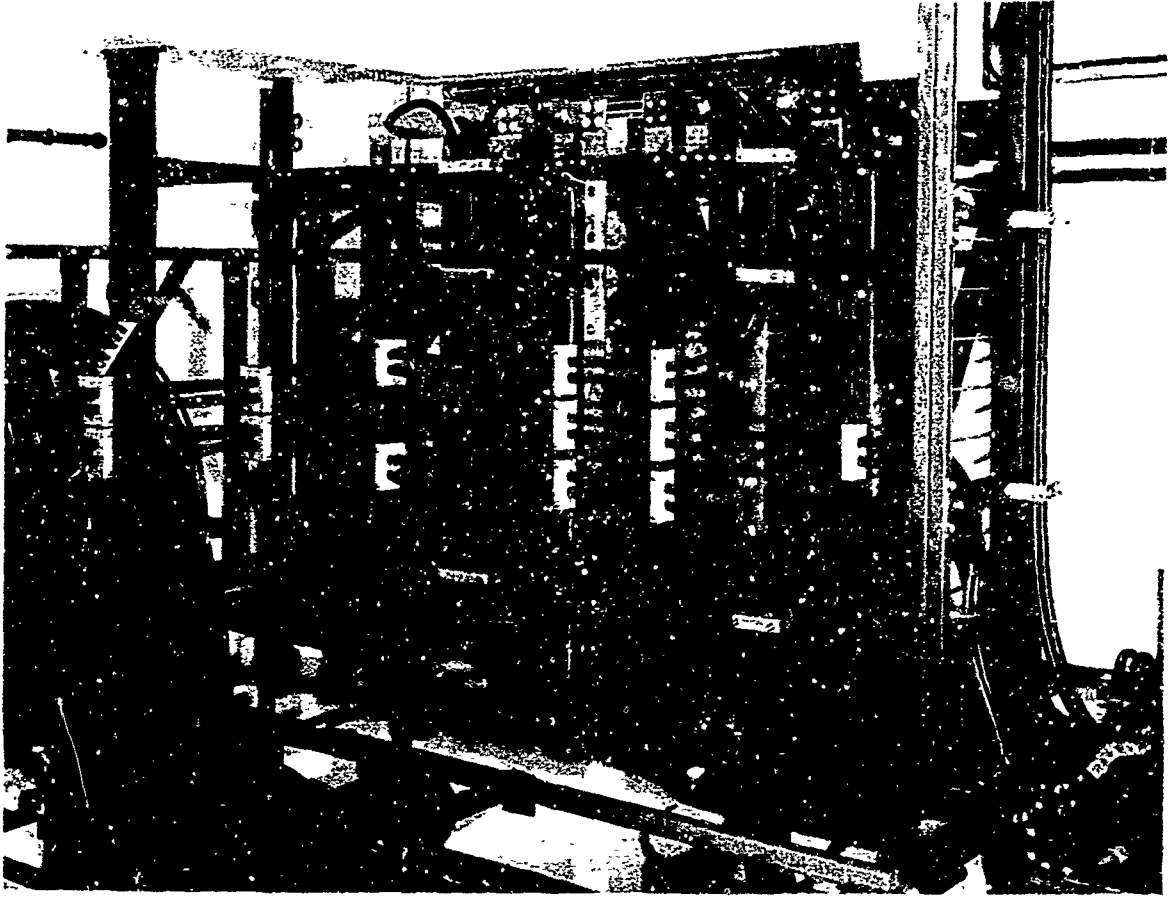


Fig. 49 New Rectifier Bank Mounted in Discharge Circuit

electrical leads between the channel and loads, and also contains the shunts used for generator control and instrumentation.

#### b. Generator Control

The burner control system was modified to allow operation of the generator in either single circuit or pulse mode. Several new safety interlocks were added, and the fast acting valve and pulse load circuit breaker integrated into the system. Generator startup for single circuit operation is identical to the Mark V, with the only difference for pulse production being the operation of the fast acting valve and the load circuit breaker.

Due to the high excitation rate obtained by the pulse channel configuration ( $\approx 3000$  amperes per second), it is necessary to have a device to prevent overexcitation of the magnet, as well as an automatic control to initiate pulse production at a predetermined, precise magnet current.

These devices are two amplifiers that pick up a voltage corresponding to a definite magnet current. The first amplifier acts as a function device which fires a silicone controlled rectifier, which in turn ignites the explosive charge operating the fast acting seed valve. This amplifier can be adjusted to fire at magnet currents between 5000 and 25,000 amperes. The second amplifier is similar to the first, but more stabilized, having a temperature drift of plus or minus 1/2% of set point from 5000 to 30,000 amperes, and is used as a safety device. The set point on amplifier #2 is slightly higher than amplifier #1, and is used to prevent overexcitation. The signal from amplifier #2 first shorts out the pulse load by closing the circuit breaker, then shuts off all fuels for the combustion chamber, giving a shutdown procedure identical to the original design. Amplifier #1 is also used to activate instrumentation to record the pulse.

In pulse testing, immediately after the desired pulse time has been achieved, the pulse load is shorted out automatically. This immediately reduces the magnet voltage to that encountered in the normal magnet decay; (i. e., single circuit operation).

To obtain this orderly shutdown under all operating conditions, including emergency shutdown, an interlocking timer is used to prevent burner shutdown until the load circuit breaker is closed. If for any reason, therefore, the test is to be terminated before pulse production, the opening of the main burner fuel valve switch or any safety interlock immediately activates the timer and at the same time shorts out the pulse load by closing the load circuit breaker. The timer can be set to close all fuel valves from 25-500 milliseconds after activation. This operating procedure prevents the occurrence of high potentials and provides for a normal shutdown.

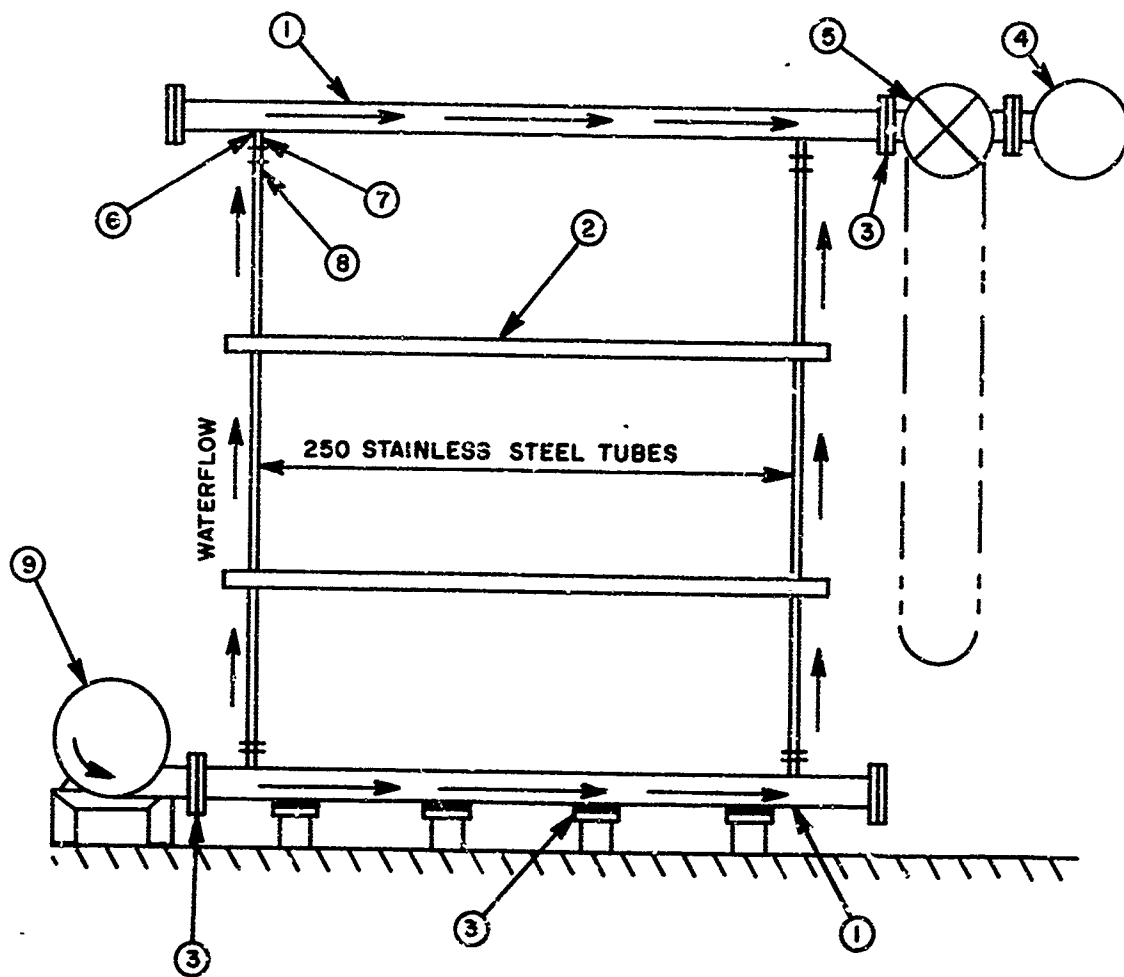
The load circuit breaker is a standard double pole circuit breaker capable of breaking the circuit at a current of 20,000 amperes and 2000 volts, and is therefore suitable for single circuit operation. For the pulse phase of the program, the circuit breaker is used as a safety device and is in a normally open position. During pulse production a high potential exists across the channel and load, the value of which depends upon the pulse duration. The breaker is capable of making at the high potentials and is used to short out the pulse load after the pulse is delivered. The remaining stored energy in the magnetic field can then be dissipated in an orderly fashion through the rectifier bank over the normal magnet decay time.

#### 4. Load Resistors

The original load resistor bank consists of 1000 stainless steel tubes having a total cooling water flow of 18,900 liters/minute. The load resistors are water-cooled stainless steel tubes, grouped in four sets of cooling water manifolds having 250 tubes each. The stainless steel resistor tubes are assembled vertically with a water inlet manifold on the bottom and a water outlet manifold on the top. Each cooling water inlet and outlet manifold is electrically insulated from one another and from ground. The insulation is furnished by the electrically non-conductive hose and phenolic insulation as indicated in Figure 50.

A study into load resistor requirements for the single circuit and pulse mode revealed that the existing load resistor bank could be utilized to meet the requirements of both operating modes. There was a question as to the integrity of insulation in the load system; however, as each tube is insulated from the common manifolds and the manifolds in turn are insulated from inlet and outlet cooling water heaters and from ground. Theoretically, the insulation was sufficient for pulse production, but before assuming the system was safe, the 20,000-volt, 2-ampere power supply was used to test system integrity. The tests showed that the tubes in the loads were sufficiently insulated to withstand potentials much higher than those expected during pulse operation.

Based on these tests the loads were electrically rearranged to give the desired resistances for single circuit and pulse production.



- |                       |                   |
|-----------------------|-------------------|
| 1 Manifold            | 5 Control valve   |
| 2 Tube supports       | 6 Hose adapters   |
| 3 Phenolic insulation | 7 Insulating hose |
| 4 Discharge header    | 8 Hose clamps     |
| 9 Inlet header        |                   |

Fig. 50 Load Resistor Schematic

## F. INSTRUMENTATION

The operation and evaluation of the MHD generator requires the monitoring and recording of certain pertinent data.

### 1. Burner Monitoring Instrumentation

To properly evaluate burner operation requires the recording of pressures and temperatures for the burner and auxiliary systems.

Pilot burner operation is evaluated by recording the fuel manifold, oxygen manifold and chamber pressures.

Main burner operation requires a knowledge of the pressures in the fuel manifold, oxygen manifold, and combustion chamber. The bulk temperature rise and cooling water discharge pressure for the burner are monitored at six locations.

The cooling water pump discharge pressure and temperature is recorded as is the temperature and pressure of the main burner oxygen as it flows through the flow control venturi.

The total bulk temperature rise and discharge pressure for each of the four load resistor manifolds is also indicated.

To best display, record, and reduce the data of the single circuit mode, an instrument panel on which the values could be displayed with fairly inexpensive meters and gauges was set up and photographed. To photograph these instruments two surplus K-25 aerial cameras are used.

For power testing one camera is operated continuously at a speed of one frame per second to record very closely the magnet pre-excitation, burner startup, and magnet self-excitation.

The film produces a picture which is 4 in. x 5 in. and sixty frames long. Using adapter lenses for fixed distances, it is possible to record the entire panel with each camera, so that all data is on a single roll of film.

The total magnet current and voltage is monitored and recorded as well as the total battery supply output. The magnet current is measured on a shunt connected between the channel self-excitation electrodes and the magnet. The magnet voltage is measured across the full magnet while the battery current is taken from a shunt on the battery switchboard.

The total magnet current is recorded on a multi-channel oscillograph recorder and is duplicated on a meter for the instrumentation panel.

As a further check on the magnet pre-excitation rise time, there is a time indicator displayed on the instrumentation panel which starts when the exciter circuit switch is closed.

## 2. Channel Monitoring Instrumentation

Figure 51 is a sketch showing the location of the various points on the channel at which provisions for electrical, pressure and temperature measurements are provided.

Pressure taps located in the electrode wall are used to measure the axial centerline gas pressure distribution. As can be seen in the figure, 14 centerline taps were installed, three in the inlet section, one at the start of the power section, and ten others through the power section.

In order to calibrate and check the cooling water flow in the channel, pressure taps were placed in the manifold cover plate. One tap was in the inlet manifold to the inlet bars, while another was in the inlet manifold to the power section bars. The cooling water flow through the tubes was precalibrated for the inlet pressure and discharge pressure so that the exact flow through the wall was checked out under pump operating conditions and flow orifices were then modified.

Provisions were made on the channel so that each copper bar on the insulating wall had an instrumentation connection point. It was not planned to utilize all of these connection points in the initial program, but they were installed in the channel and sufficient instrumentation wiring was made available.

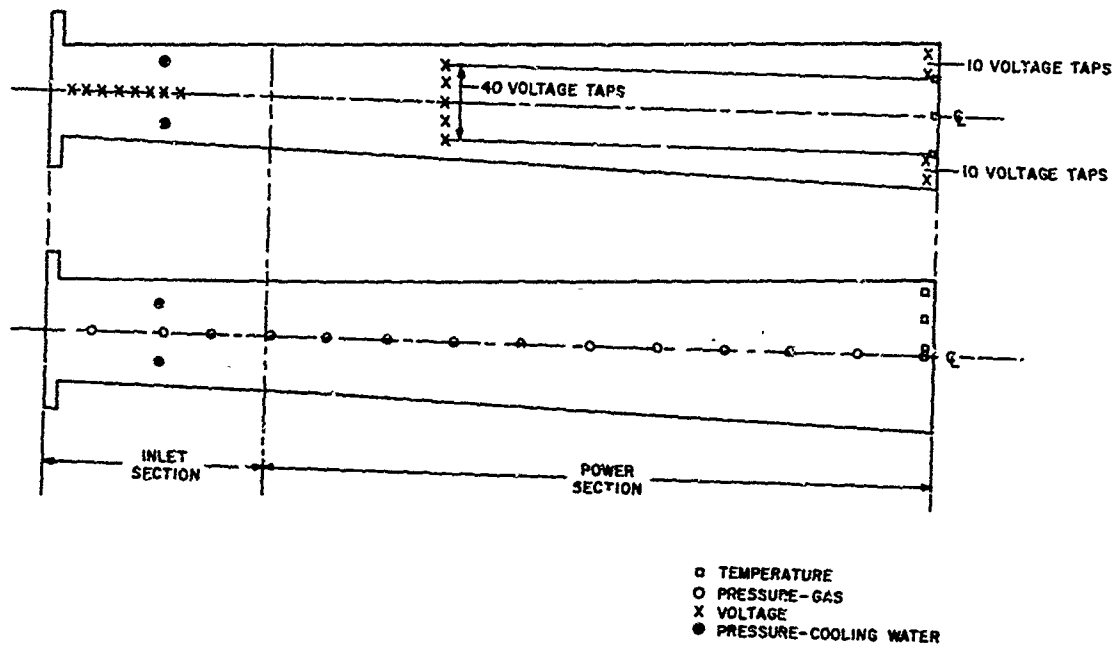


Fig. 51 Channel Monitoring Instrumentation

### III. TESTING PROGRAM

#### A. INTRODUCTION

The startup of the pulse generator required a complete shakedown and testing of all new components, as well as all the old components which had not been operated for some period of time. This shakedown included testing of the water and fuel systems, electrical circuitry, safety interlocks, and the calibration of all new systems and components.

When the generator was completely assembled for operation, a complete check of electrical insulation was conducted using the high voltage power supply. Once these tests had been completed and the low resistance areas improved, a magnet test was made to check out the magnet and battery dumping circuitry.

The battery bank was set up for six strings on ten batteries which would place a voltage of 120 volts across the magnet and a current flow of 2500 amperes. The excitation of the magnet was as expected; however, due to an error, the magnet discharge circuitry was not properly connected, thus allowing the energy in the magnetic field to be dissipated in an arc, which damaged the contactors of the circuit breaker in the battery circuit.

The damage to the circuit breaker was such that it was necessary to return it to the factory for repairs. In order to continue testing another circuit breaker was obtained and installed for temporary service.

The first complete configuration test was to be conducted in the single circuit mode of operation. This test was aimed at investigating self-excitation of the magnet rather than achieving a substantial net power output from the generator. The reason for this was that it is desirable to obtain the startup and excitation characteristics of the new generator configuration. The test plan, therefore, was to excite the magnet up to a magnet current of 10,000 amperes. The test was to be performed with a mass flow of 40 Kg/sec, using a fuel mixture of 50% ethyl alcohol and 50% methylcyclohexane with 1.4 mole % potassium in the combustion gases at 1 atm pressure and a temperature of 3000°K.

The test was, however, terminated during startup in an emergency shutdown. The reason for this was due to delayed ignition of the pilot burner which caused deterioration of the pilot burner liner thus cutting off the cooling water flow which led to burnout of the pilot chamber. This in turn led to damage of the main burner injector and backplate.

A program was immediately initiated to manufacture a new copper backplate. In the interim it was determined that a stainless steel

backplate which was used in the old Mark V program could be utilized to continue testing. To utilize this backplate required modifications to the fuel distribution manifold and the interconnection of the fuel-nitrogen purge system.

To provide safer operation of the pilot and igniter burners it was decided to change the fuel from ethane to methane. The methane is a high pressure gas which cannot condense under the required operation conditions. A check of pilot operation revealed that nitrogen dilution must be increased to provide equivalent pilot burner heat transfer. The ethane control system was then adapted to accommodate the new fuel.

The igniter and pilot burners were operated to verify their performance using methane. These tests were satisfactorily completed and the generator was prepared for excitation testing. This included installation of the repaired battery circuit breaker and a generator hookup such that the magnet was the only load on the generator. This was done to observe only the excitation of the generator so as to keep the test procedures as simple as possible.

The next test was conducted using the identical goals previously described. The generator was started at 1200 amperes magnet current and terminated ten seconds after burner firing. All phases of generator startup and shutdown were normal; however, the magnet current at shutdown was only 2500 amperes and was primarily supplied by the battery bank. Hence, the generator failed to self-excite.

Examination of test data revealed that the automatic nitrogen valve used to purge the fuel manifold failed to seat properly and the proper amount of fuel and seed failed to enter the combustion chamber. This resulted in reduced fuel mass flow and unstoichiometric combustion, giving a gas temperature too low for power generation.

All other generator components performed satisfactorily. A dynamic cooling water pressure check of the channel was performed using the main pump and no water leaks were observed. The channel insulating and electrode refractory was intact and no damage was found.

The nitrogen purge system was modified slightly and the valve operator was adjusted to provide more positive closing action. The burner was disassembled to inspect the stainless steel backplate and liner. At this time additional reinforcement was added to the burner end magnet support which was necessary to be able to bring the magnet to a current of 20,000 amperes.

Excitation Test #2 was conducted using a mass flow of 40 Kg/seconds and a burner firing point of 1200 amperes magnet current. Figure 52 shows the excitation characteristics of the new configuration.

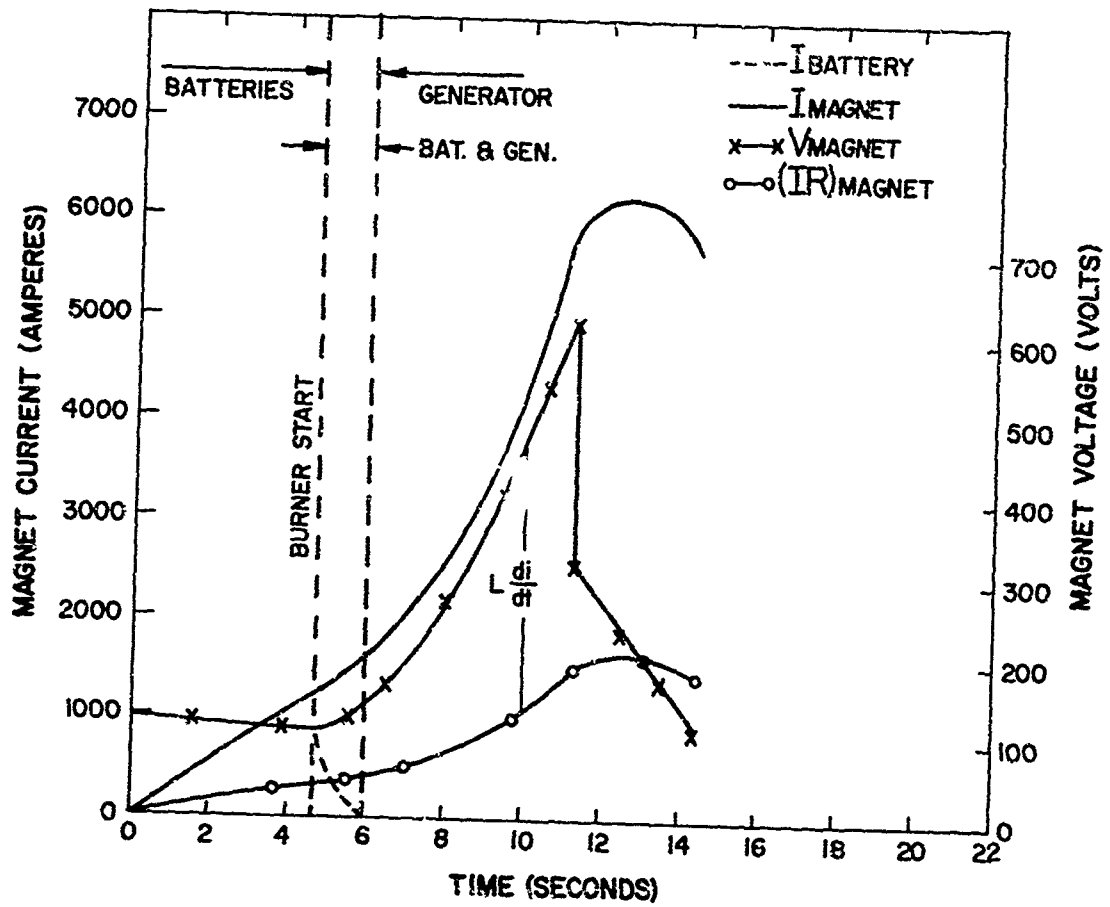


Fig. 52 Characteristics for Excitation Test #2

As can be seen from the curve there was a rapid excitation to a magnet current of 5900 amperes and a voltage of 620 volts. At this point there existed an  $L \frac{di}{dt}$  of 433 volts corresponding to a net power output of 2.55 Mw. A sharp drop in magnet voltage then occurred and the magnet current leveled off. This drop in magnet voltage was caused by a severe water leak in the very first bar in the electrode wall of the channel. The water leak developed when the bar burned out due to a lack of cooling water. Post-run inspection revealed that the gasket which was cemented to the inlet manifold cover plate had become detached and blocked the water inlet gland, thus cutting off the cooling water flow through the bar. The center section of the bar burned out, allowing water to enter through the discharge gland and flow into the channel, thus derating generator performance. With the exception of the damaged electrode bar the remainder of the channel was in excellent condition including refractory used as insulation and electrode material. The gasketing on all four channel manifold cover plates was modified to eliminate this situation.

The overall performance of the generator up to the failure of the channel bar was as predicted. Figure 53 is a plot of the axial channel pressure distribution measured along the centerline of the electrode wall. The curve shows the expansion from a pressure of 2.42 atm in the inlet section to 0.5 atm at the channel exit without the presence of shocks and flow separation at a mass flow which was 80% of the design flow.

Inspection of the main burner showed that the chamber liner was slightly burned on the injector end. This burning was directly attributable to using the old stainless steel injector backplate in lieu of the copper injector plate. The stainless backplate projects 1.90 centimeters less into the main chamber than the newer copper version of the backplate. The "O" ring which seals the cooling water passage on that end of the liner was thus located in such a position that there existed a small uncooled area of the liner which was only shielded by nitrogen injection. The backplate had been previously operated under similar conditions at a mass flow of 40 Kg/sec without damaging the liner. The safety factor from burnout using this backplate was proven to be marginal and the continued use of the stainless steel backplate would thus require a decrease in mass flow. However, lower mass flows would lead to flow separation which in turn could damage the channel and result in questionable test data. It was therefore decided not to continue testing with the stainless steel backplate.

To repair the burned areas of the chamber liner required complete disassembly of the burner and a welding cycle to fix the liner.

The new copper injector plate was received, installed, and cooling water flow checked along with associated safety interlocks. A burner test was performed at a mass flow of 40 Kg/second for a duration of 5 seconds. This time limit was chosen as it allowed sufficient time for thermal equilibrium to be achieved, yet short enough to minimize any damage if some local overheating occurred. Inspection of the burner backplate after testing revealed no damage or overheating and all components

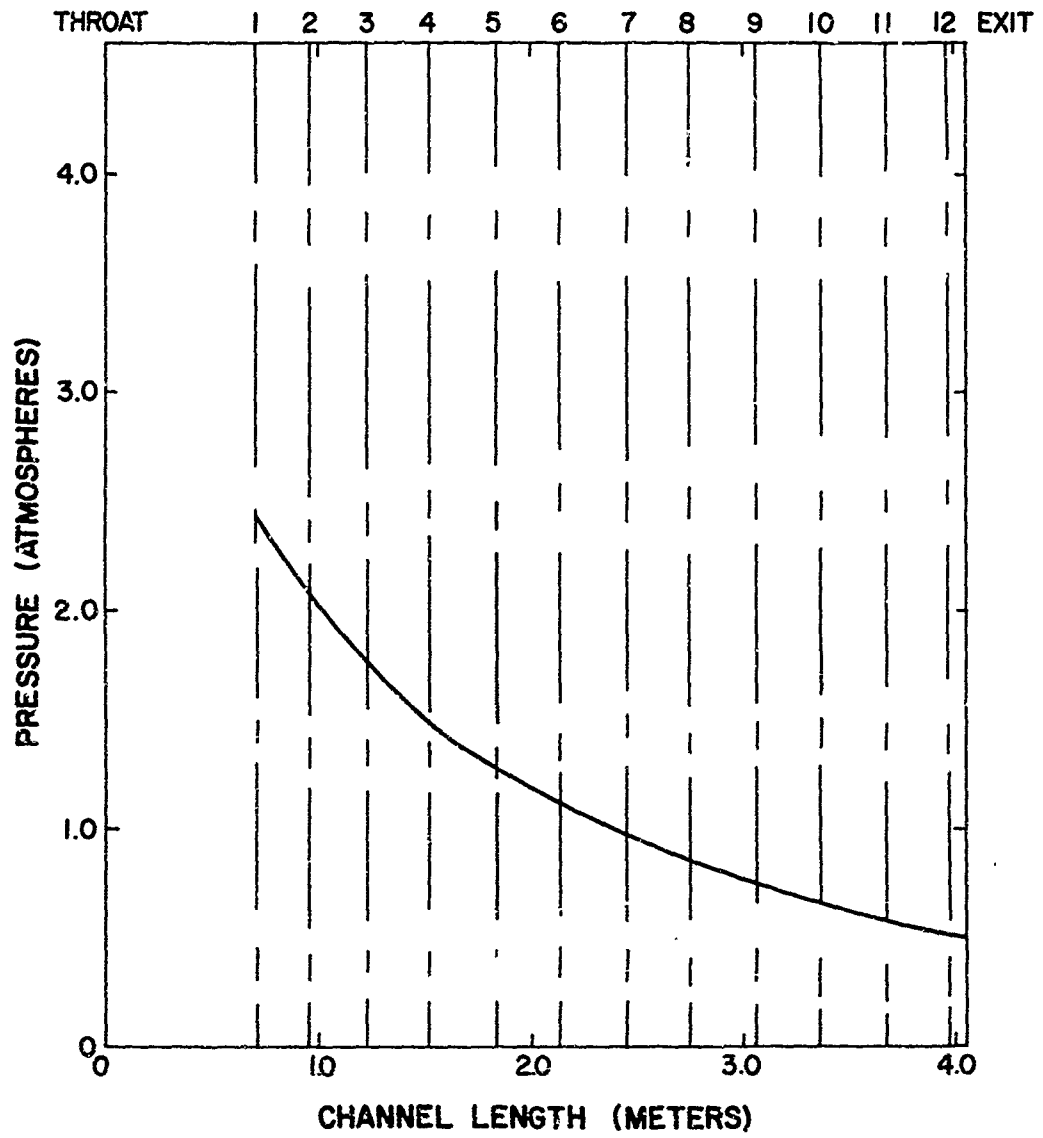


Fig. 53 Axial Channel Pressure Distribution for Excitation Test #2

indicated no further problems. The measured heat flux for the new back-plate was in close agreement with that presented under the original pulse burner testing program.

The program had now reached the stage where all components were operating reliably and single circuit power testing could be started.

## B. GENERATOR TESTING

The first test with the intention of producing net power was performed with a mass flow of 45 Kg/second using a fuel mixture of 50% ethyl alcohol and 50% methylcyclohexane with 1.5 mole % potassium in the combustion gases at 1 atm and a temperature of 3000°K. The procedure for the test was to excite the magnet using the battery bank to a magnet current of 1500 amperes where the main combustion chamber would be ignited. The limits for the test were not to exceed 15,000 amperes magnet current or a total running time of 20 seconds, and to open the load short circuiting switch. The excitation characteristics for the test are shown in Figure 54. The burner was fired at a magnet current of 1500 amperes, from where it excited to a magnet current of 15,000 amperes where the load short circuiting switch was opened causing the large drop in generator voltage shown, resulting in a negative  $L di/dt$ , hence decreasing magnet current. The load resistor was set at 0.05 ohms giving a voltage drop across the load resistor of 750 (V) at a current of 15,000 amperes as can be seen in Figure 54. Under these conditions the maximum net power level in the load was 11,000 kilowatts. Excitation proceeded smoothly until the generator output voltage reached 780 volts or a magnet current of 9500 amperes. From here until the test was terminated slight arcing occurred in the inlet section of the channel decreasing the generator output voltage which in turn caused the  $L di/dt$  to go negative after the load resistor short circuiting switch was opened.

The arcing was determined to be caused by the superimposing of the open circuit voltage in the inlet section of the channel upon the transverse voltage distribution across the channel, resulting in a local voltage gradient in excess of design conditions. To decrease the steep voltage gradient in the inlet section all bars and walls which comprise the inlet section were shorted together thereby decreasing the gradient, after which testing was resumed.

Power Test #2 was performed at a mass flow of 50 Kg/sec using identical fuel and seed conditions as in the preceding power test. The test procedure was to fire the main combustion chamber at a magnet current of 1500 amperes and open the load short circuiting switch while also having test limits of 20,000 amperes magnet current and burner operation time of 20 seconds. The excitation characteristics for this test are shown in Figure 55. The burner was ignited at a magnet current of 1500 amperes from where the generator excited to a magnet current of 18,000 amperes where the load short circuiting switch was opened, again causing a large drop in magnet voltage resulting from a negative  $L di/dt$  and decreasing magnet current. The maximum power during this test was 15,200 kilowatts. From the figure it can be seen that the voltage output of the generator was increasing rapidly until it reached 750 volts. From here until the test was terminated a water leak and slight arcing occurred in the inlet section of the channel decreasing the generator output voltage which in turn again caused the  $L di/dt$  to go negative after the load resistor short circuiting switch was opened.

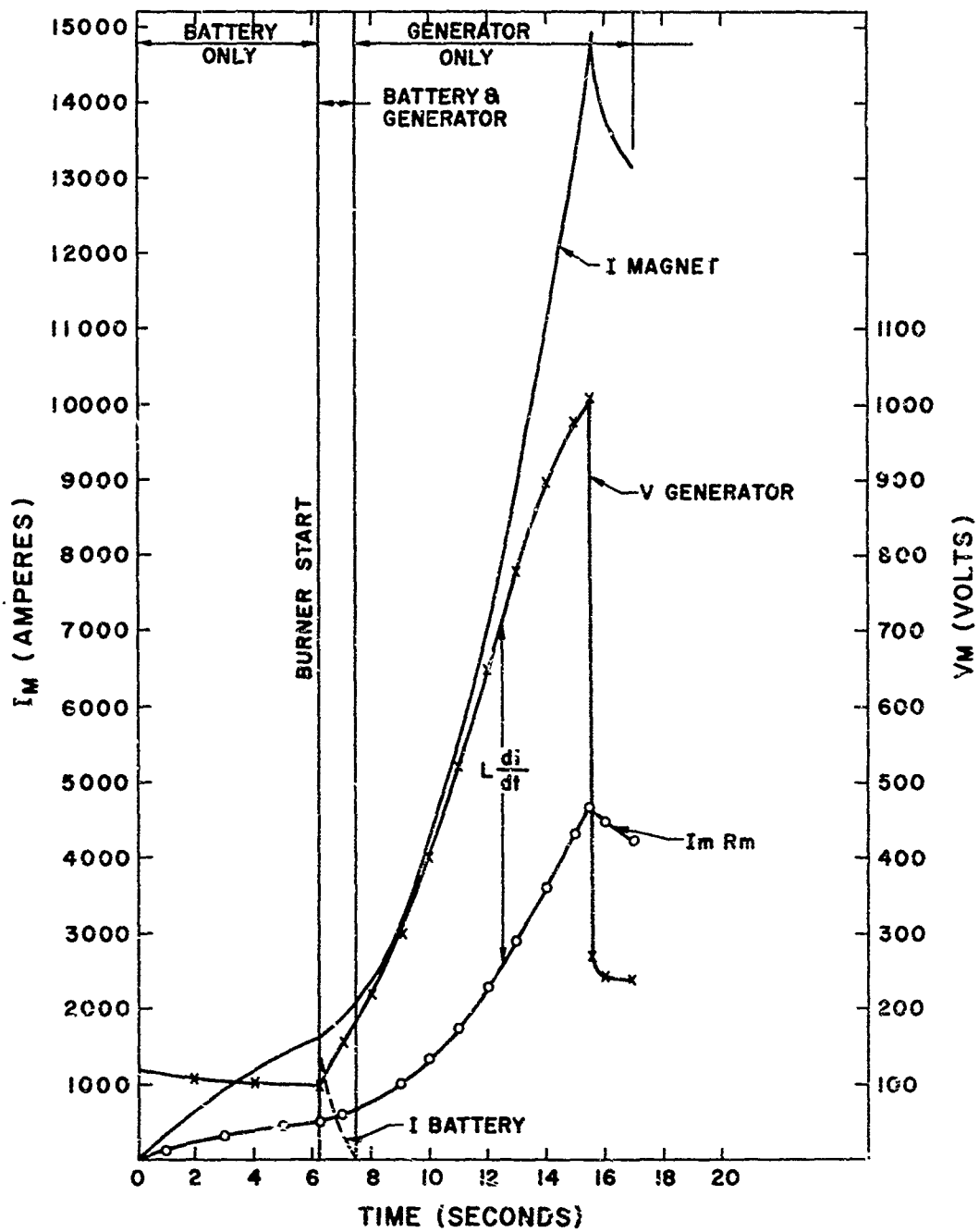


Fig. 54 Excitation Characteristics for Single Circuit Net Power Test #1

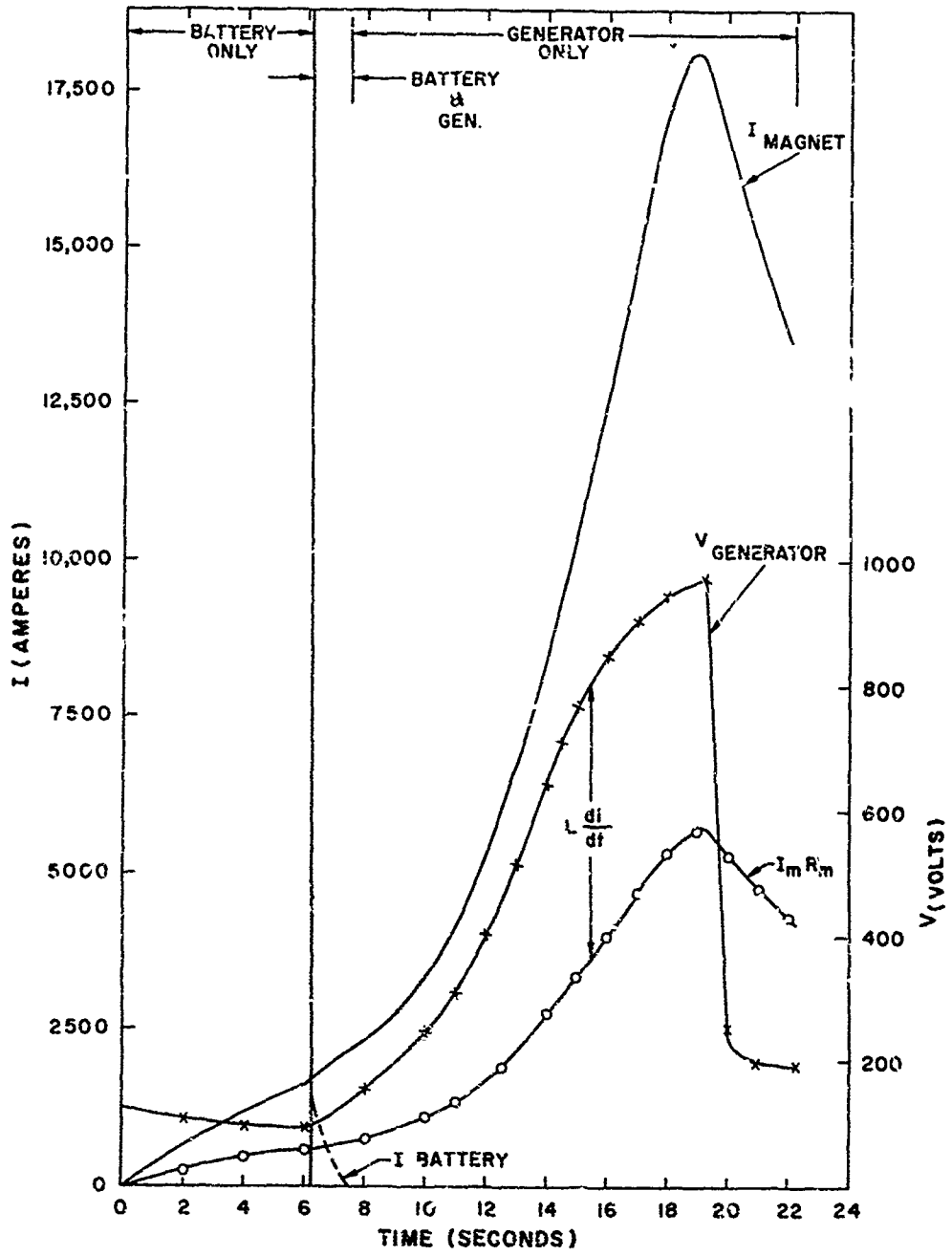


Fig. 55 Excitation Characteristics for Single Circuit Net Power Test #2

Examination of the burner after the test revealed a water leak in the burner caused by a partial "O" ring failure on the burner liner. The amount of water entering was not sufficient to jeopardize any of the burner components, but was of sufficient magnitude to seriously derate the generator performance.

To further protect the inlet section from the voltage gradient caused by the superposition of the open circuit voltage on the transverse voltage distribution across the channel, a nitrogen injection system was installed in this critical area before making Power Test #3. The nitrogen injection system was designed, installed and calibrated for a flow rate of 1 #/sec into both corners of the insulating walls and the positive electrode wall in the inlet section of the channel.

Net Power Test #3 was performed at a mass flow of 50 Kg/second using identical fuel and seed conditions as the preceding power test. The test procedure was to fire the main combustion chamber at a magnet current of 1500 amperes and open the load short circuiting switch at 20,000 amperes while also having test limits of 20,500 amperes magnet current, and burner operating time of 20 seconds. The excitation characteristics for this test are shown in Figure 56.

The generator excitation was quite similar to that experienced in the previous test with the exception that the generator was allowed to excite to 20,000 amperes before the load short circuiting switch was opened. At this time the voltage drop in the load was equal to the full voltage output of the generator which again resulted in a negative  $L di/dt$ , thus explaining the magnet current decay.

Inspection of the channel revealed slight arcing in the critical section where the nitrogen had been injected. The arcs were not as severe as has previously been experienced and allowed the generator to attain a slightly higher output voltage for a particular magnet current than in the previous test. At 18,000 amperes, however, the arcing in the inlet section of the channel resulted in a cooling water leak which derated the generator performance. This is indicated in the diagram by the dip of the generator output voltage after time 18 seconds.

From the data obtained in Power Tests #2 and #3 the measured static pressure distribution in the channel indicates that the expected open circuit voltage is developed. From this it can be concluded that the failure of the generator to develop sufficient output voltage to maintain steady state 20,000-kilowatt net power output can be directly attributed to too high an internal voltage drop. A high internal voltage drop may result from either too high an internal impedance or the existence of a large eddy current in the inlet section due to arcing. In this case it was believed the problem was a combination of both these factors.

To overcome these difficulties, the insulation capability of the inlet section was improved as well as a new fuel mixture which would

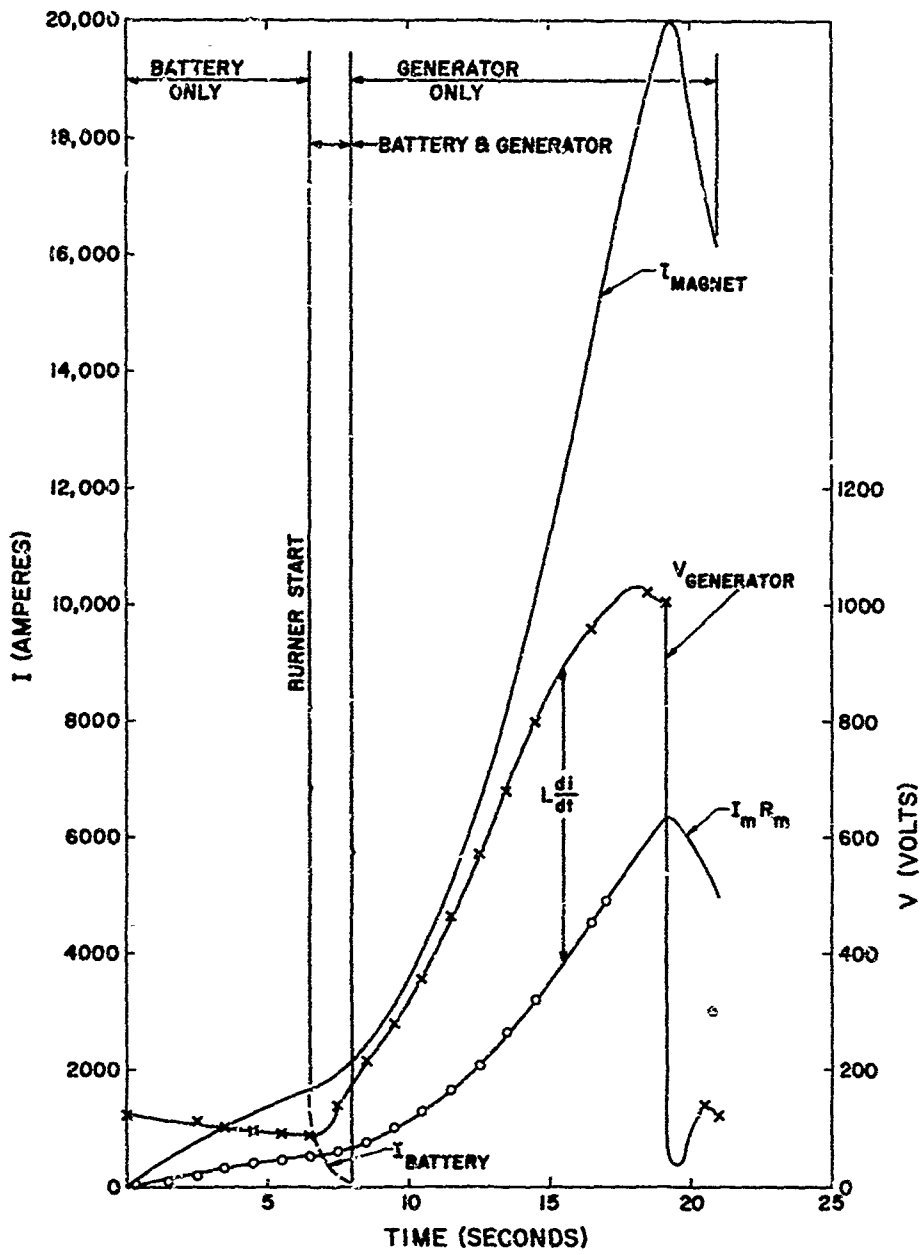


Fig. 56 Excitation Characteristics for Single Circuit Net Power Test #3

lower the internal impedance of the generator (increase the effective gas conductivity) was used. The new fuel, a mixture of "toluene" and alcohol seeded with potassium hydroxide, was used to increase the gas conductivity.

Net Power Test #4 was made using a mass flow of 50 Kg/sec. A fuel mixture of 67% toluene and 33% alcohol was used which contained sufficient potassium to give 1 mole % K in the combustion products at 3000°K and 1 atm. The burner was started at a magnet current of 1700 amperes and the single circuit load was set at 0.045 ohms with the load circuit breaker to be opened at a magnet current of 15,000 amperes. At a magnet current of 15,000 amperes, however, the test was aborted, before the load circuit breaker was opened, due to a fault which developed in the generator monitoring system.

The net results of this test were still profitable in that it demonstrated that the channel insulation had been improved since no arcing occurred. The new fuel mixture gave a higher gas conductivity which resulted in increased voltage output and faster excitation.

Based on the data obtained in Test #4 the next test (Test #5) was conducted with a seed concentration of 1.3 mole % K and an external load set at 0.0425 ohms. The excitation characteristics for this test may be seen in Figure 57. The burner was started at a higher magnet current than in the previous test, 2000 amperes, to achieve a smooth transition from battery only to generator only operation due to the increased seed concentration. The excitation rate was slightly better than that of the previous test. When the magnet reached 16,000 amperes the load circuit breaker was opened, after which the generator was operated for another four seconds and steady state conditions were achieved. At this time the current was 17,000 amperes giving a net power output of 12,300 kilowatts.

To further increase the generator output voltage in Test #6 the seed amount was increased to 1.55 mole % K. The external load was reduced to 0.040 ohms to allow the generator to steady state at a higher magnet current than in the previous test.

In Power Test #6 the burner was again started at a magnet current of 2000 amperes, and the net power load was put into the circuit at 17,500 amperes. The test continued for seven seconds with the load in the circuit and only a slight indication of continued excitation was observed at the end of the test. The maximum net power output for the test was 13,000 kilowatts at 18,000 amperes. Inspection of the channel revealed slight arcing in the beginning of the inlet section. To overcome this problem in future tests the insulating portion of the inlet section was extended to reduce the voltage gradient.

In order to further reduce the internal impedance of the generator it was decided to use two separate fuel systems whereby a saturated solution of seeded alcohol would be used in one and pure "toluene" would be used in the main fuel system. In this manner a more highly conductive

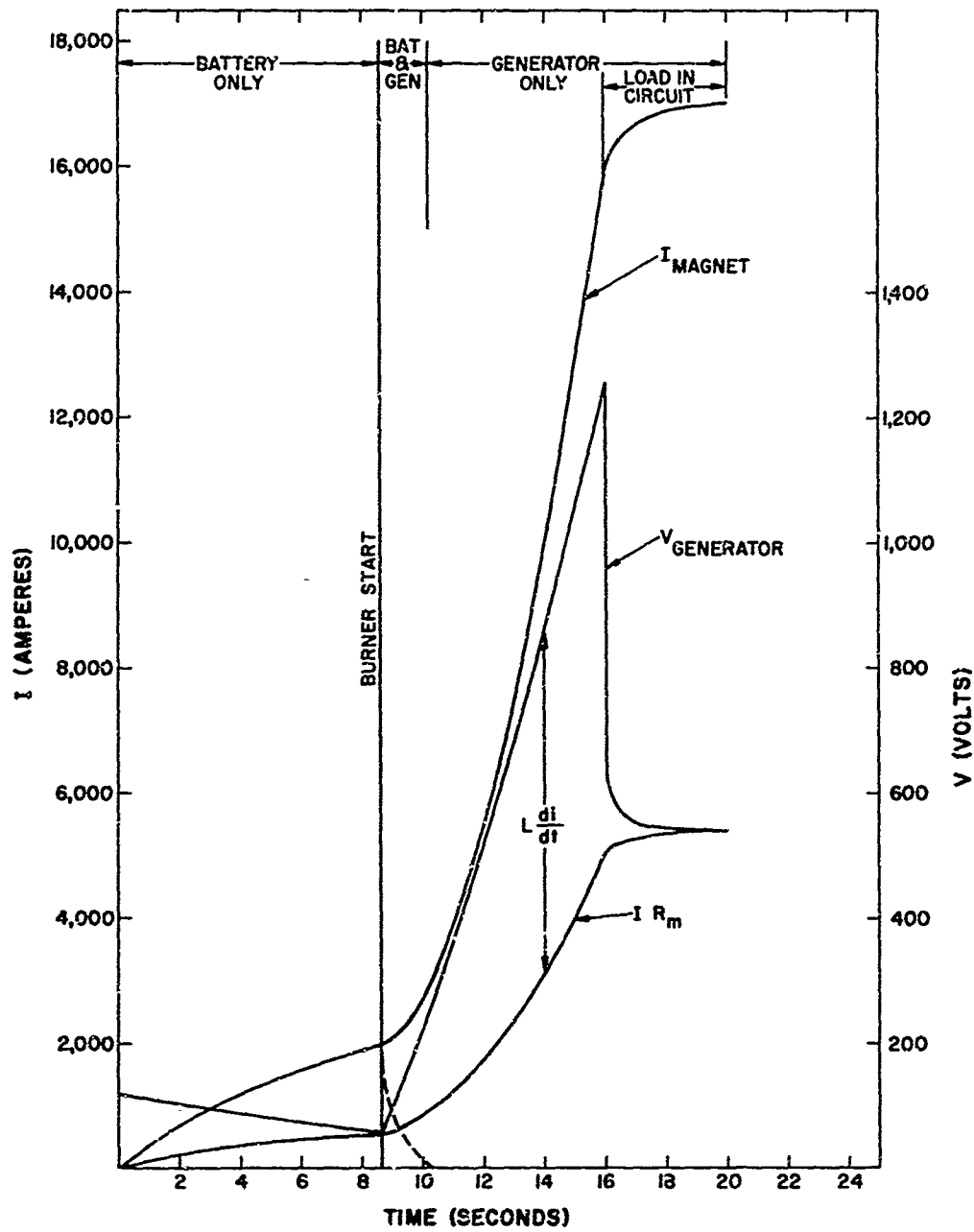


Fig. 57 Excitation Characteristics for Single Circuit Net Power Test #5

working fluid can be generated by reducing the mass flow of alcohol and creating a higher combustion temperature. The seeded fuel system to be used in the pulse operation was now utilized to inject the seeded alcohol flow to the combustion chamber.

Test #7 was conducted using a total mass flow of 56 Kg/sec and 1.3 mole % potassium in the combustion products. The mass flow was increased from 50 to 56 Kg/sec to increase the flow velocity, hence a higher voltage output. The load was set at 0.045 ohms. As can be seen in Figure 58, the main burner was fired at 8 seconds. The generator was allowed to excite to 19,000 amperes magnet current, at which time the load was placed in the generator circuit. The generator output voltage at this point was 1320 volts. The generator was, however, unable to sustain operation at the high value of magnet current and the test was terminated at 24 seconds. When the load was switched into the circuit the generator output voltage dropped to approximately 475 volts, while the voltage required to maintain magnet operation at 19,000 amperes was in excess of 600 volts.

Slight damage from arcing was again experienced in the inlet section of the channel, as the voltage gradient in this section of the channel was too high. It was therefore decided that before another test would be made the entire channel would be shifted to move the inlet section into an area of lower magnetic field, and thus lower the voltage gradient between the grounded channel inlet section and the beginning of the insulating section. To accomplish this required relocation of the combustion chamber and its associated fuel, oxidizer and cooling water piping, and the rearrangement of the cooling water inlets to the channel. In addition, by moving the channel, the eddy currents present in the inlet section will be reduced, resulting in increased power output.

Power Test #8 was conducted using the dual fuel system and the same test conditions as in the previous test, except that JP-4 was substituted for "toluene," to further increase the gas conductivity. When the generator had self-excited to 18,200 amperes magnet current the load short circuiting switch was opened. The test continued for 15 seconds and the generator stabilized at a current of 17,000 amperes and a load voltage of 810 volts, giving 13,800 kilowatts net power output. Figure 59 shows the excitation characteristics for Power Test #8. Examination of the channel after the test revealed that the relocation of the channel and the insulation modification had eliminated the arcing problem in the inlet section.

To provide more flexibility during testing the ability to change the load resistance was incorporated. A switch was utilized to partly short out the load resistor and thereby make it possible to decrease the generator load in one step during a test. Test #9 was therefore performed with an initial load resistor value of .053 ohms which could be reduced to .047 ohms at the operator's discretion. The mass flow was 56 Kg/sec with a combustion gas composition equal to that in Test #8. The generator was excited to 18,300 amperes at which time the 0.053-ohm load was placed into the circuit. When it became obvious that the generator decay was rapid, the load

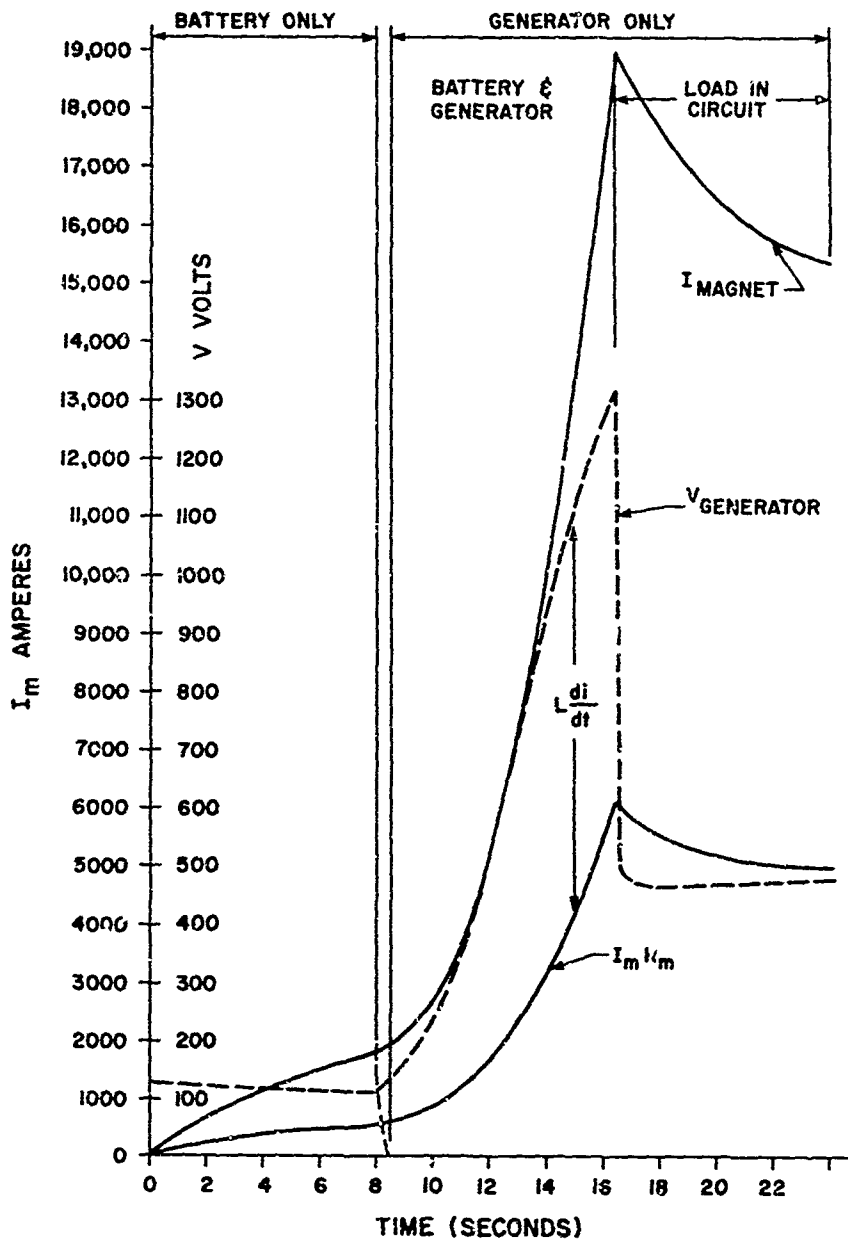


Fig. 58 Excitation Characteristics for Single Circuit Net Power Test #7

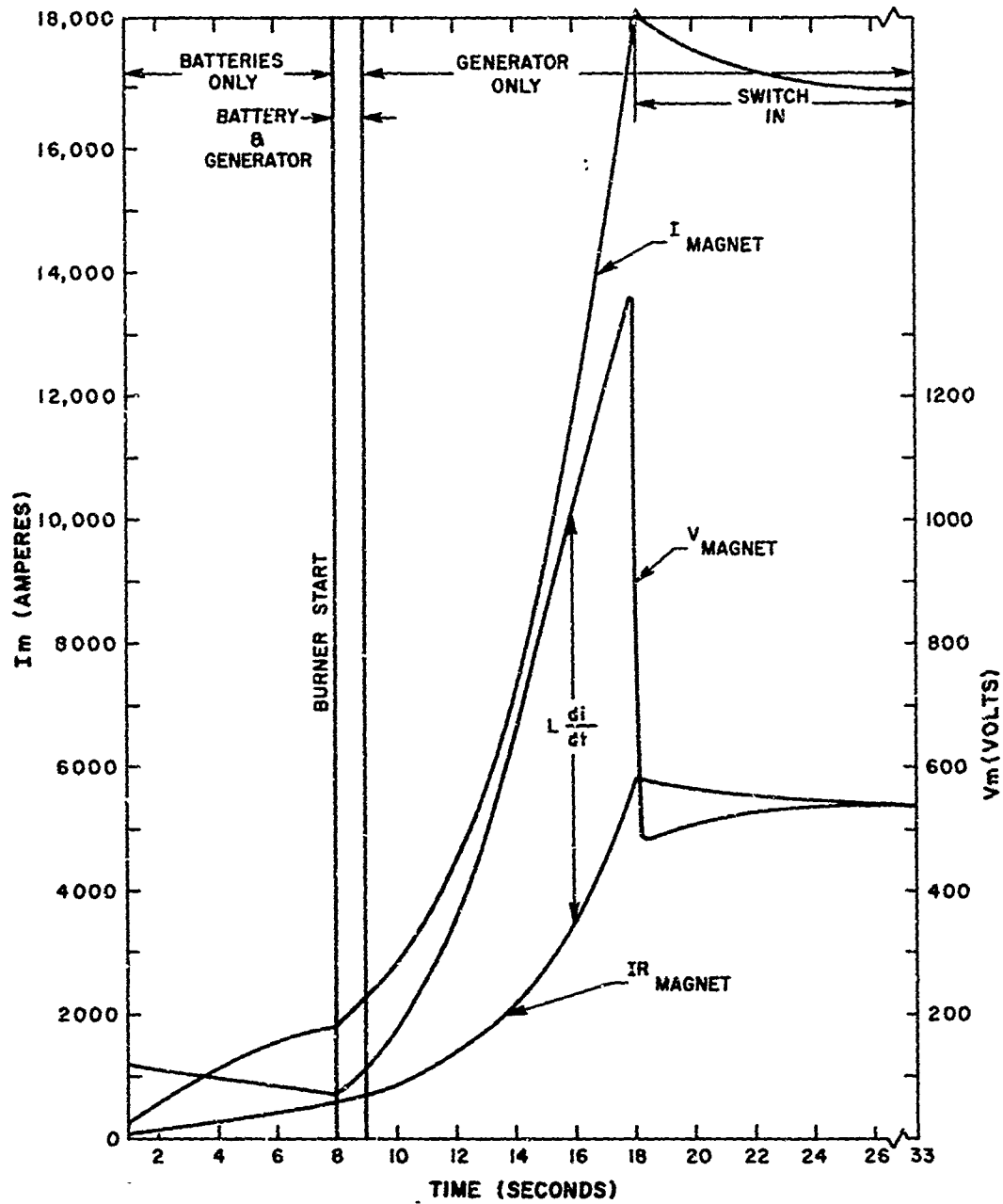


Fig. 59 Excitation Characteristics for Single Circuit Net Power Test #8

was changed to 0.047 ohms. The generator steady stated at 13,500 amperes approximately 6 seconds after the second load value was in the circuit.

Since post-run check of the channel showed no signs of arcing or water leaks which could have derated the generator performance, all indications were that, with the existing channel configuration, it was the internal impedance of the generator which prevented the completion of the 20,000-kilowatt, single circuit, steady state output phase of the program. During the previous tests the generator flow composition had been optimized in respect to gas conductivity and the last remaining device to lower the internal impedance of the generator channel was to use cesium as the seed material.

The electrical gas conductivity of the generator working fluid would be improved using cesium instead of potassium as the seed material due to the fact that cesium has a lower ionization potential, 3.87 ev versus potassium's 4.32 ev. Cesium hydroxide is extremely expensive (on the order of a hundred times the cost of potassium hydroxide), and since it requires more cesium than potassium on a weight basis for a given particle density, only the amount of cesium required to get the necessary increase of the gas conductivity was procured for one test. The cesium hydroxide was dissolved in alcohol, together with potassium hydroxide to obtain the near saturated solution.

The main fuel for Test #10 was "toluene" with the seeded fuel in the auxiliary fuel system. The load resistance was dropped slightly so that .050 ohms and .045 ohms were the two settings. The generator was excited to 18,250 amperes at which time the load circuit breaker was opened. When the magnet current started to drop, the load was switched to 0.045 ohms and the generator steady stated at 16,250 amperes. The test was allowed to continue for 15 seconds but the output never varied from the 12,000-kilowatt level. The test was terminated when it became obvious no further excitation was possible, and the seeded fuel was about to be dissipated.

The examination of the test data revealed pulsations in the seeded fuel flow. These pulsations were believed to be caused by the presence of a stem pipe in the seeded fuel flow system. Although the average seeded flow was as expected, the effective gas conductivity was decreased due to the gas conductivity not being a linear function of the seed flow rate.

Figure 60 is a typical pressure distribution obtained during single circuit testing. In the diagram four pressure distributions are given for various values of magnet current, indicating various levels of interaction between the working fluid and the magnetic field. A comparison of these measured values with the theoretical values shown in Figure 10 indicates good agreement, considering the accuracy of the instrumentation.

The single circuit power testing program was halted at this point because the contract period was nearing completion.

## STATIC PRESSURE DISTRIBUTION IN CHANNEL POWER SECTION (TEST #8)

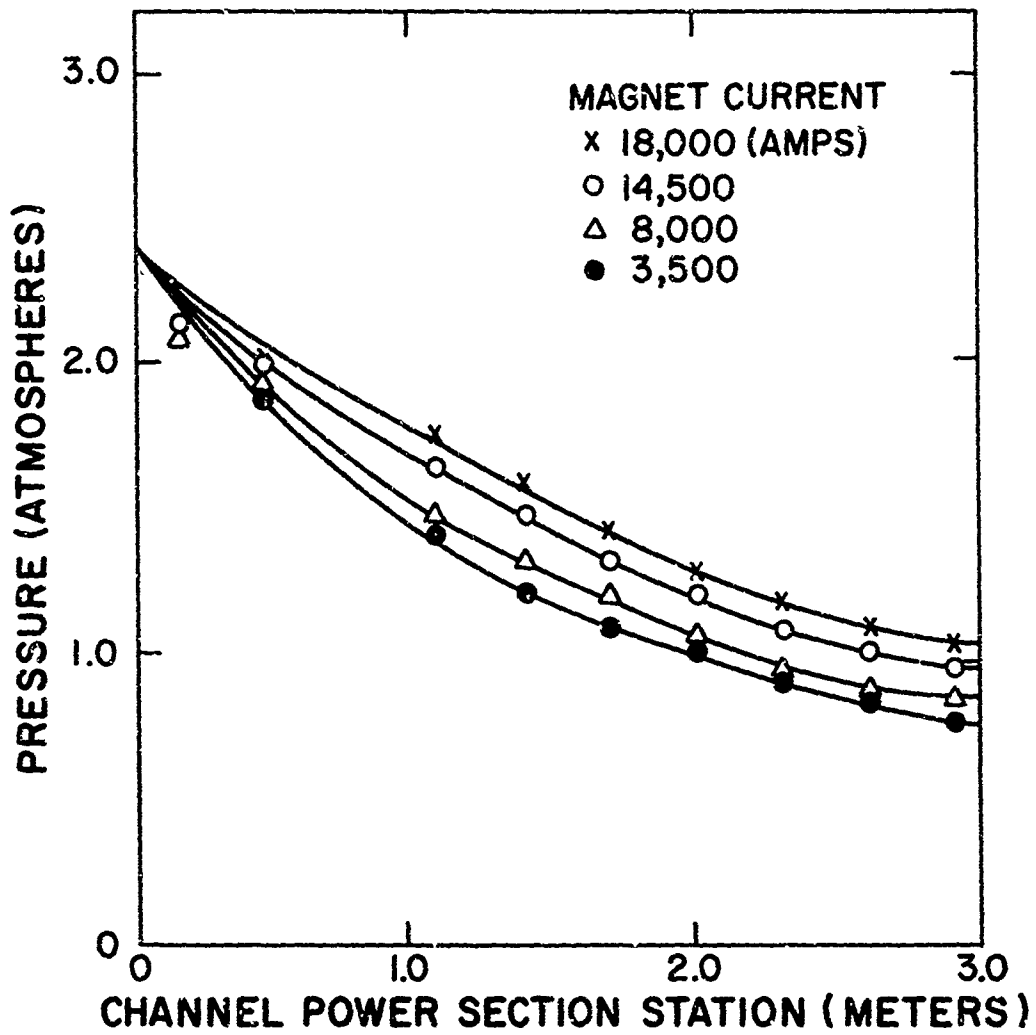


Fig. 60 Typical Pressure Distribution for Single Circuit Operation

The generator configuration which has been tested during this program has a very important practical advantage over the previous Mark V configuration in that a constant single-circuit output voltage is obtained rather than a multi-circuit, multi-voltage output. This advantage, however, is not obtained without difficulties. In comparison with conventional D.C. generators the Mark V generator is comparable to a shunt wound generator and the pulse generator to a series wound generator. By nature, however, a series wound generator has a disadvantage in that the generator external characteristics are too easily altered.

A series wound generator is no exception to the above mentioned in that this generator's output characteristics are largely influenced by the internal impedance of the MHD channel. Since the internal impedance of the generator for a given mass flow and a given gas composition is dependent on the channel configuration, the importance of the channel aspect ratio is hereby clearly indicated.

At the end of the program three attempts were made to pulse the generator. The first two attempts failed because proper generator self-excitation was not obtained. This was directly attributable to difficulties with the new pulse auxiliary fuel system. To conduct these tests, the special valve, described in the Auxiliary Systems section of this report, was mounted and the sixty connections made from the valve to the individual fuel nozzles. The tests were set up to dissipate  $10^7$  joules of the energy stored in the magnetic field at a magnet current of 20,000 amperes in 100 milliseconds, which would give a peak reverse voltage of 5000 volts.

The third test was made at a mass flow of 50 Kg/sec and a seed rate of 0.8 mole % potassium. The generator excitation was as expected, and at a magnet current slightly over 19,000 amperes the explosive charge was fired, shutting off the seeded fuel flow. Figure 61 is a diagram of the generator voltage characteristic for the period immediately before the valve was fired until the breaker short circuited the magnet.

As can be seen in the figure, the generator voltage was 1100 volts when the seed valve was fired and the voltage dropped to zero within the first 100 milliseconds but did not reverse. Instead, the voltage rose again to approximately 160 volts. At time  $t_2 - t_1 = 1.25$  seconds the load circuit breaker was closed and the main burner was shut off through the automatic control system. No voltage reversal, hence no pulse was attained. What actually occurred was that the voltage across the generator dropped to zero when the negative  $L di/dt$  plus the magnet IR drop was exactly equal to the generator channel output voltage. As the negative  $L di/dt$  became smaller the voltage across the generator recovered some voltage before the combustion chamber was shut down explaining the rise of the generator voltage.

The reason for not obtaining a voltage reversal; hence, no pulse, lies in the fact that a sufficient gas conductivity decrease was not

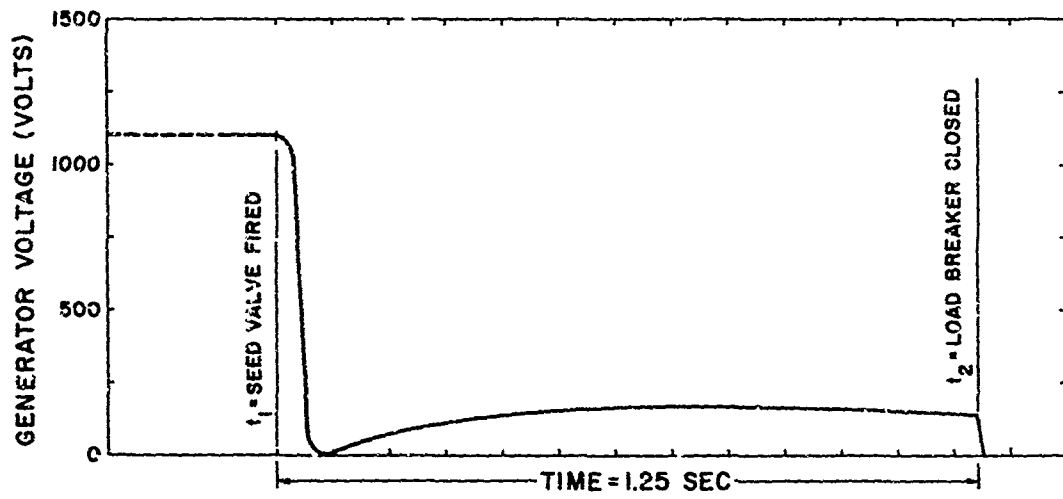


Fig. 61 Magnet Voltage During Pulse Test

obtained. It can be seen in Figure 7 that the test data corresponds to a gas conductivity change of a factor of 5,  $\sigma/\sigma_1 = 0.2$ , for a generator voltage equal to zero.

No further attempt was made to pulse the generator, and since the above mentioned test was performed without using the purge system of the seeded fuel flow due to lack of time, one has to consider any statement about this generator's capability of producing electrical impulses premature.

If time had allowed, a natural course to have been taken was to utilize the purge system for the seeded fuel flow and to use a purge flow containing an electronegative such as chlorine in order to obtain a sharper gas conductivity decrease in the generator.

#### IV. CHANNEL DESIGNS FOR HIGH NET POWER OUTPUT

Within the scope of this program a study in respect to maximum net power output was performed. The object was to evaluate the maximum net power capability of the Mark V generator using the present magnet and operating within the limits of the present flow facilities, but without regard of capability to deliver short duration impulses.

The power density of an MHD generator is proportional to the product of the gas density and the square of the gas velocity, and approaches a maximum at a Mach number slightly less than 2.0. Operation at this high inlet Mach number and low discharge pressure requires a controlled discharge to the atmosphere by use of a diffuser to avoid boundary layer separation in the channel. The diffuser is therefore a necessity in an optimized design, since this design requires the utilization of a higher pressure ratio within the MHD channel than otherwise is possible to obtain with a generator having a final discharge to the atmosphere directly from the channel exit, as was done with the present channel to facilitate short impulse operation.

The two designs presented below, therefore, utilize this high inlet Mach number coupled with a diffuser. The working fluid used in these designs is the stoichiometric combustion products of JP-4 and oxygen seeded with potassium at a rate giving 1 mole % potassium in the products at a temperature of  $3000^{\circ}\text{K}$  and at a pressure of 1 atm. The design magnetic field strength chosen corresponds to a magnet current of approximately 20,000 amperes, which is the upper limit due to the  $j \times B$  load on the magnet structure.

The first design discussed utilizes the present Mark V burner and magnet coupled with a new nozzle, channel and diffuser. The maximum capability of the existing combustion chamber, which is 56 Kg/sec at chamber pressure of 8.6 atm, was used in this design calculation. The design for the above stated conditions is shown in Figure 62, which shows the generator voltage-current characteristics and Figure 63, which shows the general channel configuration.

As can be seen from Figure 62, the design magnet current is 19,400 amperes with a generator output voltage of 2370 volts. This results in a gross power output of 46,000 kilowatts. At 19,400 amperes the steady state voltage drop in the magnet is 620 volts, corresponding to a magnet power requirement of 12,000 kilowatts, leaving a net power output of 34,000 kilowatts at a load voltage of 1750 volts.

Figure 63 shows the general channel configuration, illustrating the insulating wall placed within the magnet as well as the electrode wall. As can be seen, the channel is of a straight wall design with rectangular cross sections and diverging in area from  $0.167 \text{ m}^2$  to  $0.465 \text{ m}^2$  within the power section.

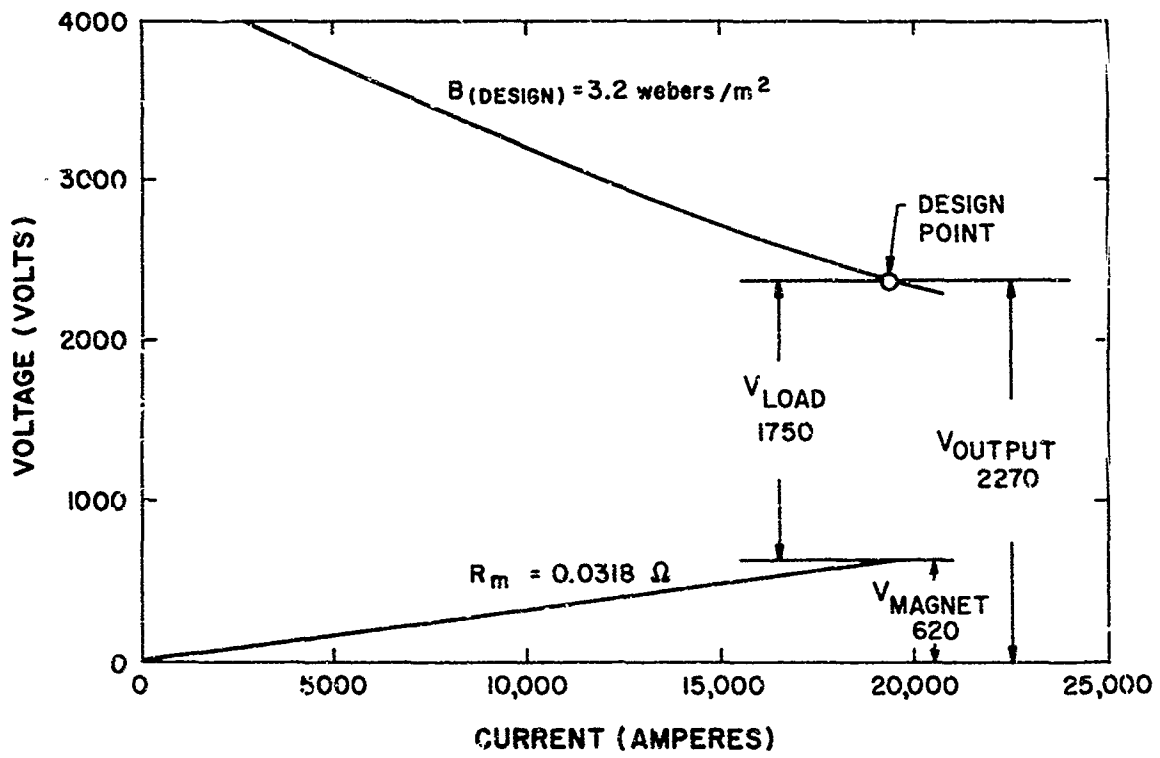


Fig. 62 V-I Characteristics for the 56 Kg/sec Generator

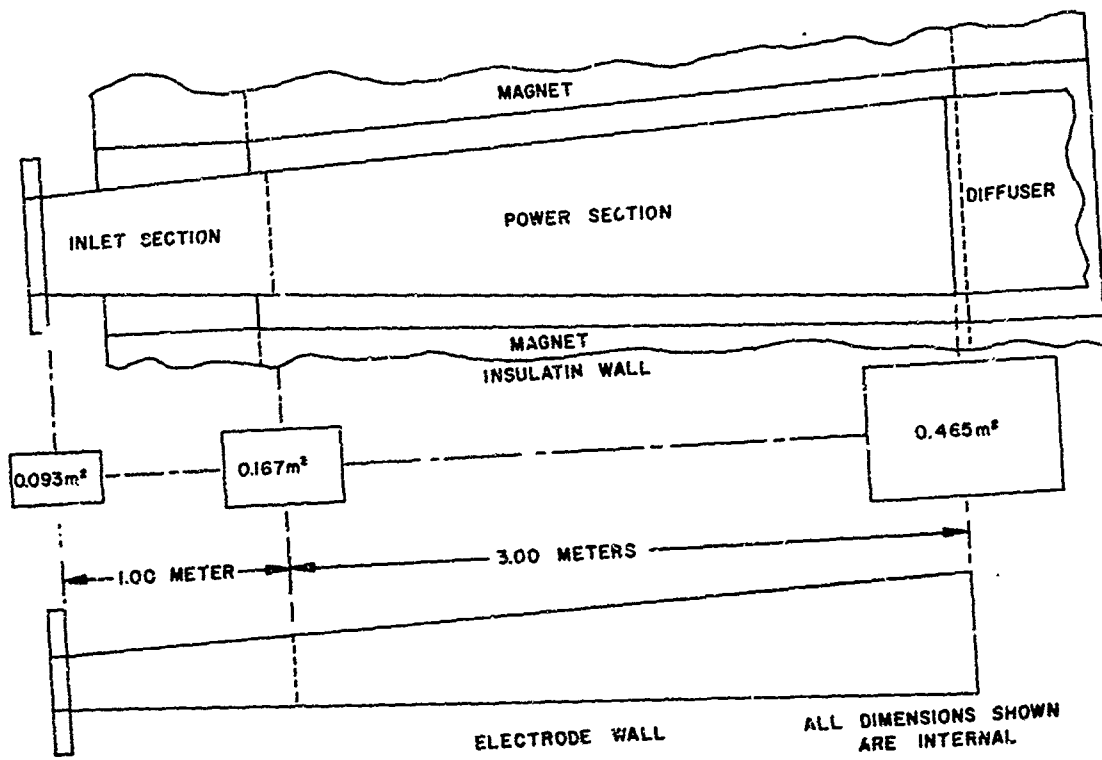


Fig. 63 Channel Layout for the 56 Kg/sec Generator

The second alternative presented is based on the maximum channel dimensions that can be used within the present field coil. The mass flow requirement for this channel configuration is 90 Kg/sec which is within the capability of the flow facility for 90-second operation. However, this design would require a new burner, nozzle, channel and diffuser.

Figure 64 shows the V-I characteristics of the generator for the design field strength of 3.2 Webers/m<sup>2</sup>. As can be seen, at the design point, the generator output voltage is 2370 volts at a total current of 36,000 amperes giving a gross power of 85,300 kilowatts. For the design field strength the magnet power requirement is again 12,000 kilowatts, leaving a total net power output of 73,300 kilowatts. However, this net power output will not be obtained in a single output due to the lower current requirement of the magnet. At the magnet current flow of 19,500 amperes a resistor in parallel with the magnet is required to bypass the additional 16,500 amperes. The power in this bypass load is thus 10,300 kilowatts at a steady state magnet voltage of 620 volts, leaving a maximum single circuit power output, in a load resistor in series with the generator channel, of 63,000 kilowatts at a load voltage of 1750 volts and a current flow of 36,000 amperes.

Figure 65 shows the channel layout for the 90 Kg/sec design. As can be seen, the channel is of a square cross section with the power section area increasing from 0.268 m<sup>2</sup> to 0.746 m<sup>2</sup> in a length of 3.0 meters. The dimensions given are the inside channel dimensions, and represent the maximum channel configuration which can be used within the magnet allowing for water cooled channel walls.

From the designs presented above, it can easily be seen that magnetohydrodynamic power generation makes it feasible to convert the exhaust energy of a modern chemical rocket into vast amounts of electrical power with relatively simple, low cost equipment.

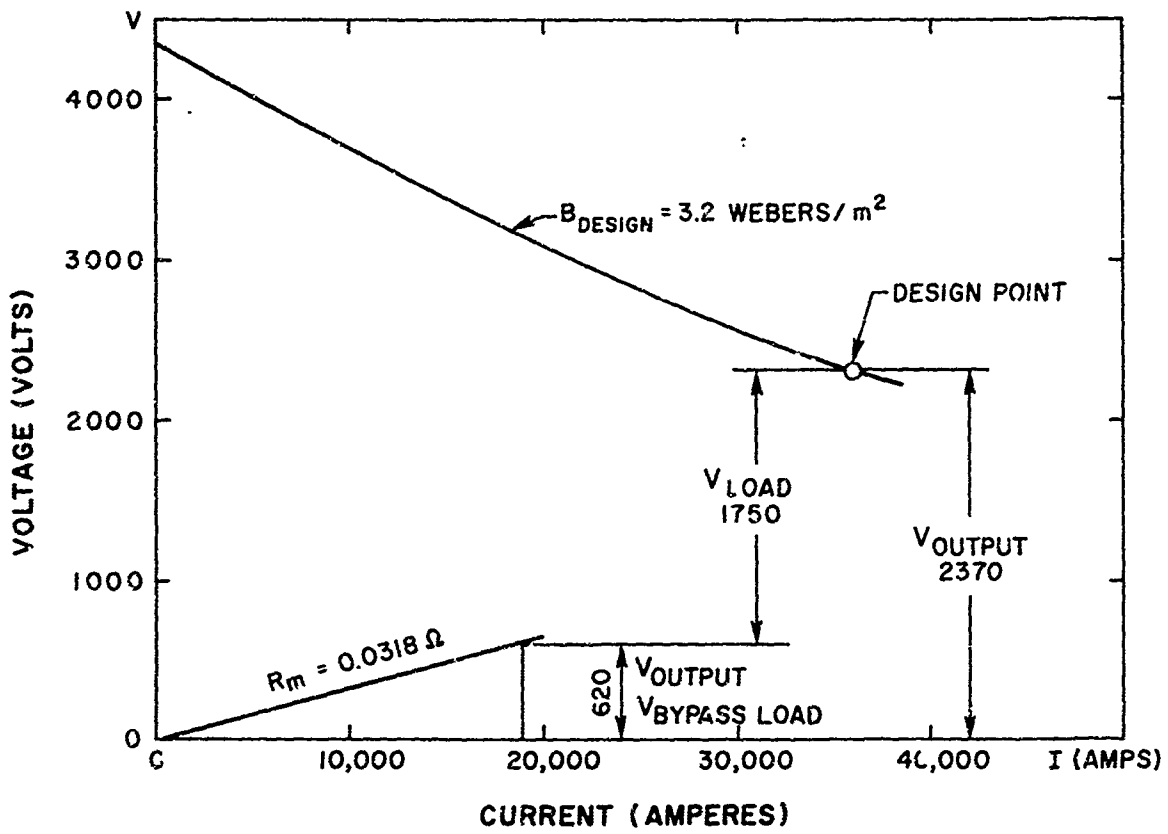


Fig. 64 V-I Characteristics for the 90 Kg/sec Generator

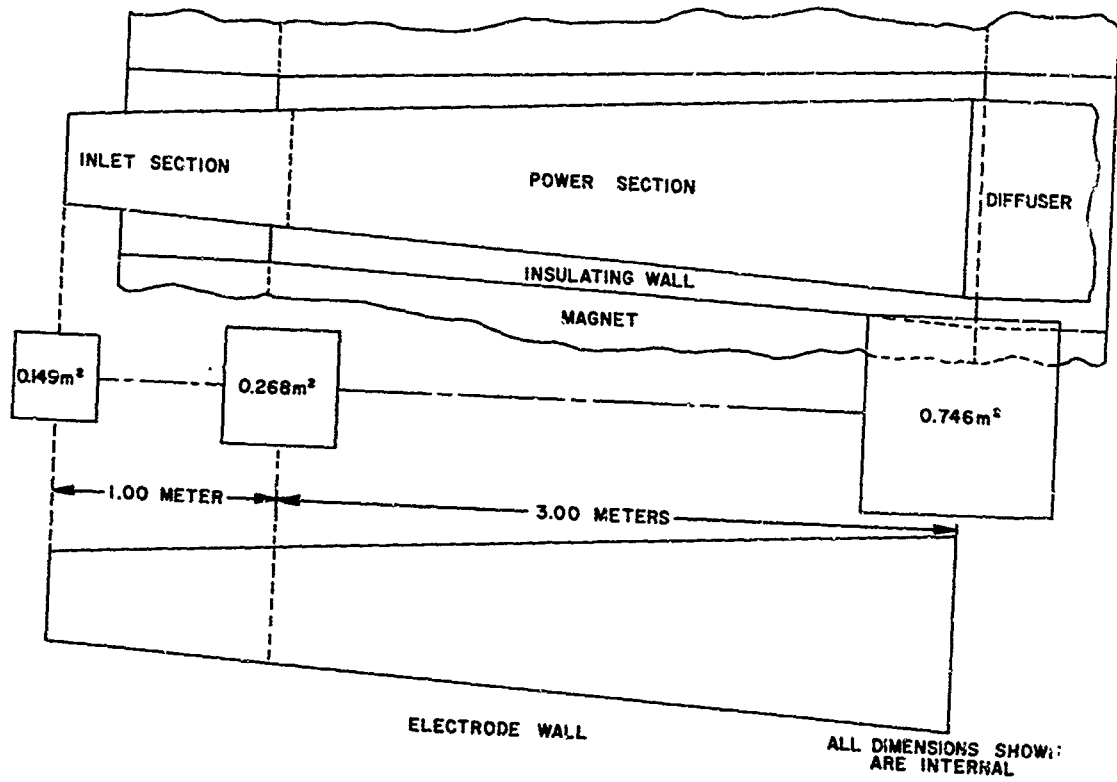


Fig. 65 Channel Layout for the 90 Kg/sec Generator

## V. CONCLUSION

The specific purpose of the program was to investigate and demonstrate the feasibility of using more or less standard combustion heat sources to drive MHD generators of essentially unlimited outputs with the emphasis in this particular study being on single circuit output generators.

The modified Mark V single circuit output channel has demonstrated the feasibility of producing high power levels using a rocket exhaust with the very important practical convenience of having one output rather than a multiplicity of outputs.

The objectives of the present study were two-fold; namely, to demonstrate the feasibility of a single circuit generator system at high power levels (tens of megawatts) and to demonstrate the feasibility of employing a combustion driven self-excited MHD generator for the production of repeated high energy (tens of megajoules) electrical impulses using the generator field as an energy storage device and the generator channel as both an energy source and a circuit breaker. Accordingly, since a single channel was to be used in the study, the channel was designed with compromises being made so that both objectives of the program could be met; the most important of these compromises involving deviations from the conditions for optimum power. The first objective of this study was accomplished; the maximum net power output generated was approximately 14 Mw, thus establishing the feasibility of single circuit high power generation. This power output is below the design value of 20 Mw, but the reasons for this are entirely explainable in terms of compromises to the original design, higher than expected electric field intensities on certain portions of the insulating walls leading to breakdown and degradation of performance, and degradation due to eddy currents. The maximum gross power output obtained during the current tests was 25 Mw; the original Mark V channel operating in the segmented output Faraday mode produced 32 Mw gross. If the generator had been optimized for steady state power output, the predicted power output would have been 34 Mw. It was not possible in the allotted time to accomplish the second objective of the program.

The rapid excitation obtained demonstrated that the generator output was more than sufficient to produce repeated electrical impulses. A  $di/dt$  in excess of 3000 amperes/sec was easily obtained and is sufficient to produce repeated pulses on the order of  $10^7$  joules at a rate of approximately one pulse per second.

One factor which remains unknown is the capability of the channel to withstand the high impulse voltage since the program was concluded before impulse testing could be carried out. In retrospect because of the arcing which occurred in the transition section, it seems that it would have been better to have provided transverse as well as axial insulation capabilities in the insulating section between the burner and the power section by utilizing a peg design.

We believe that as a result of this program it is possible through magnetohydrodynamic power generation to convert the exhaust energy of a modern chemical rocket into vast amounts of electrical power having single voltage output with relatively simple, low cost equipment.

Unclassified  
Security Classification

DOCUMENT CONTROL DATA - R&D		
<i>(Security classification of title, body of abstract and indexing annotation must be entered when the overall report is classified)</i>		
1 ORIGINATING ACTIVITY (Corporate author) Avco Everett Research Laboratory 2385 Revere Beach Parkway Everett, Massachusetts		2a REPORT SECURITY CLASSIFICATION Unclassified
		2b GROUP
3 REPORT TITLE AN INVESTIGATION OF THE CAPABILITY OF A COMBUSTION DRIVEN SELF-EXCITED MHD GENERATOR TO PRODUCE HIGH ENERGY ELECTRICAL IMPULSES		
4 DESCRIPTIVE NOTES (Type of report and inclusive dates) Final Technical Report 1 May 1965 through 31 December 1966		
5 AUTHOR(S) (Last name, first name, initial) Avco Everett Research Laboratory		
6 REPORT DATE June 1967	7a. TOTAL NO OF PAGES 116	7b. NO. OF REFS 3
8a CONTRACT OR GRANT NO. AF 33(615)-2846	9a. ORIGINATOR'S REPORT NUMBER(S) Budget Program Sequence Number 5(638173 62405214 and 5(680100 61430014 AP)	
b PROJECT NO 5350	9b. OTHER REPORT NO(S) (Any other numbers that may be assigned this report)	
c	AFAPL-TR-67-67	
d		
10 AVAILABILITY/LIMITATION NOTICES Qualified requesters may obtain copies of this report from DDC.		
11 SUPPLEMENTARY NOTES	12. SPONSORING MILITARY ACTIVITY Air Force Aero Propulsion Laboratory Air Force Systems Command Wright-Patterson Air Force Base, Ohio 45433	
13 ABSTRACT The program described in this report is directed to the design, construction and performance evaluation of a single circuit output, Faraday magnetohydrodynamic generator channel. The design corresponds to a conventional DC generator with the field coil and load in series. As a second objective, the feasibility of employing a combustion driven self-excited MHD generator for the production of repeated high energy (tens of megajoules) electrical impulses has been investigated. In this application the MHD generator combines the functions of electrical energy generation, storage, and delivery in a single unit basically identical with a conventional self-excited MHD generator configuration. Such a combination is effected by utilizing the generator field coil as an energy storage device and the generator channel as both energy source and circuit breaker. The report describes the channel design analysis, channel construction, modifications to an existing MHD generator (the Mark V) and the testing program. The net power capability of the channel design was strongly compromised in favor of other characteristics judged to be desirable for the pulse application, where high net output from the channel is not the prime requirement. Thus, the maximum net output from the single circuit channel has been approximately fourteen (14) megawatts. Difficulties encountered during the testing program include voltage mismatch between electrode and insulating wall segments in the transition section between burner and channel, arcing in this transition section, and two dimensional current flow effects due to the shorted Hall currents. Solutions to these problems are indicated. An analysis of channel configurations designed primarily for single circuit net output, rather than pulse operation, is also presented. The program was concluded before evaluation of the impulse mode of operation could be carried out.		

DD FORM 1473  
1 JAN 64

Unclassified  
Security Classification

14 KEY WORDS	LINK A		LINK B		LINK C	
	ROLE	WT	ROLE	WT	ROLE	WT
1. Generators, magnetohydrodynamic						
2. Magnetohydrodynamic power generation						
3. Mark V MHD Generator						
4. Single circuit output MHD generator						
5. Generators, Rocket driven						
6. Power generation						
7. Magnet, aircore						

INSTRUCTIONS

1. **ORIGINATING ACTIVITY:** Enter the name and address of the contractor, subcontractor, grantee, Department of Defense activity or other organization (*corporate author*) issuing the report.
- 2a. **REPORT SECURITY CLASSIFICATION:** Enter the overall security classification of the report. Indicate whether "Restricted Data" is included. Marking is to be in accordance with appropriate security regulations.
- 2b. **GROUP:** Automatic downgrading is specified in DoD Directive 5200.10 and Armed Forces Industrial Manual. Enter the group number. Also, when applicable, show that optional markings have been used for Group 3 and Group 4 as authorized.
3. **REPORT TITLE:** Enter the complete report title in all capital letters. Titles in all cases should be unclassified. If a meaningful title cannot be selected without classification, show the classification in all capitals in parenthesis immediately following the title.
4. **DESCRIPTIVE NOTES:** If appropriate, enter the type of report, e.g., interim, progress, summary, annual, or final. Give the inclusive dates when a specific reporting period is covered.
5. **AUTHOR(S):** Enter the name(s) of author(s) as shown on or in the report. Enter last name, first name, middle initial. If military, show rank and branch of service. The name of the principal author is an absolute minimum requirement.
6. **REPORT DATE:** Enter the date of the report as day, month, year, or month, year. If more than one date appears on the report, use date of publication.
- 7a. **TOTAL NUMBER OF PAGES:** The total page count should follow normal pagination procedures, i.e., enter the number of pages containing information.
- 7b. **NUMBER OF REFERENCES:** Enter the total number of references cited in the report.
- 8a. **CONTRACT OR GRANT NUMBER:** If appropriate, enter the applicable number of the contract or grant under which the report was written.
- 8b, 8c, & 8d. **PROJECT NUMBER:** Enter the appropriate military department identification, such as project number, subproject number, system numbers, task number, etc.
- 9a. **ORIGINATOR'S REPORT NUMBER(S):** Enter the official report number by which the document will be identified and controlled by the originating activity. This number must be unique to this report.
- 9b. **OTHER REPORT NUMBER(S):** If the report has been assigned any other report numbers (*either by the originator or by the sponsor*), also enter this number(s).
10. **AVAILABILITY/LIMITATION NOTICES:** Enter any limitations on further dissemination of the report, other than those

imposed by security classification, using standard statements such as:

- (1) "Qualified requesters may obtain copies of this report from DDC."
- (2) "Foreign announcement and dissemination of this report by DDC is not authorized."
- (3) "U. S. Government agencies may obtain copies of this report directly from DDC. Other qualified DDC users shall request through \_\_\_\_\_."
- (4) "U. S. military agencies may obtain copies of this report directly from DDC. Other qualified users shall request through \_\_\_\_\_."
- (5) "All distribution of this report is controlled. Qualified DDC users shall request through \_\_\_\_\_."

If the report has been furnished to the Office of Technical Services, Department of Commerce, for sale to the public, indicate this fact and enter the price, if known.

11. **SUPPLEMENTARY NOTES:** Use for additional explanatory notes.
12. **SPONSORING MILITARY ACTIVITY:** Enter the name of the departmental project office or laboratory sponsoring (*paying for*) the research and development. Include address.
13. **ABSTRACT:** Enter an abstract giving a brief and factual summary of the document indicative of the report, even though it may also appear elsewhere in the body of the technical report. If additional space is required, a continuation sheet shall be attached.  
  
It is highly desirable that the abstract of classified reports be unclassified. Each paragraph of the abstract shall end with an indication of the military security classification of the information in the paragraph, represented as (TS), (S), (C), or (U).  
  
There is no limitation on the length of the abstract. However, the suggested length is from 150 to 225 words.
14. **KEY WORDS:** Key words are technically meaningful terms or short phrases that characterize a report and may be used as index entries for cataloging the report. Key words must be selected so that no security classification is required. Identifiers, such as equipment model designation, trade name, military project code name, geographic location, may be used as key words but will be followed by an indication of technical context. The assignment of links, rules, and weights is optional.